A.H. Reerink

Field Analysis through Integrated Modeling and Simulation

Field Analysis Through Integrated Modelling and Simulation

By

A. H. Reerink

in partial fulfilment of the requirements for the degree of

Master of Science
in Petroleum Engineering

at the Delft University of Technology,
to be defended publicly on March 29th 2018 at 04:00 PM

Supervisor:	Prof. dr. ir. J.D. Jansen	TU Delft
Company supervisors:	Ir. P. Oosthoek	Total
	Ir. G. Van Der Ham – Nijmeijer	Total
	Ir. M. Janzen	Total
Thesis committee:	Prof. dr. ir. J.D. Jansen	TU Delft
	Prof. dr. J.E.A. Storms	TU Delft
	Prof. dr. H. Hajibeygi	TU Delft

An electronic version of this thesis is available at http://repository.tudelft.nl/.

TUDelft

Abstract

Simulation to predict the well and reservoir performance is a very important and established process in reservoir engineering. Integrated production modeling allows improving the understanding of the field's performance and production network, fluid flow behavior and optimization at any stage and level during the life of the field through reservoir modeling processes.

This work forms an in depth study of the production data from the K5-F field in the Dutch sector of the Southern North Sea in which the field is analyzed through integrated production modeling to remove the uncertainties coupled with this field. Due to the absence of individual flow meters for the three wells producing from the K5-F field, a first step was the determination of a production split per well. This production split is then used to quantifying the water gas ratio which forms the input data for material balance modeling. The effect of a changed production history per well on analysis and parameter estimation is also studied.

The well test analysis results and corrected production history incorporated in the material balance software allowed the estimation of other unknown reservoir parameters such as volumes, saturation, relative permeabilities and compartmentalization per well. Using material balance modelling as a tool for history matching, and taking into account the local geology the K5-F reservoir showed that the K5-F1 is a segmented reservoir behaving as separate compartments. Through interference testing it was found that is communication between K5-F1 and K5-F3 through a shared aquifer that is giving additional pressure support to the K5-F1 field. K5-F2 is not in communication with a different reservoir. For both K5-F1 and K5-F2 a reservoir pressure and water saturation match within a 2% range is found

Even though the K5-F field is one that has many production difficulties, unknowns and uncertainties, the workflow used and presented in this thesis allowed for the successful development of an integrated production model based on the most recent ideas and developments. The designed and simulated reservoir model resulted in cumulative production match around 3% and good reservoir pressure, wellhead pressure and gas rate match for K5-F1. K5-F2 found a cumulative production match of 4,8% which is above the acceptable 3%. With the assumptions and optimizations made throughout this study it was possible to create a reservoir model capable of forecasting the K5-F1 and K5-F2 well performance.

This research has shown that the amount and quality of production history available for a field and/or wells can have a huge impact on the analysis on reservoir parameters and model estimations. Besides the quality of the production data being used, the amount of production history plays a large role in well test analysis. Small amounts of production history for instance can influence in the late stage of the pressure build up derivative which can lead to an underestimation of the skin. Even something as simple as a new production split has led to a 16,76% lower cumulative production for K5-F1 and a 13,21% higher cumulative produced volume for K5-F2. Therefore it can be stated that the quality of a reservoir model and history match of a field has a direct correlation with the quality of the production and field data.

Table of Contents

Table of Figures

7

1. Introduction

Around the 1970's it was recognized that there was a need for integrated modeling of oil and gas fields. It became better understood that in order to have an efficient field management, oil and gas companies must gain a better understanding of the field and its system interactions. This led to the development of integrated production modeling software which main intention is to duplicate the performance of a reservoir numerically by including the known reservoir properties.

History matching has become an important part of the modeling and simulating of reservoirs and lies at the basis of this thesis. In history matching the aim is to find a way to describe a reservoir in which the difference between observed data and simulated data is minimal for a past production period. History matching can help to confirm reservoir parameters such as initial gas in place and help identify production problems.

In history matching production parameters are transformed into reservoir parameters while for reservoir simulation the opposite is done. There is no direct relationship in which the data can be used to estimate variables, which makes history matching an inverse problem with complex combinations of reservoir simulations. Multiple configurations of the reservoir properties and variables can result in similar simulated production data which means there is more than one reservoir model which describes the historical production with an equally low mismatch between observed and simulated data. In a perfect world all the possible reservoir models are constructed and the best one selected based on quality of the match but this is not feasible. Therefore a history match based on a logical reservoir model and a low mismatch is considered a good basis for future planning until new data becomes available.

Once a model has been built, checked and verified, the model can be used for a variety of different analyses such as the testing of different development and production scenarios or economic optimization.

This report describes a study about the production difficulties seen in the K5-F field in the Dutch sector of the Southern North Sea. In this work, the field production problems will be analyzed by determining a production split between the three wells connected to the subsea manifold, quantifying the water gas ratio with this split, and creating a history matched model.

1.1 Research Objectives

The purpose of this thesis is to study the effects of historical production data on history matching and field analyses through the reservoir modeling of the Total Exploration and Production Netherland's K5-F field.

In this MSc thesis available data is gathered, analyzed and used to create a dynamic model which helps to create a history match with realistic parameter estimations. It attempts to obtain a satisfactory forecasted model taking into account the major uncertainties on the various input parameters from geophysics, geology and reservoir engineering that plague Total's K5-F gas field. Additionally, the influence of the difference in production split is investigated as well as the impact of the choice of different Vertical Lift Performance and Inflow Performance Relationship correlations.

The general steps taken to study the effects of historical production data on history matching and the analysis based on this are the following:
1. Update and review production history
2. Define water and gas production split between wells
3. Define connectivity and approximate origin of water within field
4. Establish hypothesis for to explain reservoir behavior
5. Develop an Integrated Production Model for the K5-F field
6. Forecast field

2. Geological Background

2.1 Brief Field History and Location

The field studied in this research is located in the southern part of Total Exploration and Production Netherlands's (TEPNL) 'pistolet' in the Dutch sector of the North Sea. This field was first discovered in 1999 through an exploration well referred to as K5-11. This exploration well found the entire Lower Slochteren gas bearing. After discovery the field was developed as a unitized field covering three blocks, K4bK5a, K5b and K6. A subsea development was made with 2 wells tied in: K5-F1 is a tie back of exploration well K5-11 and K5-F2. The produced gas travels via satellite platform K6-N for separation to K6-CC for treatment and compression and finally transported via the Noordgastransport pipeline to shore. K5-F1 saw its first production in September 2008 after which the production of formation water was first seen in the K5-F1 field in 2011. In 2015 the water separation capacity limit of the K6-N platform was reached resulting in the first large production stop. Through pressure data analysis, a strong pressure support is seen but the cause for this pressure support has never been verified.

K5-F2 saw its first production in November 2008 and started producing water in 2013 where after a similar trend of water gas ratio increase is seen. It is feared that with the current increase in water gas ratio, the well could stop producing in 2018. Unlike K5-F1, K5-F2 does not show any significant additional pressure support.

A third well, K5-F3, was drilled in 2016 in the theoretically undrained North East panel and tied into the same subsea development as K5-F1 and K5-F2. However, the production results of this well are extremely disappointing. The quality of the reservoir is mediocre and the maximum the well produces is 30 KNm3/d instead of the expected 750 KNm3/d. The well also shows some depletion and potential water encroachment from the bottom of the reservoir.
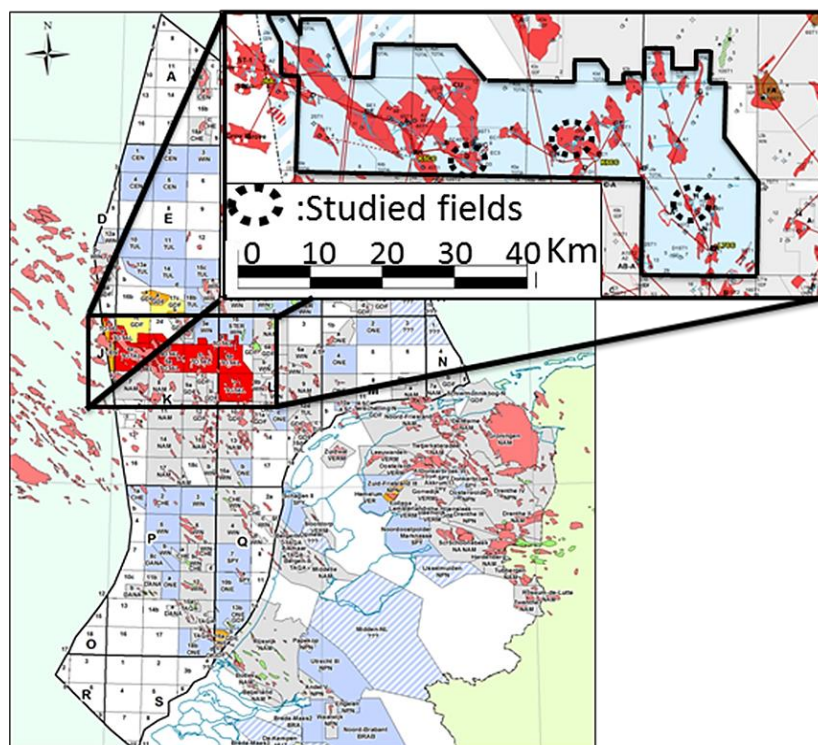
Figure 1: Topographic map of the Netherlands overlain with a thematic map showing the spacial distribution of gas (red) and oil (green) fields on and offshore. The zoomed window focusses on the offshore area owned by Total E&P NL also referred to as the 'pistolet'.

2.2 Regional Geology

The studied gas field is part of the Cleveland High which is a structural high South West of the Central Graben.

2.2.1 History of the Regional Geology

The Westphalian reservoir succession is one of the oldest reservoirs of all of the Southern North Sea petroleum systems. The Westphalian overlays the Namurian sediments overlain by Permian Rotliegend successions. The Westphalian and Rotliegendes layers are separated by the Hercynian unconformity. During the late Devonian the North Sea started to rift until the Diantian. Here carbonates were deposited on top of the horst structures and mud dominated sediments were deposited in the down faulted regions.

Transgressive muds filled the basin in a period of maximum rifting during the Namurian causing phase relative transgression. The entire basin was filled by the time Westphalian sediments were deposited after which the area became dominated by braided fluvial systems, alluvial planes and lake environments. This caused a coarsening upward sediment succession in the south prograding deltaic sediments (Collinson J.D., 1993).

As previously mentioned, the Westphalian deposits are post-rift sediments and therefore only affected by little cooling down subsidence leading to an even distribution of sediment containing homogeneous thicknesses throughout the basin. In the syn-rifted sediments no thermal cooling evidence is found leading to conclude that the Southern North Sea basin was a foreland basin formed by flextural dip (Quirk, 1993). Both mechanisms of the basin formation are possible but according to the structural setting the latter mechanism, the foreland basin, is the most likely approach. The basin was sourced from sediments from the Fenno-Scandinavian shield in the North (Ziegler, 1990) and (Ramsbottom, 1978).

Due to tectonic forces from the South, the London-Brabant massif became the prominent sediment source in the Permian. In the late Carboniferous, or Stephanian, and Early Permian volcanic activity and rifting events dominate the area and a period without deposition occurred which resulted in the formation of normal faults with an NW-SW and E-W tilted fault block structures. This resulted in the Hercynian or Saalien unconformity which forms the end of the Westphalian period.

The Westphalian sediment succession is relatively heterogeneous, especially when considering the sand to coal ratio. The total Westphalian succession contains six sand-mud rich cycles with each cycle taking approximately 10 million years (Lippolt, 1988).Each cycle can be subdivided into third order cycles which each take around 1.5 million years. These cycles show different overall net to gross ratios depending on their position to the Fenno-Scandinavian sediment source. Net to gross ratios decrease when traveling more South in distal direction. The main Westphalian components are:
  ➢ Lower Westphalian A
  ➢ Upper Westphalian A - (Langsettian)
  ➢ Westphalian B - (Duckmantian
  ➢ Lower Westphalian C - (Bolsovian)
  ➢ Upper Westphalian C
  ➢ Westphalian D (Early Stephanian)

The reservoirs, especially reservoirs in Westphalian A and B are formed during a period of high lake-levels. At the lake margins, prograding delta systems change from progradation systems into aggradation systems as it tries to keep up with lake level rise. As a result, braided river channels form amalgamated stacked channels forming sheet-like sands which are good reservoir targets. A second mechanism is avulsion of the braided channels that form sheet-like sand-bodies. Important to state is that the channels do not have sufficient energy to erode and as a consequence no incised valleys develop and hence the formation of sheet-like sand bodies is possible. Also take into account that during the lake level rise the sediment derived from the Fenno-Scandinavian shield is kept on the alluvial plains more northwards in proximal direction and as a result the net to gross decreases towards the south in distal direction.

Although the Westphalian sediment succession contains several interbedded sand-mud successions, the Westphalian does not contain intra-Westphalian sedimentological traps. This is due to the fact that during the Permian rifting event shales were breached causing leakage of the lower Westphalian reservoirs. Hence the Hercynian unconformity, also known as the Saalien unconformity, forms the seal as the most lower part of the

Permian Rotliegend is mud dominated. Due to volcanic activity, tectonic activity and geomorphological highs, the mud layer of the Early Rotliegend is not distributed equally across the area and at some place even absent. Westphalian reservoirs then do not contain a seal and are in direct communication with Lower Slochteren reservoirs.

In contrast Westphalian A reservoirs are sometimes isolated by the mud-rich Westphalian B. Westphalian B is the muddiest compartment of the Westphalian sediment succession and can be subdivided into three parts; a lower part which is fining upwards and mud dominated, a middle part where the maximum flooding surface is recorded and a upper part which is slightly coarsening upwards. The upper part also contains occasional mouth bar sands forming the only reservoir potential in this Westphalian B compartment.

According to well log data and a sedimentary facies interpretation an overall depositional environment has been established as stacked braided river channel deposits with low sinuosity and little/no lithic fragments. Due to the lack of extra data and widespread well spacing it is thought that the channel sands are amalgamated and form sheet like sandbodies. This makes these reservoirs have a layer-cake reservoir architecture where complexity is due to small scale heterogeneities and third order sequence variation.

2.3 Geological Setting

The Westphalian succession was deposited in the Carboniferous. The area was stable during deposition which can be seen in through the even distribution of thickness of the subunits in the following figures. During the Late Carboniferous (Stephanian) the region became tectonically active under North to South tectonic compressional stress. This resulted in the development of East – West trending anticline and syncline structures. During a later extensional phase a series of normal faults developed generating the paleo-morphology.
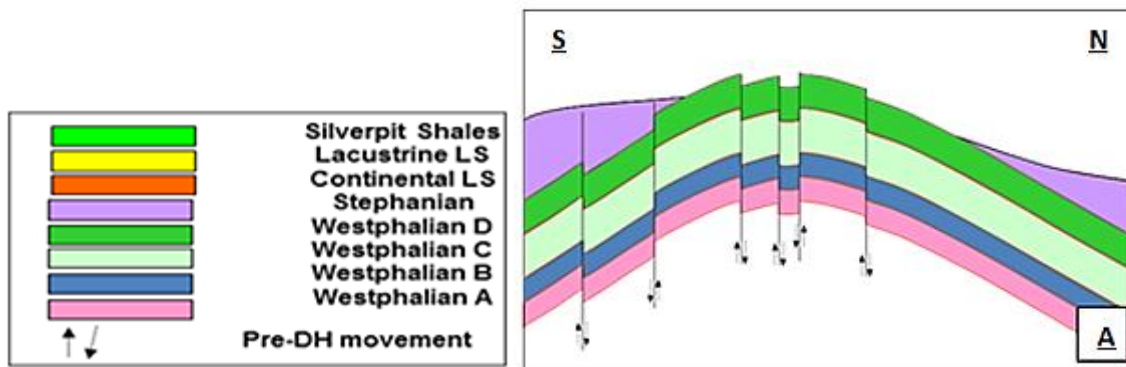
Figure 2: Late Carboniferous

A period of non-deposition and erosion is recognized as the Early Permian. In this period the angular Hercynian Unconformity, also referred to as Discordance Hercynienne (DH), which was formed as a result to prior North to South compression and extension. This compression and later extension was due to the Laurussia and Gondwana continental plate colliding forming Pangea.
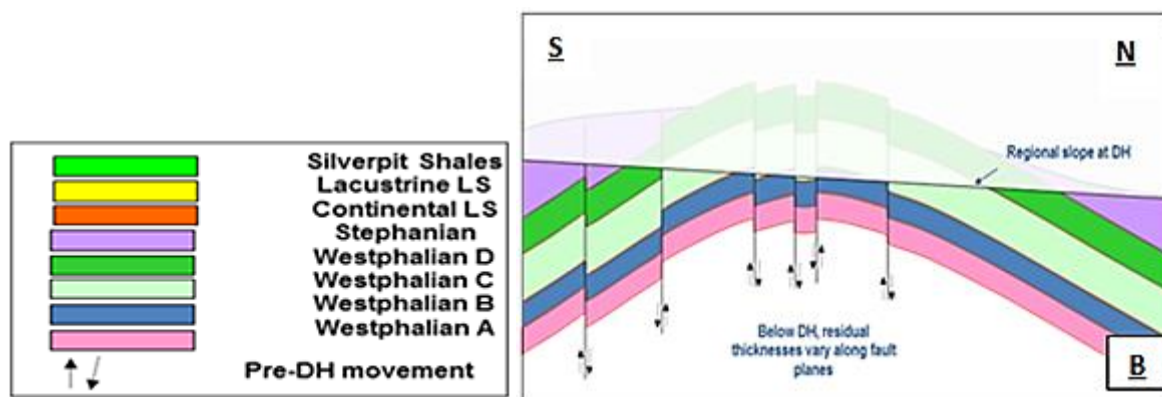
Figure 3: Early Permian

Due to internal cyclicity of Westphalian strata, each sub-unit contains different characteristics. Westphalian A & C are more competent sub-units than Westphalian A & D. Therefore, Westphalian A & D are more eroded forming a depression in the landscape whereas A & C are less eroded and form a local relief. The Permian Rotliegend deposition is effected by this morphology distribution of the cyclicity.
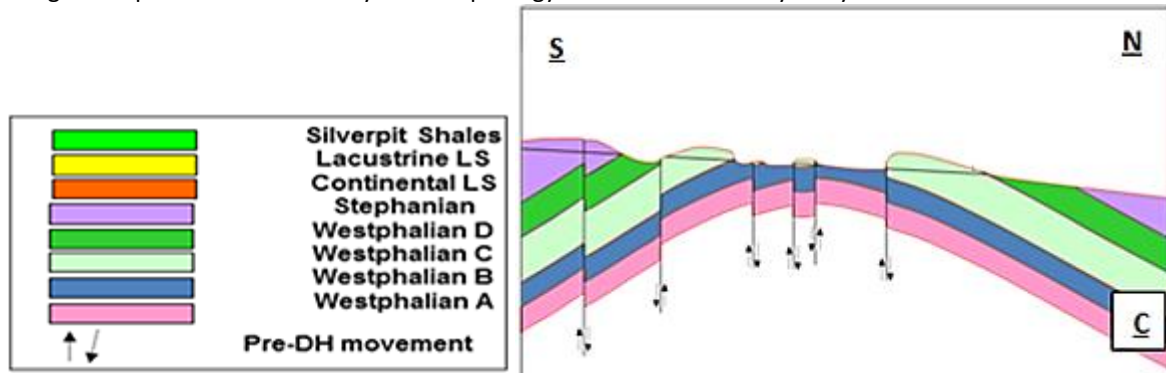
Figure 4: Permian Rotliegend

The Lower Slochteren, a sub-unit of the Rotliegend Group, is deposited during Early Permian. The Lower Slochteren fills in the depressions and thins out on the local morphology. Therefore, the Lower Slochteren thickness is variable, according to the paleo-morphology and hereby to the Hercynian unconformity placement. Later the Lower Slochteren will act as the main reservoir in the studied area.
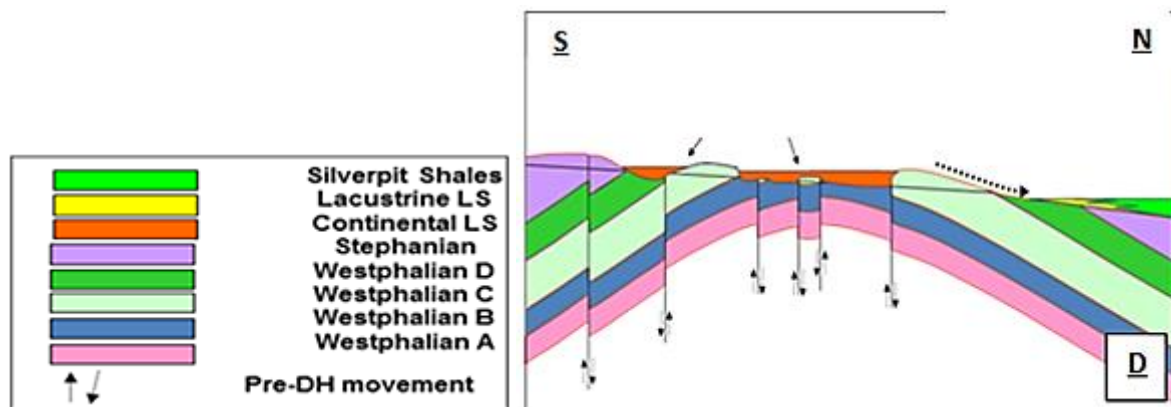
Figure 5: Lower Slochteren

Subcrop maps from the depth of the Hercynian unconformity clearly indicate the East to West trending anticline structure where Westphalian A, is the oldest sub-unit, forms the center of the anticline and Westphalian D, the youngest sub-unit, is present at the flanks of the anticline. This is shown in . Since the Lower Slochteren is the main reservoir in the landscape it is expected to be thickest when underlain by Westphalian sub-unit B or D. Most wells in the area have therefore been drilled where Westphalian B or D are present as seen in . During multiple tectonically active periods conjugate sets of normal faults have been developed with NW to SE and NE to SW trends. The NW to SE facing faults are normal faults formed as a result of late Permian extension, where the NE-SW conjugate faults have formed due to an associate strike-slip movement. This system of faults has a significant impact on the gas field distribution, size and aquifer properties.

13
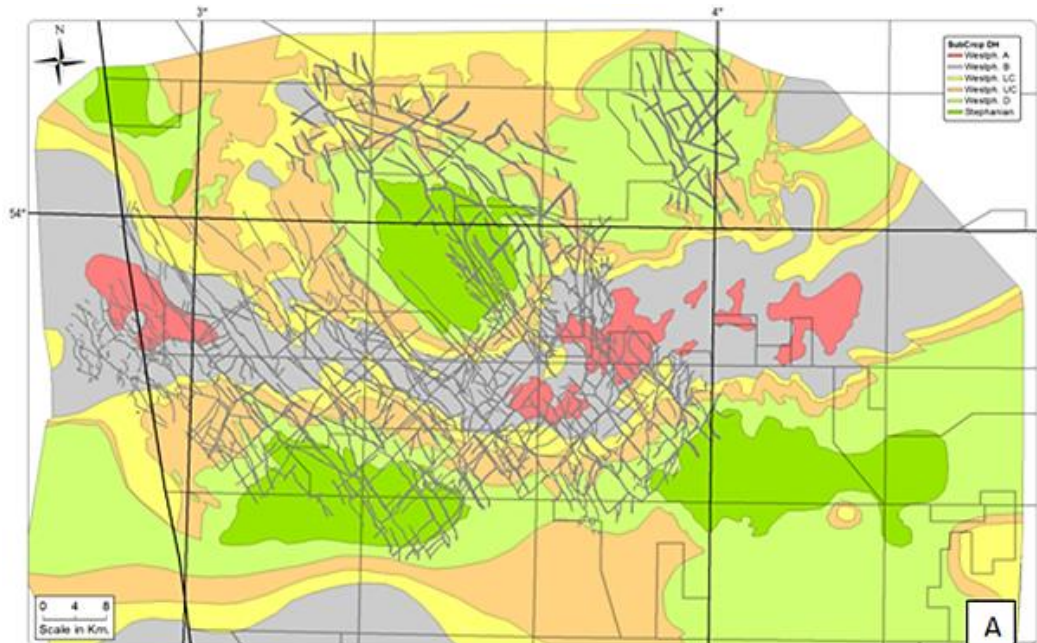
Figure 6: Subcrop map of Lower Slochteren, overlain by a fault map showing two main fault patterns, NW-SE normal faults and NE-SW strike slip faults.
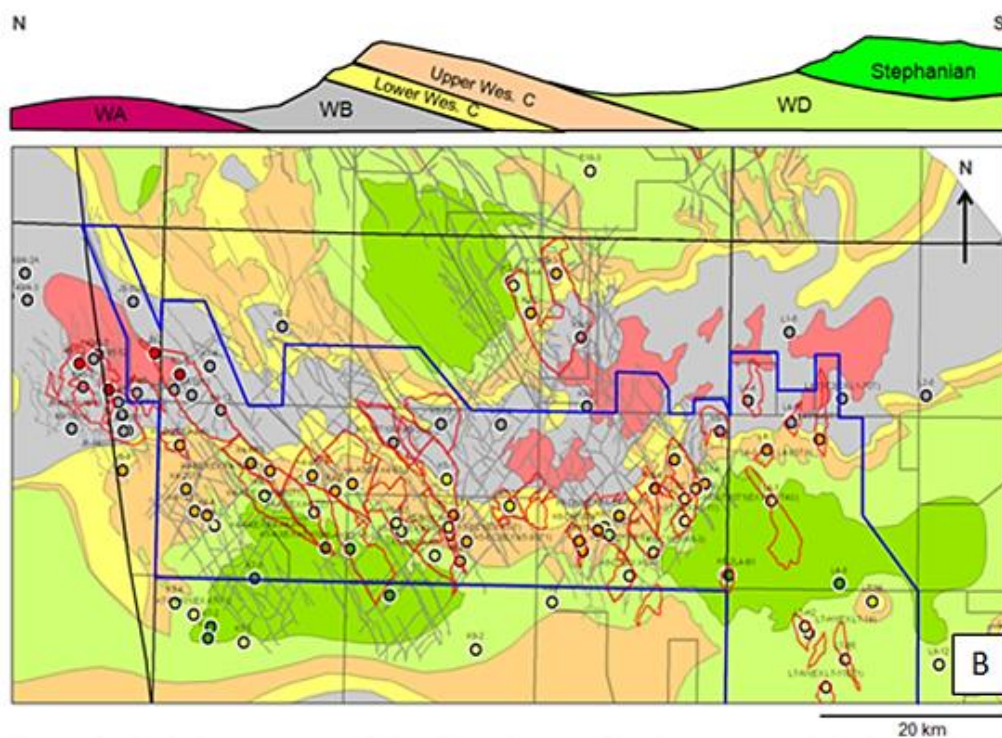
Figure 7: Subcrop map of Lower Slochteren overal by Total's offshore drilled wells and 'pistolet'. The East to West trending anticline can be recognized. Through the well distribution it can be noted that most of the wells have been drilled in the Lower Slochteren. (Total Internal Rapport)

2.4 Lower Slochteren Reservoir

The wells studied for this thesis produce gas from the Lower Slochteren reservoir. The Lower Slochteren overlays the Carboniferous Westphalian group where the Carboniferous Westphalian group acts as a source rock and is found to be mostly water bearing. This layer plays an important role in terms of water breakthrough since the sand layers of both reservoirs are sometimes communicating as seen in .

14

During the Permian, Rotliegend sediments were deposited which can be subdivided into three parts; the Lower Rotliegend, Upper Rotliegend and Zechstein. During the Upper Rotliegend the Lower Slochteren and Silverpit claystone succession were deposited. The Lower Slochteren is sand-rich and acts as the main reservoir in this area. Due to the transgressive nature, the quality of the Lower Slochteren reservoir declines towards the top until it is overlain by the Silverpit shale formation. The reservoir quality also decreases in a distal direction towards the North, until the Lower Slochteren reservoir shales out and is no longer present. This is depicted in .
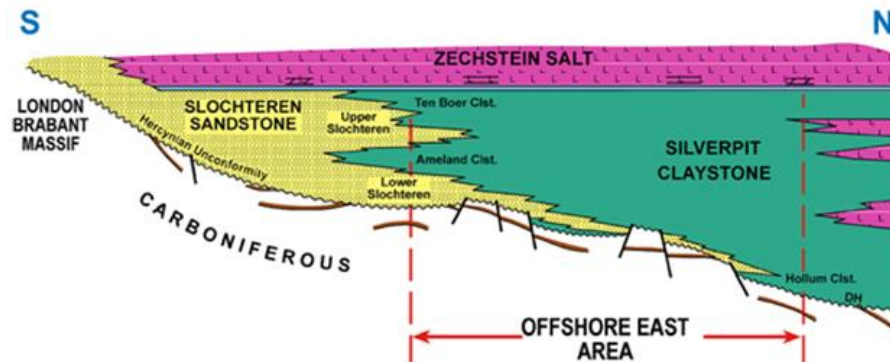
Figure 8: Schematic cross section of the Upper Rotliegend strata.

2.4.1 Depositional Environment and Facies Interpretation

The climate became drier during the Late Carboniferous and Early Permian and the fluvio-deltaic depositional environments slowly changed into dessert dominated depositional environment of wadi systems and a variety of aeolian dune systems. The distribution of the facies is dependent on the paleo-morphology and proximal/distal distance to the London-Brabant massif, the sediment source of the Lower Slochteren reservoir. The proximal/distal distance is strongly controlled by the variations in the lake level, where the several eustatic cycles can be interpreted as the arid/desert-variant of the Exxon's shallow marine succession (Sanjeev Gupta, 1998).

Figure 9: Sedimentary model of the depositional model of the Lower Slochteren reservoirs. For the Lower Slochteren reservoirs this model is valid where the marine influence is changed for lake influence and the terrestrial facies are deposited in an arid climate instead of a wet climate. (F. Lafont, 2000)

Over time the lake level gradually raised leading to backstepping of the Lower Slochteren sediments. During this lake-transgression , aggradation of Aeolian dunes and playa deposition takes place in an attempt to keep up with the lake level rise. This resulted in the development of thick Lower Slochteren reservoirs. The spatial distribution of the facies changes from East to West as a result of the paleo-East to North East wind direction and paleo North to South fluvial flow direction. Large normal faults running South West to North East constrain a fluvial wadi axis acting as a fluvial highway. Consequently, the most Eastern and Western parts of the study area, the Lower Slochteren reservoir predominantly contain Aeolian dune deposits, whereas the central area reservoir contain mostly fluvial wadi and playa deposits. A large scale interpretation of this is shown in .
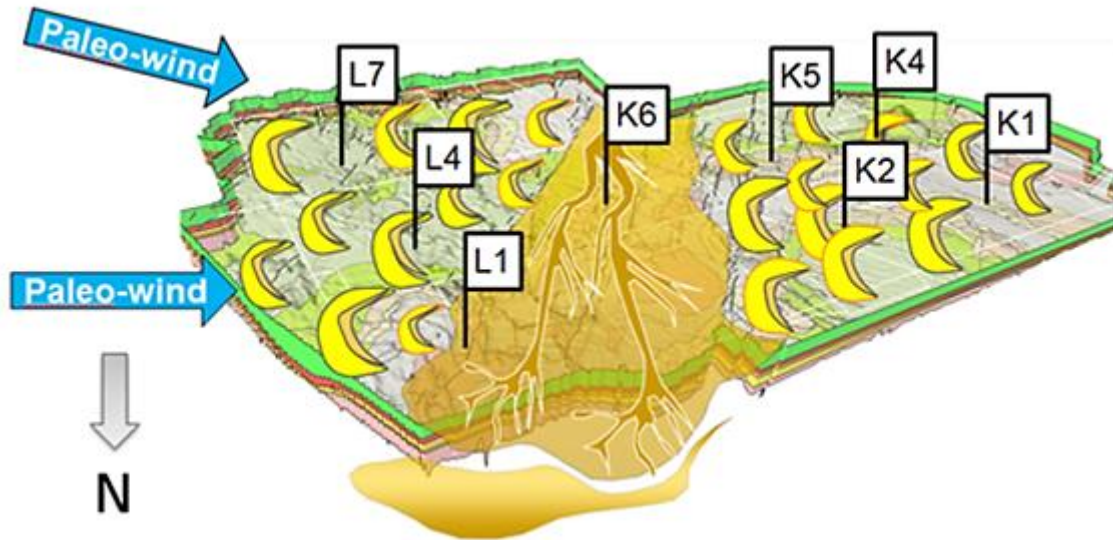
Figure 10: Large scale facies interpretation of TEPNL 'pistolet'. Note that the fluvial transport direction is perpendicular to the aeolian transport direction what impacts the facies distribution at medium scale. (Total E&P NL internal report)

In general six main types of sedimentary environments can be distinguished for the Lower Slochteren in the K4 and K5 blocks;
- Two distal ones (desert lake shales and distal sheet flood)
- Desertic fluvial channels (wadis)
- Three Aeolian sediments (dry Aeolian dune, damp Aeolian interdunes or sabkha and playa shales)

These are shown in . These six environments can be further subdivided into six petrophysical facies as shown in of which four show reservoir potential; the dry Aeolian dunes which show good reservoir quality, the damp Aeolian interdunes show fair reservoir quality, the wadis moderate and the distal sheet flood poor reservoir quality.
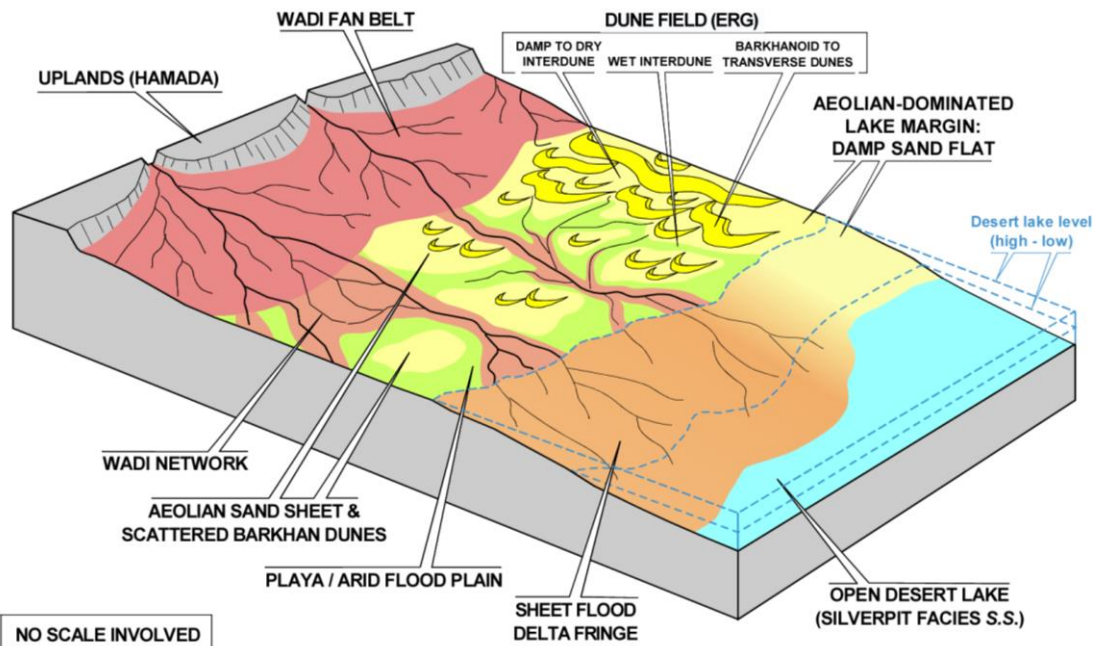
Figure 11: Schematic structural and depositional 'sandbox'model of the study area. (F. Lafont, 2000)

Class	Petrophysical facies	Reservoir Properties
I-A:	Desert lake shales	no reservoir properties
I-B:	Playa shales	no reservoir properties
II-C:	Fluvial derived, distal sheet flood delta	poor reservoir sand, porosity 2-10% and permeability <1mD
III-C:	Proximal fluvial/ wadi channel	fair reservoir sand, porosity 6-12% and permeability up to 10mD
IV-D:	Wet aeolian dunes with interdune deposits	fair to good reservoir sand, wide range of porosity, average of 12%. Best sample 15-16% porosity and permeability between 10-40mD
V-D:	Dry aeolian sheet sand to dune forests	good to very good reservoir sand, porosity of 14% and permeability between 40-100mD. However this facies can be very cemented causing permeability issues, especially in dune deposits underlain by lake flooding surfaces due to carbonate precipitation.

Figure 12: Petrophysical classification based on fluid flow properties, sedimentary mechanisms and depostional environments.

17

3. Software

Taking into account the regional geology and the issues with the field, an analytical study is performed using the following software sets and databases.

3.1 Microsoft Excel 2007

The production split between the three production wells in the K5-F field was determined through decline curve analysis using Excel 2007. This production split is then used to determine water gas ratios per well to find and analyze the production history. This software was also used for general data gathering and storage as well as simple graphical analysis.

3.2 PIE version 2014.10

Pressure Interpretation d'Essais des puits, referred to as PIE, well test analysis software is an analysis tool which allows engineers to get an understanding of the well, reservoir parameters and reservoir geometry. Data from Down Hole Gauges (DHG) and pressure vs time derivatives from Drill Stem Test (DST) are input data for this software. The parameters which can be estimated using this software are (Wilson, 2003):
- Skin factor
- Reservoir permeability
- Boundary distance
- Wellbore storage
- Areal permeability variations
- Turbulence
- Viscosity

3.3 MBAL from IPM version 10.0

A third software used is MBAL which is a material balance software that provides the possibility of defining hydrocarbon volumes and drive mechanisms which allows the recreation historical pressure and water production trends. This is necessary to create reliable production models and forecasts. The theoretical material balance behind this model will be described in Chapter 7 but as the name states is based on the principle of the Law of Conservation of Mass. This software does not take into account the orientation and placement of the wells or the reservoir geometry.

3.4 PROSPER from IPM version 10.0

PROSPER is short for Production and Systems Performance Analysis Software which models the different well components of production systems. (C. Correa Feria, 2010). PROSPER is the link between the subsurface and the surface facilities and utilizes nodal analysis. This allows the system to design, optimize and analyze well performance. The following characteristics are examples of what can be modelled through Prosper:
- PVT analysis accounts for the fluid characterization;
- Tubing pressure losses by Vertical Lift Performance (VLP);
- Reservoir inflow through Inflow Performance Relationship (IPR).

These calculations are assisted by the information of downhole completions, production rates and reservoir properties so that PROSPER can estimate the most accurate well performance curves. These performance curves in turn help in obtaining a match to the performance data.

3.5 GAP from IPM version 10.0

General Allocation Package (GAP) simulates multiphase flow through non-linear sequential quadratic programming which optimizes the production systems. Integrated Production Modeling (IPM) software links the well and reservoir model to GAP so that the whole production system is replicated in the computer software.

3.6 OFM

OFM (Oil Field Manager) is a Schlumberger Software which is a production surveillance tool that incorporates analysis and forecasting tools. As the name indicated it is a database and management software which stores the default allocated production data. Some of the data options this program offers is (Schlumberger, 2017):
- Monitor and survey performance with advanced production views;

- Forecast production with powerful decline and type curve analysis;
- Analyse any asset and share results using standards;
- View, relate, and analyse reservoir and production data with comprehensive tools, including interactive base maps with production trends, bubble plots, and diagnostic plots;

3.7 PI ProcessBook

PI ProcessBook is real time asset monitoring program which is used to simplify the data infrastructure between data from asset and process infrastructures to operational intelligence. Production data such as downhole temperature, downhole pressure, production rates, water salinities etc. are stored in this database. The program is used for data collection, finding, analyzing and visualizing current or historical data up till 8 years. The PI Processbook also offers a DataLink option in which you can make a direct link between specific PI production data and Excel. (Osisoft)

4. Production Analysis

Simulation to predict the well and reservoir performance is a very important and established process in reservoir engineering. One of the largest issues in the oil and gas industry is the generation of a reliable production model for forecasting purposes. In petroleum engineering, knowledge of the underground such as geology and petrophysics is incorporated in reservoir simulation models to better understand them.

In reservoir simulation process an estimation of the reservoir parameters and properties is made and used to compute the past field history through either production or pressure modeling. The outcome of this computational production history can be compared to the gauge data from the field to test the accuracy of the estimated parameters and properties. The idea behind this method is that, if the simulated result matches the observed data, then the model used can be considered correct and reliable. Additionally, history matching can also be used to adjust the estimation of unknown parameters in the numerical model until they closely fit the observed data.

In this research, a first step is to perform a decline curve analysis on the observed data. This was necessary to determine the production split between the wells as K5-F is only fitted with one flow meter. After this step a computer assisted history match can be performed allowing analysis through IPM modeling. More reasons for the necessity of determining a new production split will be discussed in paragraph 4.2.

4.1 Decline curve analysis

Oil and gas production rates decline over time as more of the volume initially in place is produced which depletes the reservoir through which the pressure drops. Decline curve analysis is a commonly used technique for studying declining production rates and can be used for basic predictions of future performance of oil and gas wells. A decline curve forecast model will not be very accurate, and should only be used as an indication, as it does not incorporate any well or reservoir specific data. The basis of this analysis technique is to fit a trendline through the historical production performance and assume this trend will continue in the future. This principle is applied to the K5-F production data, where care was taken to account for the difficulties characterizing this field such as the metering issues and long periods of production stops due to water handling issues on the K6-N platform.

4.2 Production split

A large difficulty in determining the production split of the wells in this field is that none of the wells are fitted with flow meters and flow is only measured on the K6-N platform where the three wells converge. Since K5-F3 only started adding to production in 2016 it was decided to perform the decline curve analysis on the production data from wells K5-F1 and K5-F2 only. This allows the assumption to be made that before 2016, when only one of the two wells is producing, that the production volume measured at that time can be considered to be the correct volume of that producing well.

Before this research, the production split was determined by engineers from Pau in France and was mostly based on downhole pressure changes or basic production rates divided over the two wells producing at the time. The unaltered production data from the K6-N flow meter is shown in .
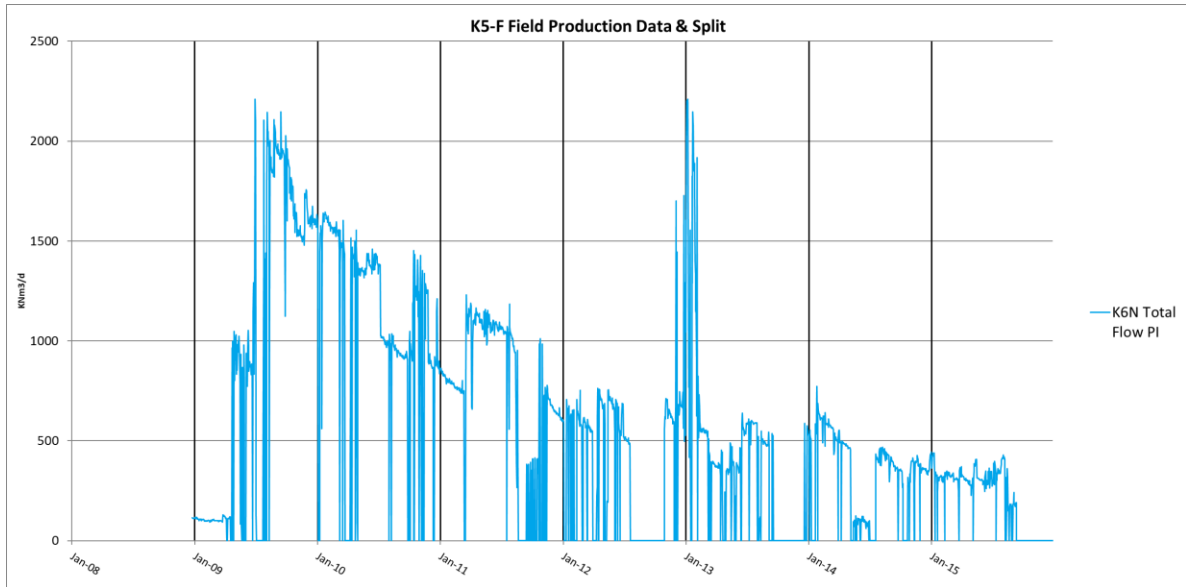
Figure 13: Total gas production of the K5-F field

The original production split made by engineers in Pau and used for all previous production analysis is shown in. The blue line represents the total production measured with the flow meter at platform K6-N, the red the resulting produced volumes for K5-F1 and in green the K5-F2 gas production.
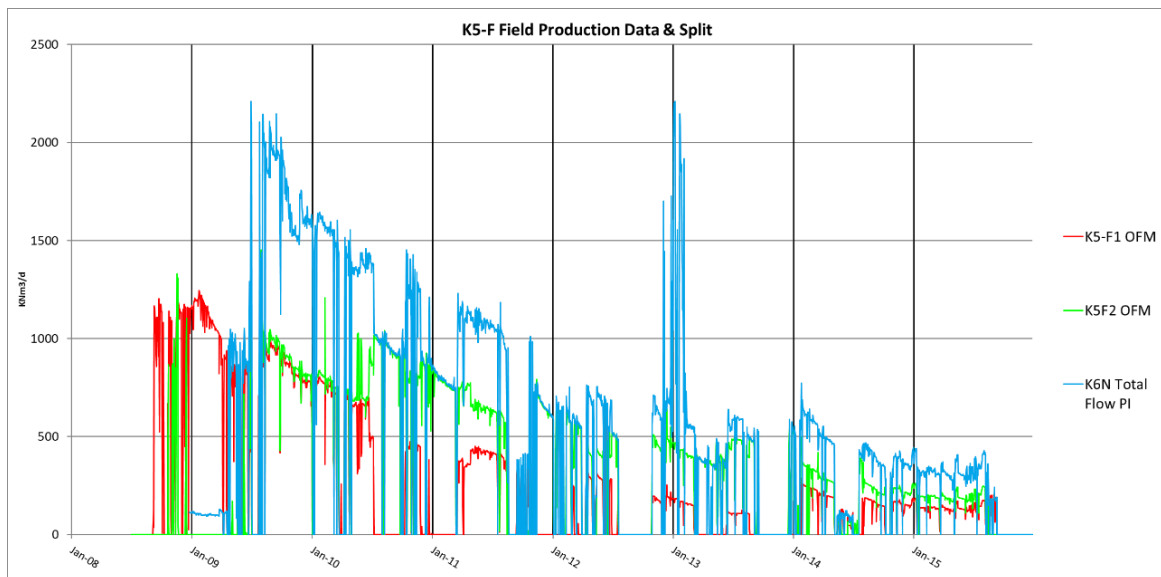
Figure 14:Total production of the K5-F field (blue) with Pau allocated K5-F1 (red) and K5-F2 (green) production.

It is not very clear what algorithm this production split is based on but when looking at the data closely one starts to question it. In Figure 14 some questionable data is seen:

- Between the middle of 2008 until approximately June 2010 the total production seems to be divided equally between the two wells. Since the wells are in different geological panels it is highly unlikely for their characteristics to be identical which makes it illogical to have the same flow for both wells;
- Production increase after unchoking K5-F1 is added to K5-F1 as well as K5-F2, where this increased production should only be allocated to K5-F1
- The low registered total production around January 2009;
- The peaks in total production in January 2013.

21

The previous reservoir models and the analysis of them have all been based on the gas production split determined in Pau. Due to the above mentioned arguments, the validity of the production data and its production split is put into questions granting the need for a new determination of the gas production per well.

Before performing production split calculations, the registered gauge data was closely analyzed and any unrealistic data was removed. Evidence of this is shown in Figure 15 where unrealistic data such as the peak in January 2013 is removed. The removal was justified through the analysis of the flow meter gauge data. This data showed that the data had been registered twice, doubling the production volume for that day resulting in the peak previously mentioned.

By plotting the moments in time when only one of the wells was producing for a longer period in time gives the following result:
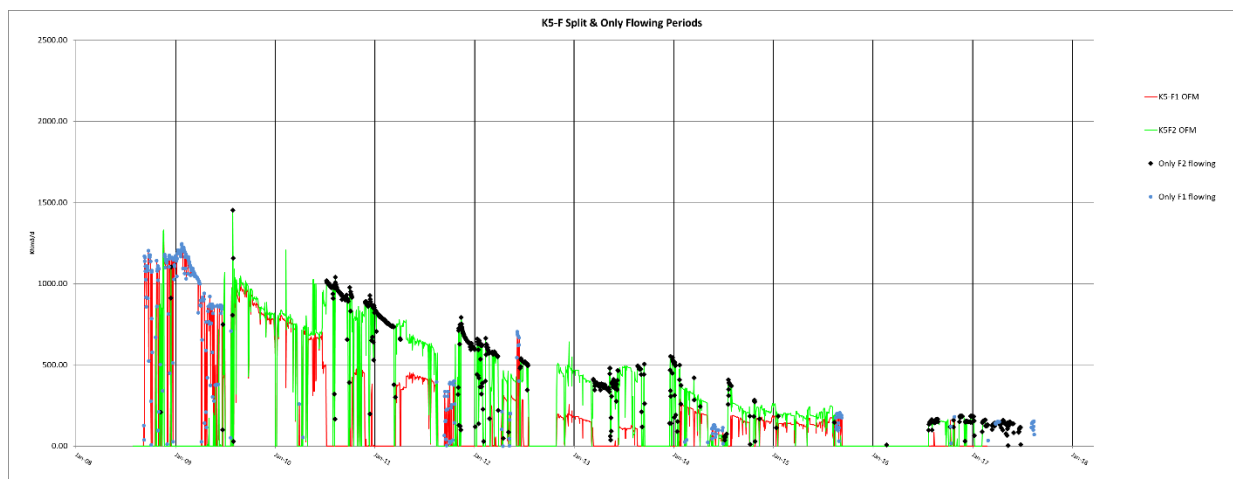
Figure 15: Pau registered production split of K5-F1 (red) with only flowing periods (purple), and K5-F2 Pau registered production (green) and only flowing periods (black)

Here the purple points symbolize the points when only K5-F1 is producing and the black points resemble the moments when only K5-F2 is producing. Figure 15 shows 6 distinct periods in which K5-F1 is the only one producing, of which one long period. Whereas, K5-F2 has approximately 12 'only flow periods' of which some are for multiple months and spread throughout the whole production lifetime. Fitting a line through these single production moments of the most reliable producer, in this case K5-F2, results in the following trend. The moments when only K5-F2 is producing are more reliable since K5-F2 is an unchoked well with more calibration points in time in comparison with K5-F1 which will results in a more accurate trendline.
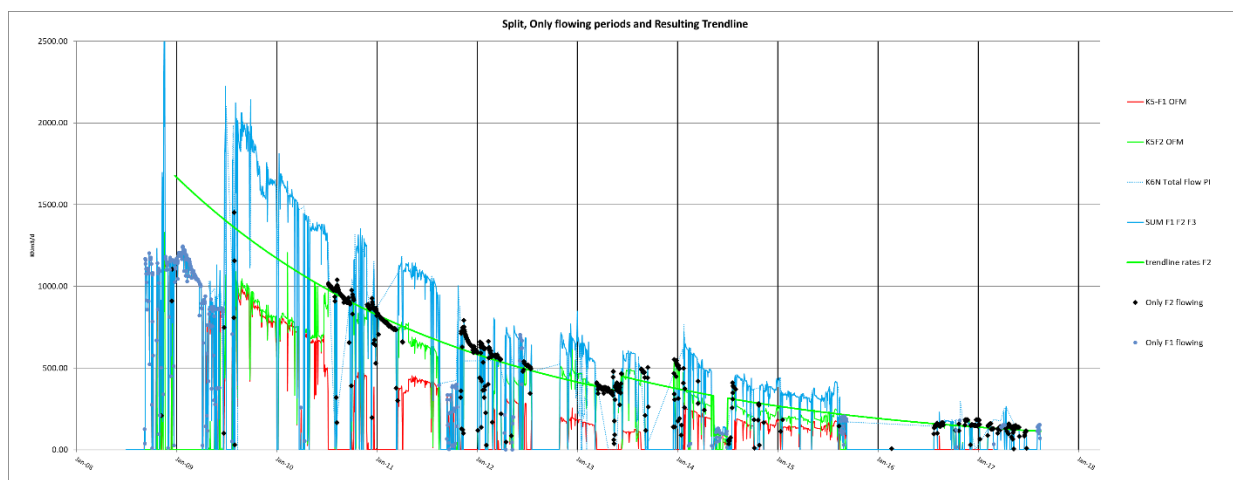
Figure 16: Trendline through the K5-F2 only production periods (black)

The trendline through the K5-F2 singular production moments is made up of two segments. The first segment is from the beginning of production till June 2013, at which time a compressor was hooked up onto the system requiring a second segment starting from the moment of compression hook-up until the present.

This trendline is assumed to depict the produced gas volumes from the K5-F2 well. Taking into account that the total flow is measured at K6-N and that the production of K5-F2 is corrected towards this trendline, a simple deduction of the total production minus the K5-F2 trendline production allows the production of K5-F1 to be calculated. To reduce the uncertainty of this calculated production split a deviation function was added to the K5-F2 trendline production calculation. This permits the user to have the system recalculate the production split according to the deviation from the trendline the user is willing to tolerate. This deviation can lie anywhere between 0% and a 100%, where 0% (Figure 17) resembles no deviation from the trendline and 100% (Figure 16) equals the Pau allocated production split.
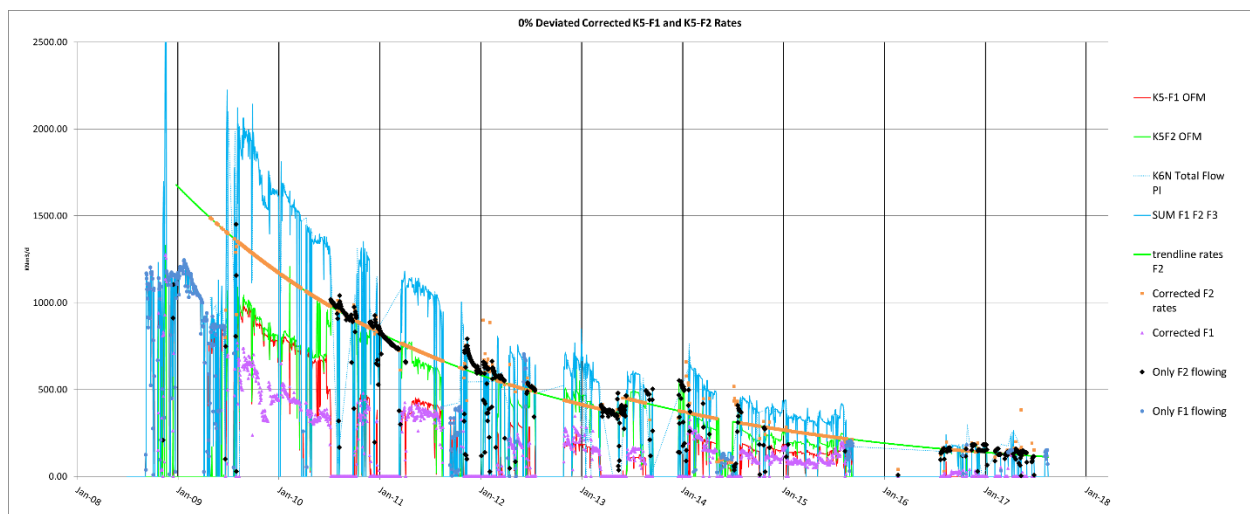
Figure 17: Production split with a 0% deviation from the trendline. K5-F1 production indicated in purple, K5-F2 production indicated in orange.

The purple points show the new production values for K5-F1 and the orange the values for K5-F2. With a 0% deviation, the value will adhere to the trendline as shown in Figure 17. For this thesis, a deviation of 15% was used for further analysis. This percentage is chosen by the Reservoir Engineers at TEPNL to account for the variations over time such as gauge failure etc. This resulted in the following production profile:
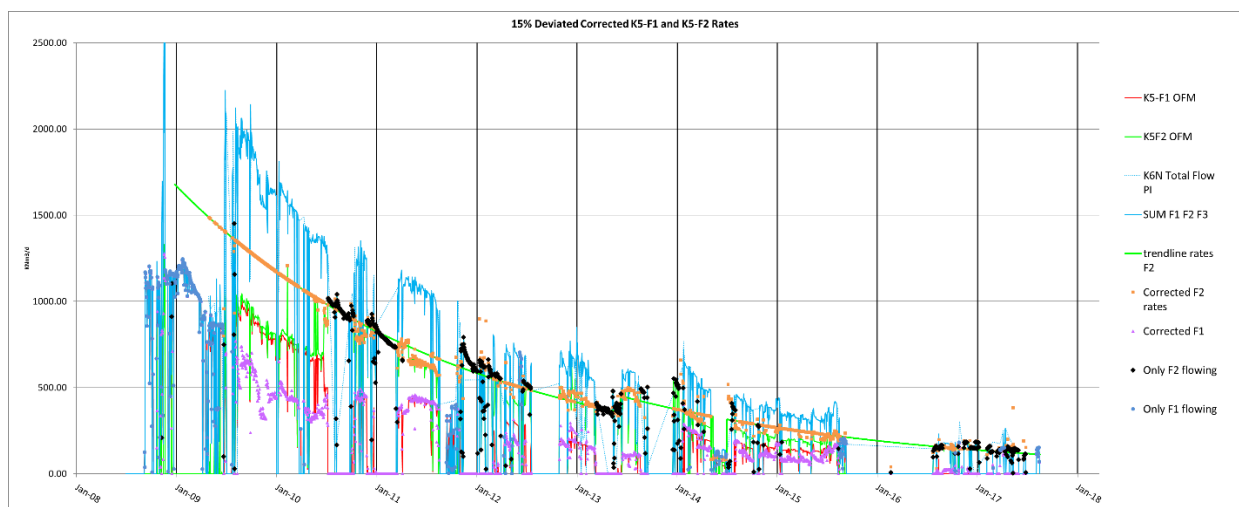
Figure 18: Production split with 15% deviation from the trendline. K5-F1 production indicated in purple, K5-F2 production indicated in orange.

23

4.3 Water production split

The flow meter at platform level records all of the production through the pipeline whether it is gas or water. As the field starts producing water from 2011 onwards it was necessary to determine a water production split as well. Figure 19 shows the recorded K6-N water volumes originating from the K5-F field. Here the red points resemble the water production registered by the flow meter and the blue dots the water production based on the corrected production history.
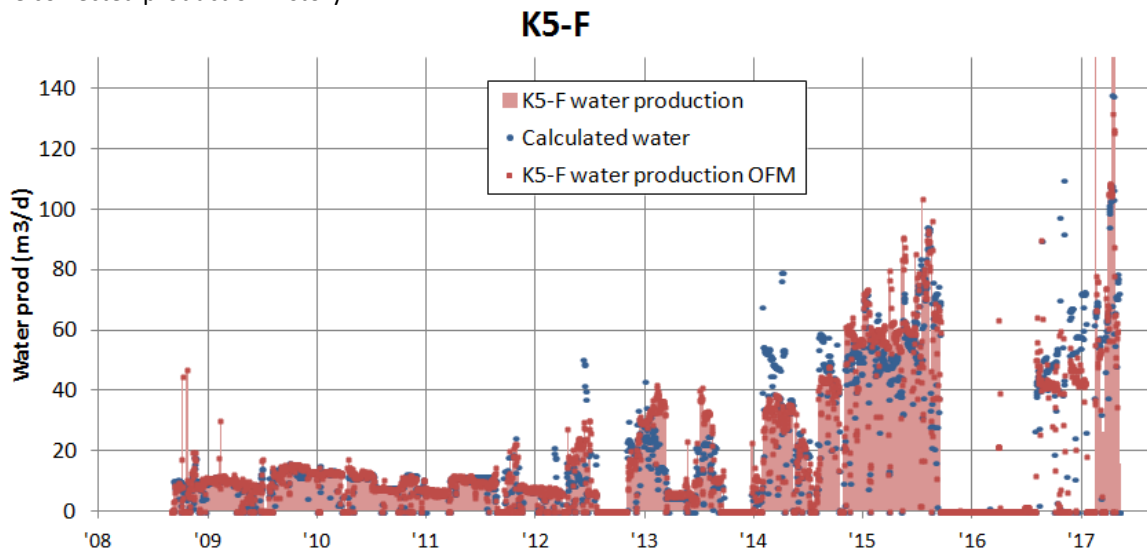
Figure 19: K5-F recorded and calculated water production over time.

The same trendline principle and therefore new gas production split was used to calculate the water volumes produced per well. Figure 19 shows a gradual increase in water production over time. Figure 20 shows the water gas ratio (WGR) calculated based on the corrected production history for K5-F1 and Figure 21 shows the WGR trend for the K5-F2 well.

Figure 20 verifies the hypothesis that K5-F1 is the first well to show water breakthrough from seen in June 2011 where after an exponential increase in water production is seen. Approximately 2,5 years later than K5-F1, K5-F2 shows water breakthrough at the end of 2013 as shown in Figure 21. K5-F1 and K5-F2 shows a similar exponential increase in water production, where this increase is steeper for K5-F2.
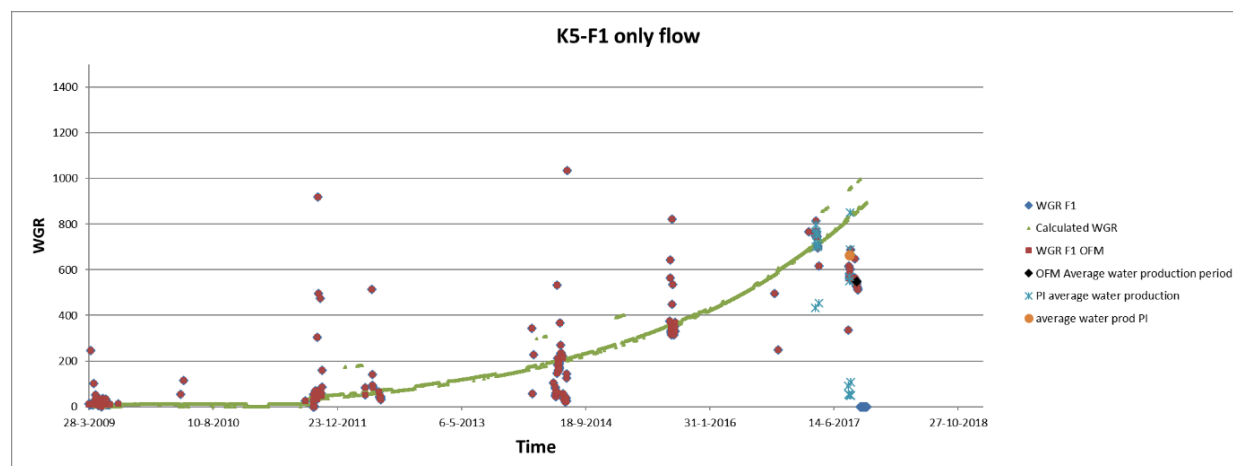
Figure 20: Water Gas Ratio change over time with the corrected production history for K5-F1.
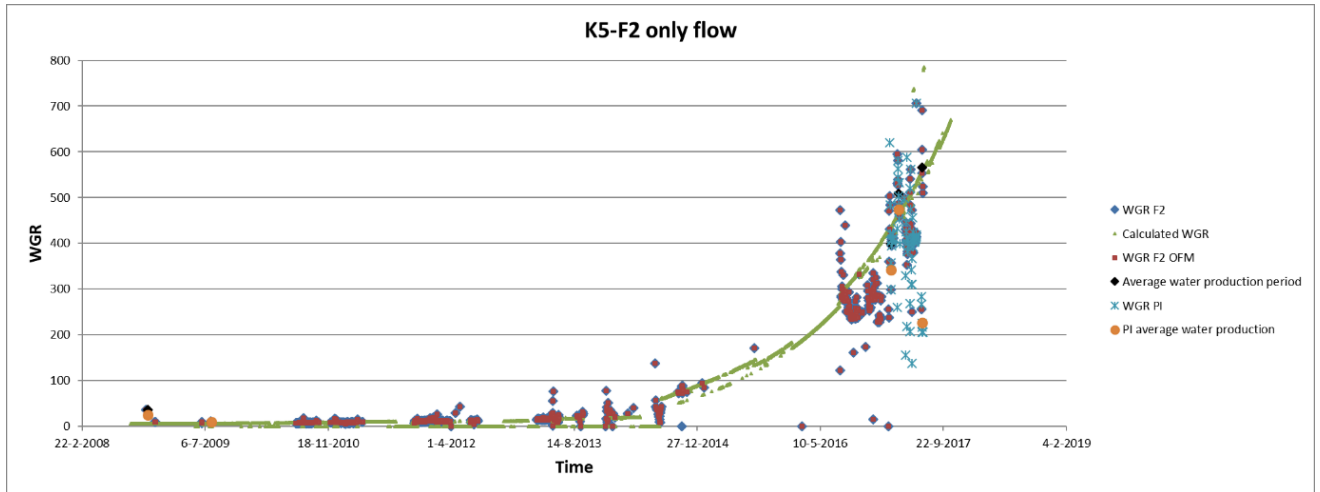
Figure 21: Water Gas Ratio change over time with the corrected production history for K5-F2.

For further analysis and for building a reservoir model it is important, to incorporate the gas and water production trends and to also understand the reservoir geometry and interconnectivity characterizing this production. Figure 22 shows the structural contour map of the K5-F field. This figure shows that K5-F1 and K5-F2, and K5-F2 and K5-F3 and different geological panels separated by large faults indicated by the black lines. This faults shown in this contour map were previously thought to be sealing with zero communication between the K5-F1, K5-F2 and K5-F3 panels. The seismic data shown in Figure 22 shows that K5-F2 and K5-F3 are likely not in communication as they do not share a fault place. However, through close analysis of the pressure data there is a chance that K5-F1 and K5-F3 are connected if the fault separating the two fields is open. One way to check this is through interference tests. Figure 23 shows the bottomhole pressure (BHP) and wellhead pressure (WHP) gauge data registered in the K5-F3 well during a period where only K5-F1 was producing. During this production time, the K5-F3 BHP and WHP pressure drop approximately 1 bar. This pressure drop is evidence of communication between the K5-F1 and K5-F3 panel dismissing the hypothesis that the three reservoirs are not in communication together.
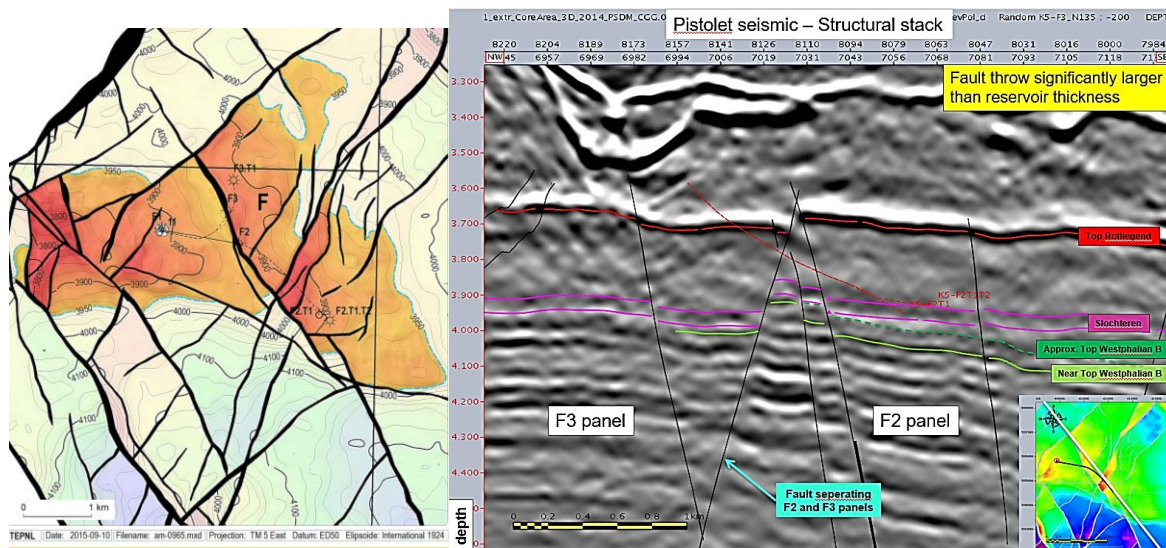
Figure 22: Structural Contour Map of the K5-F field and the K5-F1, K5-F2 and K5-F3 panels (left) and seismic cross section map showing the K5-F3 and K5-F2 separation (right).

25
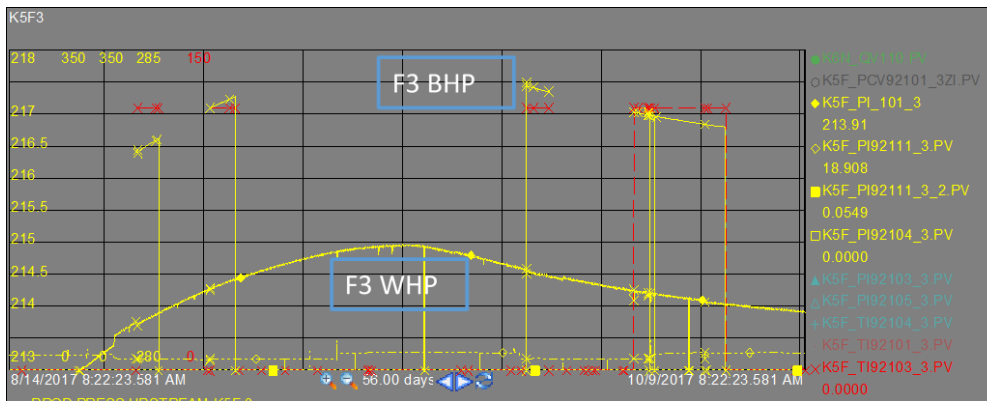
Figure 23: WHP and BHP change in K5-F3 during a period in which only K5-F1 is producing

4.4 Sensitivity & Uncertainty

This paragraph tries to grasp the uncertainty and sensitivity of the production split. Here most of the uncertainty lies at the basis of where and how the measurements are taken or stored, the measurement instruments or conversion errors. The relative uncertainty on the bottomhole pressure and flow rate gauges and rates in the field has been approximated at +/- 5%. (Blandamour H., 2013) As previously mentioned, data storage is something that has been wrong in the past. This is also shown in Figure 13 where large peaks in production were proven to be erroneous data storage where sometimes production data would be stored twice.

Another issue with data is the data source itself. Not all of the recorded data is stored, only a few data points within a day are stored. However, when pulling data from one of the databases, data from any time within the day can be requested. If the requested time is different from the time of the saved data point, the database will extrapolate the data based on the two data points closest to the requested one. This can mean that the same requested data could differ per extrapolation meaning that the corresponding values can differ per request.

Another uncertainty lies at the determination of the water gas ratio. Since this is based on the corrected production history, all of the previously mentioned uncertainties are incorporated in the water gas ratio as well. The water gas ratio used during this research is calculated through a trendline which is estimated based on the average water production when only one well is producing. This trendline is estimated by the user and is therefore prone to human error. To reduce some of the uncertainty this principle was applied to all of the data sources available within TEPNL. The database associated averages per data source are shown in Figures 20 and 21. However, when a well produces for a longer time, more data becomes available which can lead to new insights into well behavior. An example of this is shown in Figure 21 where the new production data shows that the previously used trendline for water gas ratio calculations does not fit the production data. Which is why a new trendline was estimated and applied.

5. Well Test Analysis

The aim of well testing is to gain information about a well and reservoir. To get this information, the well flow rate is changed and this change disturbs the pressure in the reservoir. Measuring this change in pressure over time and interpreting this gives information about the average properties of the part of the well involved in the compressible zone such as permeability, facies heterogeneities and enables identification of barriers. In the well test analysis it is assumed that the reservoir is homogeneous, isotropic with a constant thickness distribution throughout the reservoir limited by impermeable boundaries.

The new production split affects the whole production history of the field which makes it important to reanalyze all the previous models including the well tests. During the well testing of a gas well, pressure build up data is gathered by shutting in the well and letting the pressure increase naturally.

The analysis of the pressure increase over time can determine important reservoir characteristics which are fundamental in building the reservoir simulation models. Additionally, the influence of a new production history was studied in which new derivative curves are compared to old derivative curves.

5.1 K5-F1 Well Tests
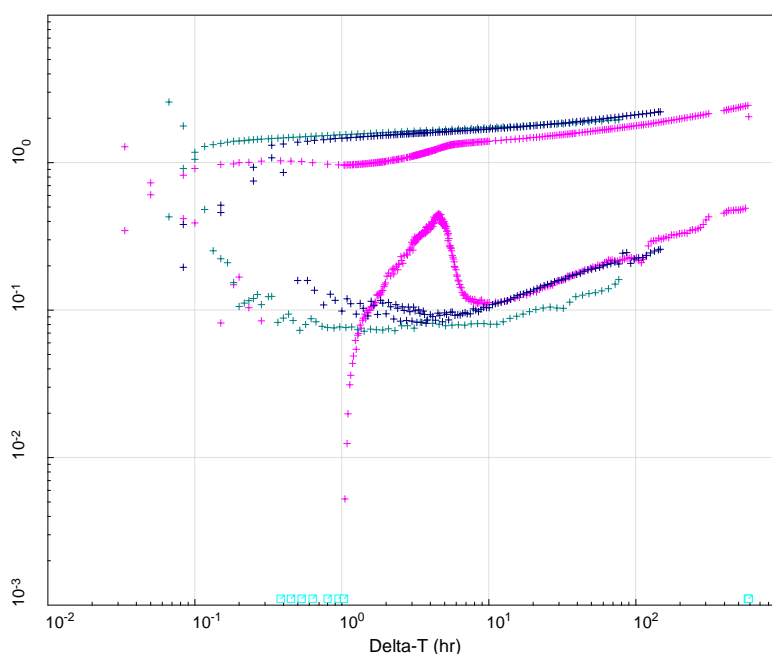
Figure 24: Derivative plot with data from all the different pressure build up data available for K5-F1 with the pink data points from the pressure build up from September 2011, blue from January 2010 and green from April 2009.

Figure 24 shows the different derivative plots of the pressure build up tests with the new production history. Known reservoir parameters are used as input data in PIE where the reservoir thickness from logs is set at 27,2 meters, gauge depth at 3228 meters and reservoir depth at 3900 meters. For K5-F1 there were two usable data sets for pressure build up analysis, one originating from April 2009 and the other from January 2010. The other data sets were all too erroneous due to incomplete data sets or pressure build up interruptions as shown in Figure 24 by the pink data set from September 2011. This interruption is caused by water dropping down the wellbore, disturbing the pressure signals.

From seismic data the field shows a lot of faulting as previously indicated by the contour map in Figure 22. Through PIE well testing software the influence of the faults in the area can be studied. Here the reservoir geometry and well trajectories are incorporated in the software as they require different calculations to be performed. The analysis for the K5-F1 pressure build up data was performed with a type curve model for a

vertical well and homogeneous radial reservoir characteristic and tested with the following boundary possibilities:

- No boundary
- 1 boundary
- 2 boundaries
- 3 boundaries.

From these different analyses it was found that the best match was obtained with the 3 boundaries setting. One boundary at a distance of 100 meters, a second at a distance of 700 meters and a third at a distance of 230 meters. The pressure build up analysis is shown in Figure 26 with on the left the derivative curve, in the middle the history match based on the derivative analysis and on the right the superposition plot. When comparing these distances with the contour map they are found to coincide with the faults closest to the K5-F1 well as shown in Figure 25.
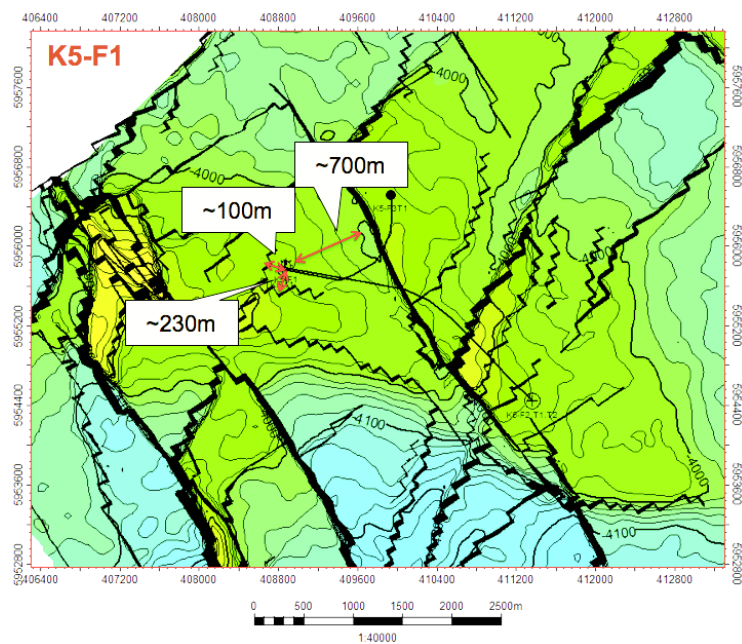
Figure 25: Fault map of K5-F block with focus on the K5-F1 well and the three well test analyzed boundaries
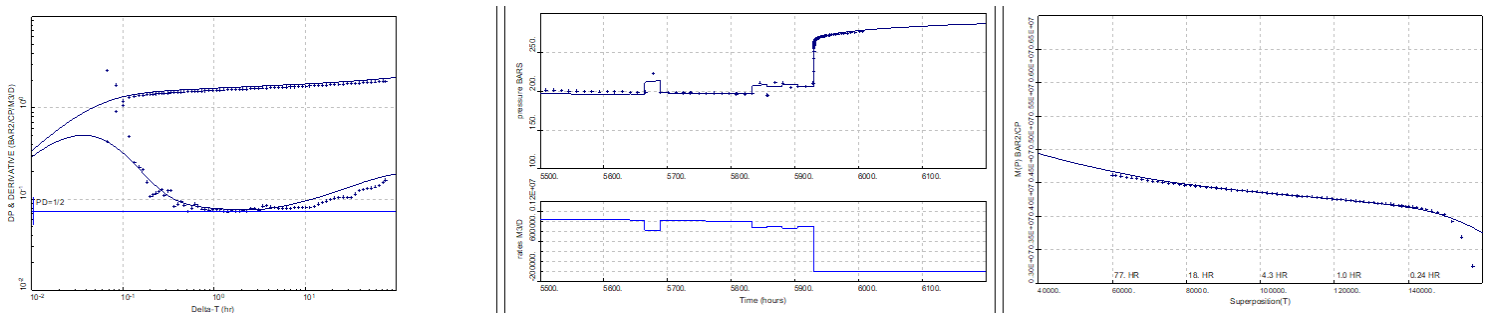
Figure 26: April 2009 well test analysis with 3 boundaries at 100m, 700m and 230m away. The derivative was matched with a wellbore storage of 0.14 m3/bar, reservoir permeability of 12.9 mD, initial pressure of 347 bar, reservoir thickness of 27.2 m and a skin of 3.9.

The pressure build up data from April 2009 allowed the first well test analysis to be performed for this well, the analysis results from this test were applied to the well test of January 2010 as a verification of the analysis results. When the analysis results also apply to the data gathered from the pressure build up in January 2010, it can be stated that the results are valid. The results of the pressure build up analysis are shown in Figure 27 with on the left the derivative plot, in the middle the history match based on the analysis results and on the right the superposition plot which is acting as a third quality check plot. Superposition describes the pressure in a reservoir

when several flow rate variations occur. Here the pressure variations due to flow rate changes are equal to the sum of the pressure drops due to each flow rate.

It was found that the same input and results from the 2009 analysis matched the well test from 2010, validating the results. The only difference with the pressure build up analysis of April 2009 is a lower initial pressure, which is normal as the reservoir is further depleted.
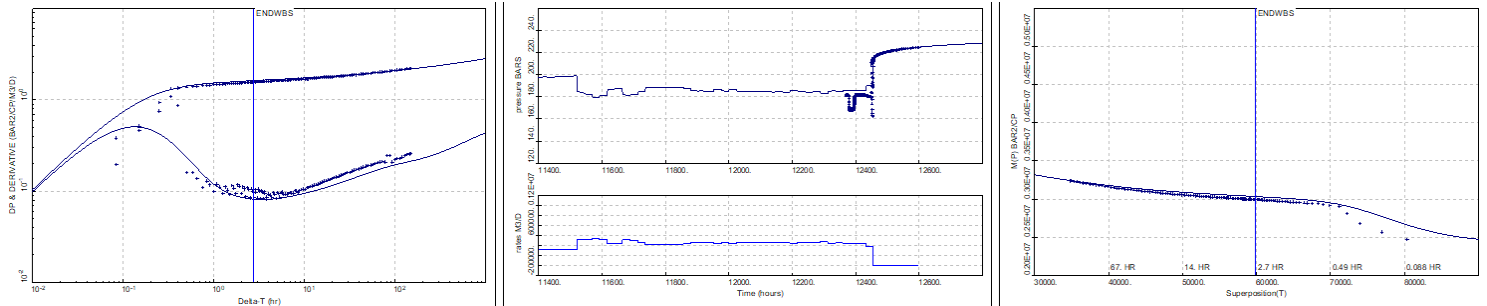
Figure 27: January 2010 well test analysis with 3 boundaries at 100m, 700m and 230m away. The derivative was matched with a wellbore storage of 0.56 m3/bar, reservoir permeability of 12.9 mD, initial pressure of 297 bar, reservoir thickness of 27.2 m and a skin of 4.

For the pressure build up data from September 2011 it was impossible to find a match since the well was opened during the build up phase of the test which interrupted the pressure build up. This disruption in data makes any interpretation results unrepresentative. The results of the two pressure build up analyses are shown in Table 1.

Parameters	2009	2010
Skin	3.9	4
Permeability	12.9 mD	12.9 mD
Initial pressure	347 bar	297 bar
Distance faults x direction	100m & 700m	100m & 700m
Distance faults y direction	230m	230m

Table 1: Well test analysis results K5-F1

5.2 K5-F2 Well Tests
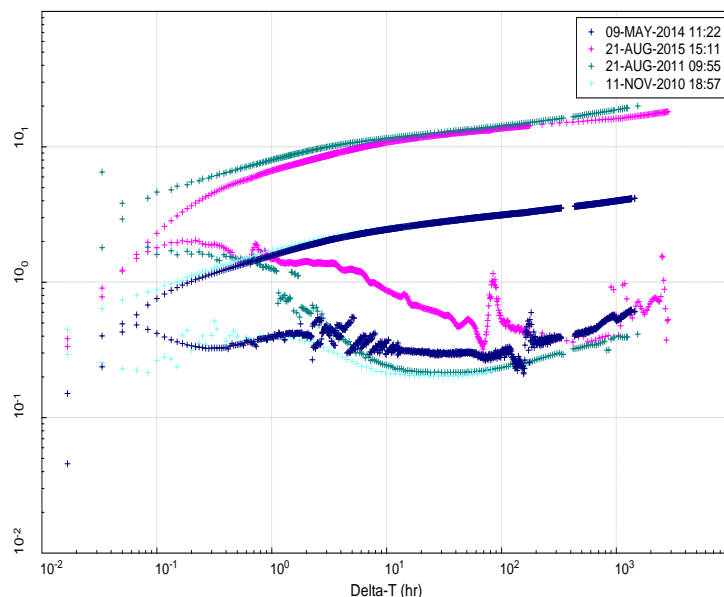
Figure 28: Derivative plot with all the different pressure build up data available for K5-F2 with Light Blue data points from the pressure build up in November 2010, Green from Augustus 2011, Dark Blue from May 2014 and pink from 2015).

K5-F2 has more pressure build up data sets available than K5-F1 which helps to create a better understanding of the reservoirs behavior over time with a higher accuracy. Figure 28 shows the pressure build up derivative
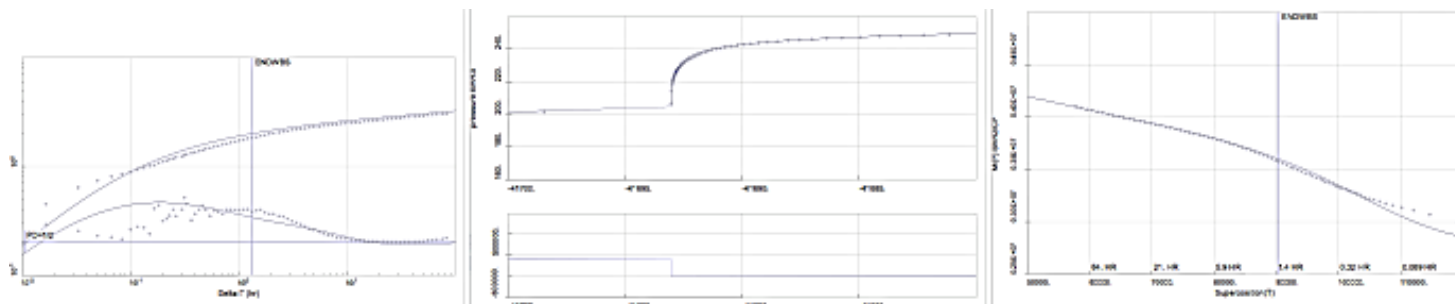
curves of the available data sets overlain on one another. Here one can see a clearly see a change in reservoir parameters and therefore characteristic, such as permeability and skin, between the pressure data from before 2011 and after 2014. The pressure build up analysis per data set will be shown individually to show this change more clearly.

Figure 29: Pressure build up data from November 2010 without boundary. The derivative was matched with a wellbore storage of 0.16 m3/bar, reservoir permeability of 7 mD, initial pressure of 285 bar, reservoir thickness of 18 m.

The best match for this build up was found to be without the influence of boundaries and a skin of -2.3 and a permeability of 7 mD. These analyses were performed with type curve models for horizontal wells and a radial, homogeneous reservoir as shown in Figure 29.

Figure 30 shows the fault map of K5-F2 where multiple faults are visible. For the pressure build up of August 2011 a best fit was found to have one boundary at a distance of 350 meters. The well test analysis performed with PIE well test software is shown in Figure 31.
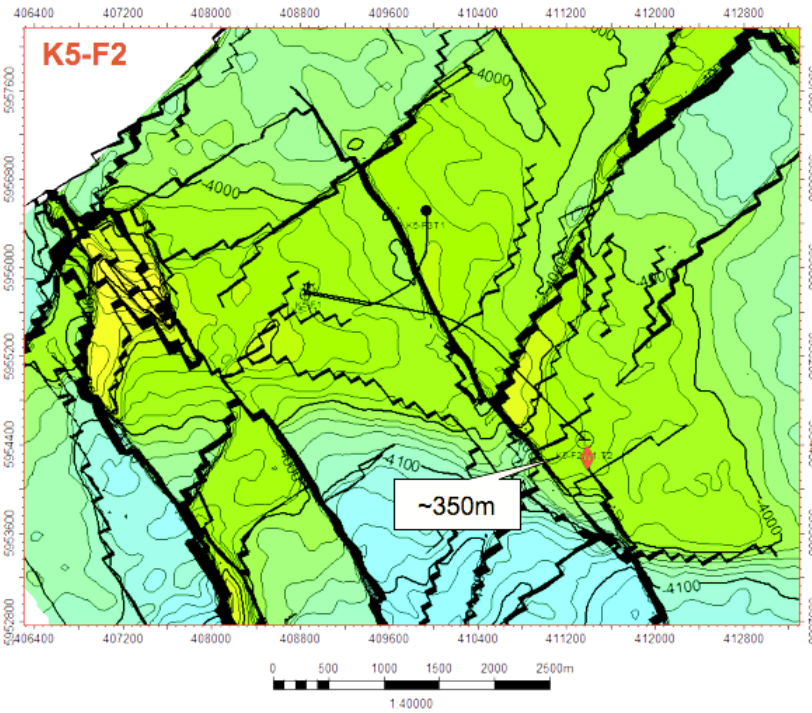
Figure 30: Fault map of K5-F block with focus on the K5-F2 well and the well test analyzed boundary at a distance of 350 meters.
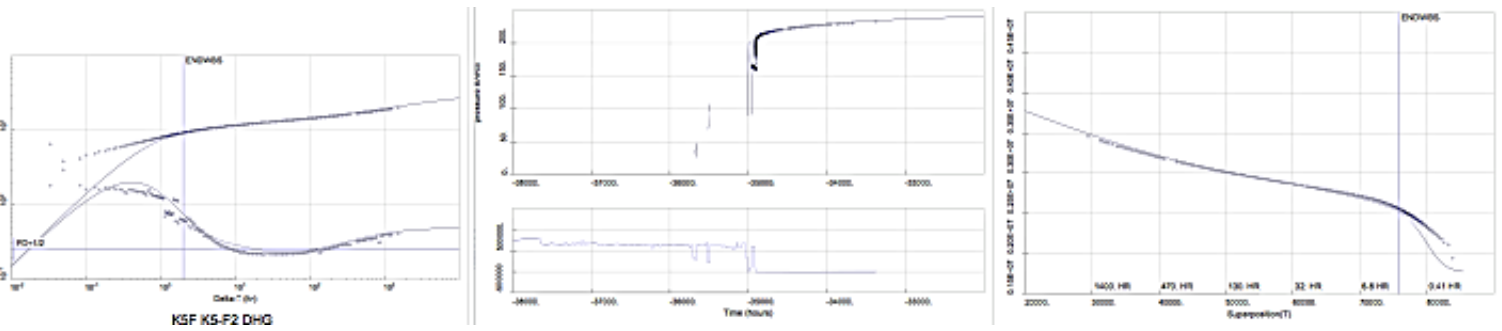
Figure 31: K5-F2 August 2011 with a boundary at 350 meters away. The derivative was matched with a wellbore storage of 0.16 m3/bar, reservoir permeability of 5.5 mD, initial pressure of 269 bar, reservoir thickness of 18 m.
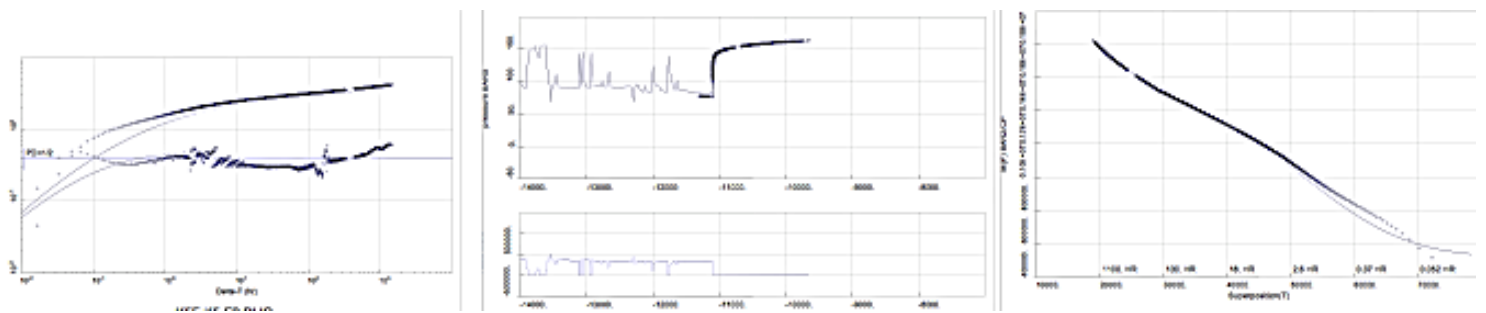
Figure 32: Pressure build up data analysis for K5-F2 June 2014. The derivative was matched with a wellbore storage of 0.71 m3/bar, reservoir permeability of 3.7 mD, initial pressure of 202 bar, reservoir thickness of 18 m.
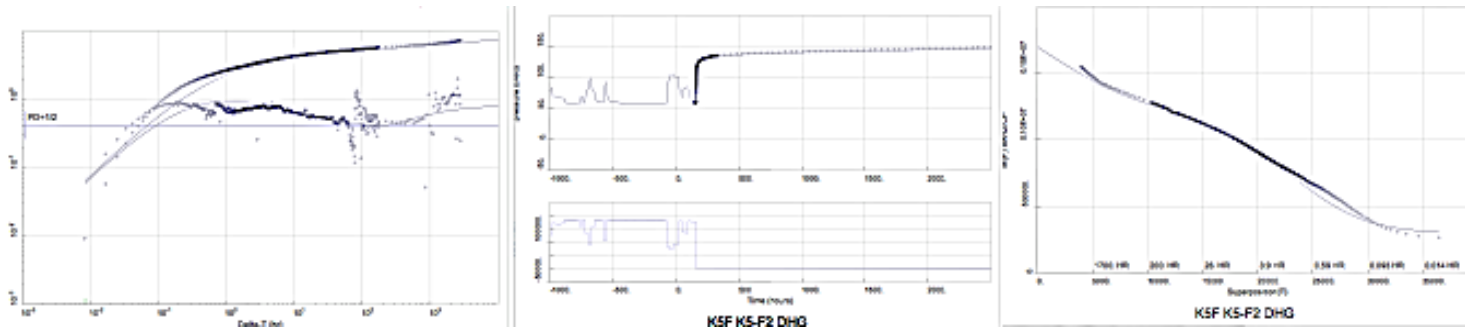
Figure 33: Pressure build up analysis for K5-F2 December 2015. The derivative was matched with a wellbore storage of 0.80 m3/bar, reservoir permeability of 2.5 mD, initial pressure of 170 bar, reservoir thickness of 18 m.

Parameters	2010	2011	2014	2015
Skin	-2.3	-2	-3	-2.4
Permeability	7 mD	5.5 mD	3.7 mD	2.5 mD
Initial pressure	285 Bar	269 Bar	202 Bar	170 Bar
Distance faults	-	350 m	350m	350m

Table 2: Well test analysis results K5-F2

Figures 31, 32 and 33 show the analysis of the pressure build up data from 2011, 2014 and 2015 respectively. Table 2 summarizes the analysis parameters of the well tests well one can clearly see a decline in reservoir permeability.

5.3   Uncertainty

Well test data is very dependent on the stability of the pressure increase throughout the pressure build up. Pressure response is interpreted after the effects of the wellbore storage have ended after which the signal is deeper in the reservoir. This signal is then likely to be in a different zone and can have a different resulting permeability value. The permeability value resulting from the analysis is dependent on the stability point chosen in the derivative plot. Stability in the derivative plot gives the kh value, therefore, when such a stable point is not very visible due to the presence of boundaries, an unrepresentative permeability value can be calculated. If one wants to know the depth of investigation, only permeability is used meaning that your height is important for determining the distance of any boundaries. However, the height is normally not well defined and approximated through pay summaries which is not necessarily the same as the production height.

6 IPM Workflow

Relationships between the observed and simulated parameters are not linear and very complex. The optimization of a simulated model is a minimization of the mismatch making it an inverse problem. These observed parameters include production rates, downhole pressure data, downhole temperature data and choke settings. Simulated parameters that are considered to have a high level of uncertainty include faults and fault transmissibility, connectivity, porosity and permeability. The simulation models are used to generate reliable production forecasts, where the reliability of the prediction is strongly influenced by the accuracy with which the input data and reservoir properties are determined. The simulation program used for this research is a threefold modeling system referred to as IPM which is short for Integrated Production Model. IPM encapsulates systems which incorporate the mass balance of the reservoir, the reservoir characteristics and reservoir dynamics. The workflow used for the development of the K5-F field model is depicted in Figure 34.
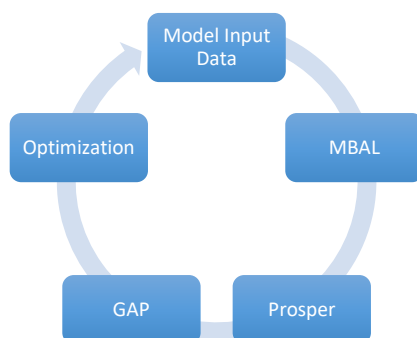
Figure 34: IPM workflow model input data (Montopoulos, 2015)

6.1 Model Input Data

The usual approach to this is to first estimate the reservoir parameters and properties, compute the past field history for reservoir pressure and production volumes and then validate this computation by comparison with observed field data. If there is no match between the data sets, then the reservoir parameters or properties are re-adjusted until a satisfactory match is found. Here it is important to change the parameters and properties to represent realistic values so as not to create an unrealistic model.

To simplify the inverse problem 4 assumptions are made (Experts, 2007):
1) The distributions are Gaussian;
2) Initial reservoir models are correct to some extent;
3) Measurements always contain Gaussian noise;
4) Simulator numerical model is correct.

6.2 Technical Input Data

The technical input data required to develop this model is based upon the following:
- Geological models and geological data
- Core sample data
- Historical production data
- PVT data of the fluid of the K5-F field and neighboring fields
- Pressure and temperature data from wells in both static and dynamic status
    o Initial reservoir pressure
    o Flowing well head pressure (WHP) and well head temperature (WHT)
    o Bottom hole pressure (BHP)
    o Pressure build up test
- Water analysis and gas analysis data
- Production downtime
- Compressor data

6.3 Sensitivity & Uncertainty

Data quality plays a large and important role within the development of a model since it dictates the accuracy of the model, the efficiency and effectiveness of its development. The studied data that was found to be incorrect was removed prior to modelling. This was done through data comparison from all the different databases used with TEPNL and in depth analysis of this recorded data. This rigorous data analysis prior to modeling helps to remove inaccuracies, erroneous gauge data and helps make decisions on which data to use and which to leave out. This was especially the case in this research as multiple databases and sources were available.

Through close examination of the available data it was found that the data values from PI Processbook change, especially when using data older than 1 year. The PI system saves data points up to a maximum of 8 years. The system does not save all the data points within a day but saves only a few values per day. This means that data taken on a day, at a different time than the exact moment the value was saved in the system, PI will extrapolate a value for the requested time based on the data points saved. This extrapolated value results in changes in PI data, and therefore inaccuracies. To try and limit the inaccuracy, it was decided to take data from each database system at the same time each day, in this case 06:00 am. By keeping the time the same in each database, a comparison between data values is possible. K5-F1 and K5-F2 are older than 8 years, so data that was gathered in Excel sheet by other engineers had to be used for the first 2 years of production life since this data was no longer available.

7 Reservoir Model Development – MBAL

One of the fundamental laws reservoir engineers adhere to is the law of mass conservation. The material balance used for reservoir analysis is also based on this fundamental law which allows calculations for reservoir parameters such as the size and type of an aquifer or the hydrocarbons originally in place. Through these calculations, historical production behavior can be imitated and a reservoir model can be made.

The equation for material balance is derived as a volume balance which compares the cumulative observed production volumes with the expansion of reservoir fluid due to a finite pressure drop (Drake, 1978). This equation is based on a theoretical tank model which does not take into account the reservoirs actual location or geometry.

7.1 Workflow

The general workflow used when building an MBAL model is depicted in Figure 35. In MBAL each reservoir is defined as a tank. To obtain the reservoir pressure behavior over time for each tank an arithmetic average of the observed pressure data is computed using the mass balance software. The average pressure is taken over a short period of time at which the wells were shut in giving a stable pressure reference point. In the soft sensing of the pressure data the following steps were taken (Ambasyha, 1990):
- Well model matched to well test;
- If bottomhole pressure is available, then the reservoir pressure is estimated by adjusting the productivity index(PI). Here it is important to make sure that the flowrate is matched to the bottomhole pressure within a margin of 5%;
- If bottomhole pressure is not available, then the reservoir pressure is estimated by first calculating the bottomhole pressure using correlations and after altering the PI data to make sure the flowrate and bottomhole pressure match within a 5% margin.

A next step is to perform a linear regression on the parameters with the highest uncertainty per tank. The parameters, which are considered known, were excluded from this process. Known parameters for K5-F are water saturation and porosity.

A simulation of the model was done to verify the quality of the match. Here, essentially, mass balance equations are used with the reservoir flow rates as input value so that the reservoir pressures can be back calculated for each tank. Well estimated input parameter values result in a properly history matched model. The difference between the simulated reservoir pressure and the measured reservoir pressure should be small between +/- 2-5%.

In MBAL two different tank model constructions were designed which are meant to symbolize the K5-F field and its reservoirs. Here, the hypothesis about the communication between K5-F1 and K5-F3 can be tested as well as the reservoirs geometries. In order to reduce the confusion between the reservoirs and wells, their model, characteristics and results will be discussed in separate sections.

The model for this field previous to the start of this research was based on the idea that none of the wells are communicating and therefore designed as three individual tanks. Due to the pressure drop seen in the K5-F3 reservoir while only K5-F1 was producing in the area has invalidated this hypothesis which has led to the development of a new MBAL model as seen in Figure 36.

The old input data was replaced with data based on the new production split. Monthly production volumes were calculated and the according monthly water-gas ratios where inserted to calculate the historical reservoir pressure and water production for each given tank. When more information and insight was gained the model was adjusting accordingly to match the observed behavior. The adjustment are made by carefully changing the parameters excluding the known parameters.

When the observed data, reservoir pressure and water gas ratios matches the simulated data within a margin of ~1% the designed MBAL model can be considered a valid imitation of the mass conservation for the field. This model will then form the basis for the next step in building the reservoir model. This process is based on trial

and error as very little is certain about the connectivity between the tanks and its size, presence and connectivity of aquifers.

It is important to bring to attention that parameters such as initial gas in place, permeability, reservoir thickness and porosity for the South and Central tank were not allowed to iterate during the regression as they tend to grow out of proportion giving unrealistic geological results. Relative permeability curves, which are representative of the tank models, were found to have the largest influence in calculating the corresponding phase volumes of gas and water.
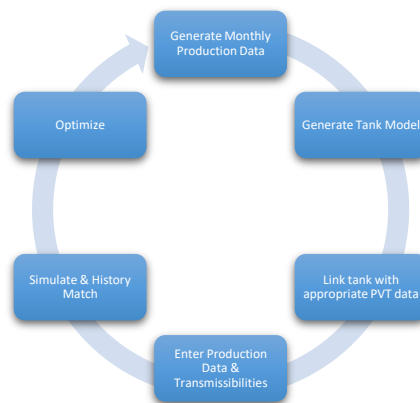
Figure 35: Workflow MBAL

7.2 Assumptions and Considerations

The tank model used in this research is shown in Figure 36. For the design of the model the following assumptions were made (Experts, 2007):
- Homogenous pore volume
- Gas cap
- Aquifer
- Constant temperature
- Uniform pressure distribution
- Uniform hydrocarbon saturation distribution
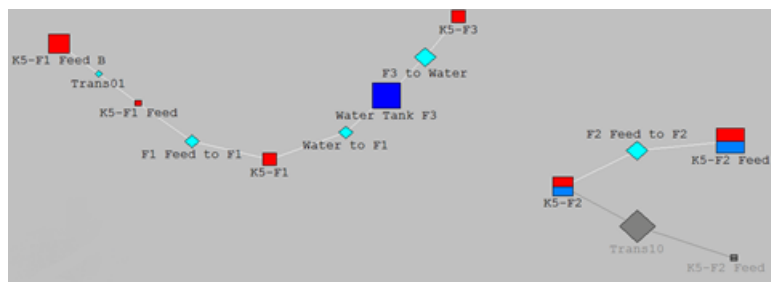
Figure 36: Theoretical Tank Model of the K5-F field.

Reservoir compartmentalization

The MBAL software does not incorporate reservoir location or general geometry which means that the drainage radius parameter carries extra importance in determining the no flow boundaries. In this model, it was impossible to find a match in reservoir pressure for K5-F1 and K5-F3 within a 2-5% tolerance margin without segmenting the K5-F1 reservoir. Without segmentation the pressure decline within the first 5 - 8 years was impossible to match, whereas the late phase was matched or vice versa. The structural contour map shown in section 4.3, shows that the K5-F1 panel has some internal faults which could act as segments, and therefore an increased slow gas supply to the system. When implementing this segmentation in MBAL a match over the entire production lifetime was possible. Here, the MBAL program assumes that the properties such as porosity and

permeability of each tank are constant but one can change the transmissibility between each segment. This allows a relative precise definition of the slow gas supply to the well.

7.3 Material Balance Equation and Important Parameters

The material balance equation is related to the volume balance where the amount of gas originally in place is equal to the amount of produced gas. Here the gas that remains in the reservoir at any pressure expands to fill the volume initially occupied. The equation for a closed gas reservoir can be written as follows (Kleppe, 2017):

$$GB_{g1} = (G - G_p)B_g$$

Where G is the gas initially in place, B_{g1} is the initial gas formation volume factor, Gp is the cumulative gas produced and Bg is the formation volume factor for gas at pressure p. Substituting for Bg from the gas law while temperature is assumed to be constant result in (Moghadam S., 2011):

$$\frac{p}{Z} = \frac{p_i}{Z_i}(1 - \frac{G_p}{G})$$

Plotting ($\frac{P_i}{Z_i}$) against G_p for K5-F1 and K5-F2 gives the following graphs. With these graphs an estimation of the volume of gas initially in place can be made. The visualization of the pressure depletion over time can also help identify deviations from the expected pressure decline curve for a volumetric reservoir.
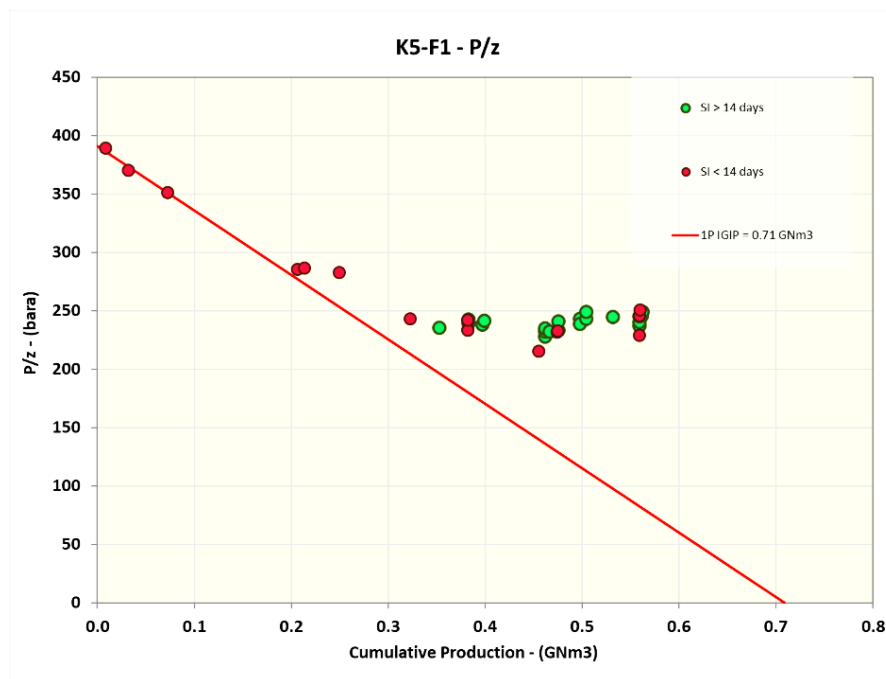
Figure 37: K5-F1 P/z plot

Figure 37 shows that K5-F1 has a clear deviation from the linear trend. This is a common indicator for an external pressure support which trend is common for water driven reservoirs. Waterdrive reservoir are characterized by a flat pressure response after some depletion (IHS Inc, 2014), in which an aquifer provides pressure support through water encroachment into the gas reservoir.

The deviation from a linear trend strengthens the hypothesis of the presence of an active aquifer pressure support. In gas reservoirs with an aquifer the rate of the gas withdrawal is directly proportional to the water encroachment. When the gas rate is high and the aquifer is strong, the chance of early water breakthrough is high due to coning (Kabir, 1983). The gas volume is reduced by the net volume of water influx when water starts invading the gas reservoir while maintaining reservoir pressure. This must also be reflected in the material balance equation (Moghadam S., 2011):

$$\Delta V_{wip} = 5.615(W_e - W_pB_w)$$

Where W_e is the encroached water, W_p the produced water at platform level and B_w the formation volume factor of the water (5.615 is a constant applied when using oilfield units). Assuming there is no water injection,

solubility of gas in water and the compressibility of rock and water are negligible, the general material balance equation can be reduced to (Moghadam S., 2011):

$$GB_1 = (G - G_p)B_g + 5.615(W_e - W_pB_w)$$

Re-arranging this leads to:

$$G = \frac{G_pB_g - 5.615(W_e - W_pB_w)}{B_g - B_1}$$

The denominator is small in the early stages of production life of the reservoir which can lead to errors in calculating the volume of initial gas in place. Therefore, this calculation should be performed throughout the multiple stages of the field's life cycle.

For K5-F2 this external pressure support is less evident as shown in Figure 38. This can either mean that pressure support visible is from an aquifer that is less strong than K5-F1 or that it is connected to another reservoir.
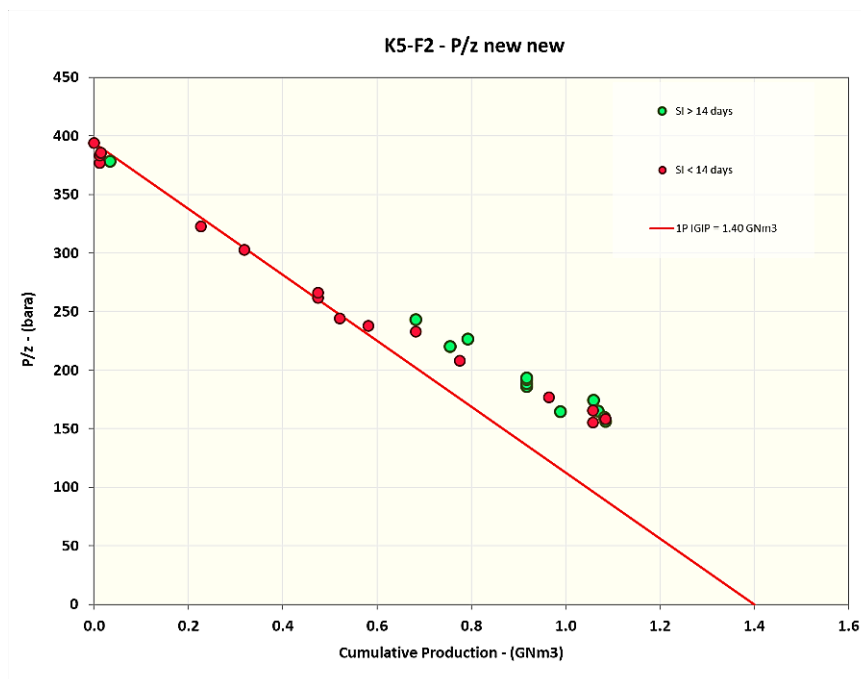
Figure 38: K5-F2 P/z plot

7.4 Relative Permeability Curves

Accurate relative permeability curves carry high importance when simulating a reservoir. In reservoir analysis a full understanding of how oil, and in this case, gas and water flow through porous media is required to create a representative model. The relative permeability curves have the ability to predict changes in phase saturations over time, therefore simulating phenomenon such as water breakthrough and increases in water gas ratios. Relative permeability curves are strongly dependent on rock and fluid properties and can be made specifically for each different sand layer. The relative permeability curves used in this research are derived from available core, well test and log data and are shown in Figures 39 and 40 with their corresponding parameters input values.

The capillary pressure and maximum pressures identify the maximum hydrocarbon saturations (S_{max}) and residual gas saturations (S_{gr}). The log analysis provided the maximum residual gas and water permeability values, krg_{max} and krw_{max}, from the sand layers which had the highest gas and water saturations. The end points were then fixed and the gas and water exponents were varied until the WGR result from MBAL matched the WGR from the field.

The fractional flow equation assumes diffusive flow conditions, where at any point in a linear displacement path, water saturations were uniformly distributed with respect to thickness. Therefore, as the water saturation was assumed to be uniformly distributed, the same was considered for hydrocarbon saturations which allowed for

the flow to be modelled by thickness averaged permeabilities (Drake, 1978). The assumptions behind the fractional flow equation affected the true representation of reservoir behaviour. However, the use of single deterministic values of water gas ratios, obtained at different stages of the wells or reservoir's production life, further affected the accuracy. This provided a deterministic forecast of the water gas ratios until the most recent production history could be used as a fixed value in the development procedure in GAP modeling. Alternatively, fractional flow matching was also performed in MBAL to generate pseudo relative permeability curves.
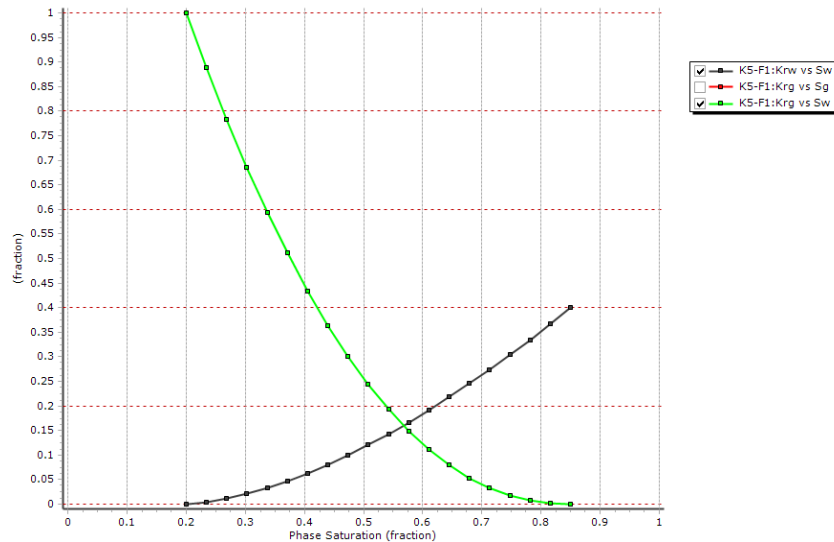
Figure 39: Relative permeability curves for the K5-F1 reservoir

K5-F1	SRES	END POINT	EXPONENT
KRW	0.2	0.4	2
KRG	0.15	1	2
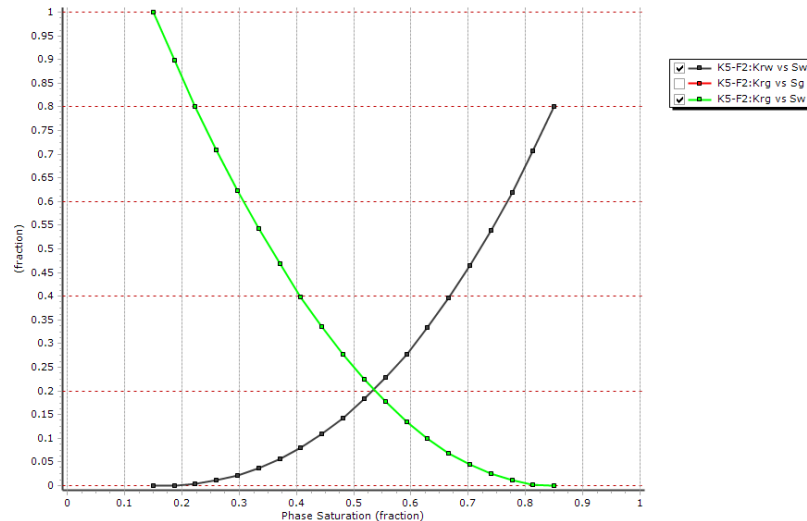
Figure 40: Relative permeability curves for the K5-F2 reservoir

K5-F2	SRES	END POINT	EXPONENT
KRW	0.15	0.8	5
KRG	0.15	1	2.7

39

7.5 Pressure History Matching

For a good pressure match, pore volumes of gas and water are defined to help size the total pore volume and the strength of the aquifer. Simulations are performed incorporating the previously defined parameters and used as input to history match the reservoir pressure change over time.

Firstly, a comparison is made between the average reservoir pressure, simulated well pressures and observed pressure values. The average reservoir pressure data used for quality control are the pressure points at which the pressure was stable for a period of 4 days or longer. MBAL associates a volume withdrawn from the reservoir with a particular pressure. Comparing these simulation results to the observed reservoir pressure points gives an indication of how well the model matches. When the simulated pressures are too low in comparison with observed pressure data, the system is lacking energy which indicates an underestimation in for example the tank volumes. The parameters with the largest influence the pressure match are (Rietz D., 2001):

- Pore volume;
- Permeability;
- Initial gas in place;
- Configuration of the reservoir;
- Compressibility.

After a satisfactory pressure match is found for the entire field, a next step is to match the saturation. The saturation match is dictated by the gas water ratio. The following paragraphs show the results of the MBAL model simulations based on the previous assumptions and calculations.

7.5.1   K5-F1

K5-F1 was modeled as a segmented reservoir, which is in communication with the K5-F3 reservoir through a shared aquifer. This communication through the aquifer is a hypothesis based on pressure changes seen in K5-F3 when only K5-F1 was producing. This hypothesis can be verified through a simulation match in the entire model.

Some degree of trial and error was required when simulating the tank model since little information about the reservoir, aquifer, transmissibility and its connectivity is known. The following figures show the simulation results per tank. Two different scenarios are tested in which modifications are made with regards to aquifer or segmentation.

Scenario 1: Basic K5-F1 reservoir segmentation MBAL model
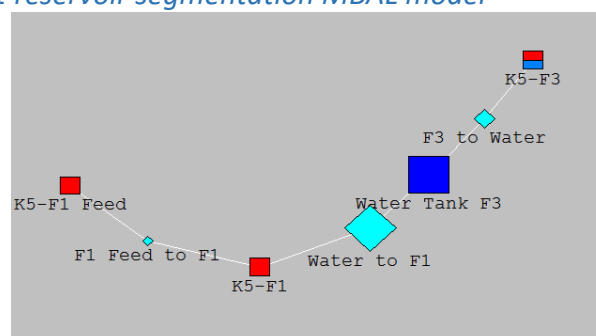
Figure 41: Basic K5-F1 MBAL tank model with connectivity to the K5-F3 reservoir
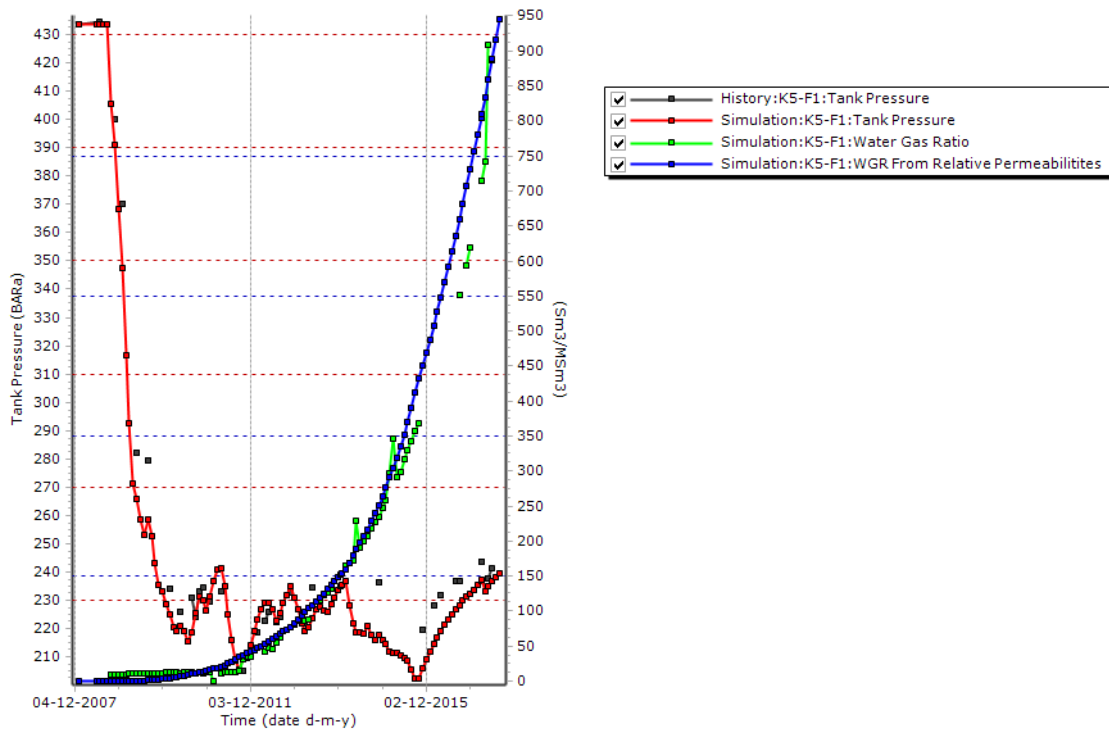
Figure 42: K5-F1 reservoir pressure and WGR reference points vs simulated reservoir pressure and water gas ratio values.
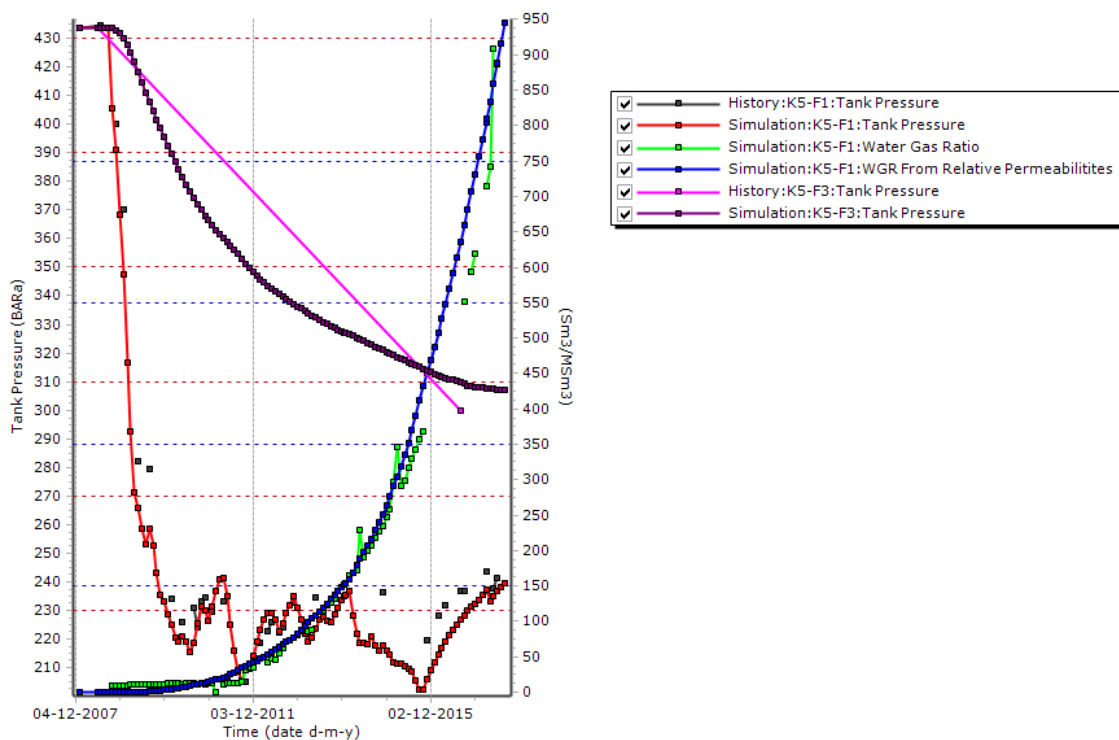
Figure 43: K5-F1 and K5-F3 reservoir pressure measured point vs simulated point. K5-F1 measured WGR and simulated WGR

Figures 42 and 43 show the simulation results between the measured average reservoir pressure reference points and the simulated reservoir pressure values. For K5-F3 there is only one reference point to use as a

measured reservoir pressure point since it has not produced enough for more relevant pressure reference points. From these figures it can be concluded that although there is a relatively good match between measured and simulated data, it is impossible to match the late stage reservoir pressure to the measured data points eventhough the match with the water is good. For K5-F3 the simulated pressure is not within the acceptable margin.

Scenario 2: Best estimate MBAL model with K5-F1 reservoir segmentation
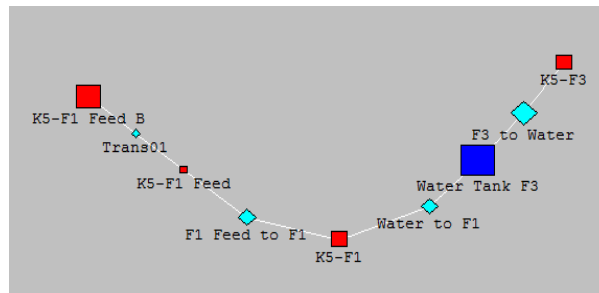
Figure 44: K5-F1 and K5-F3 tank model with K5-F1 reservoir segmentation. K5-F1 is the well, K5-F1 Feed is the first reservoir segmentation and K5-F1 Feed B is the third segmentation.
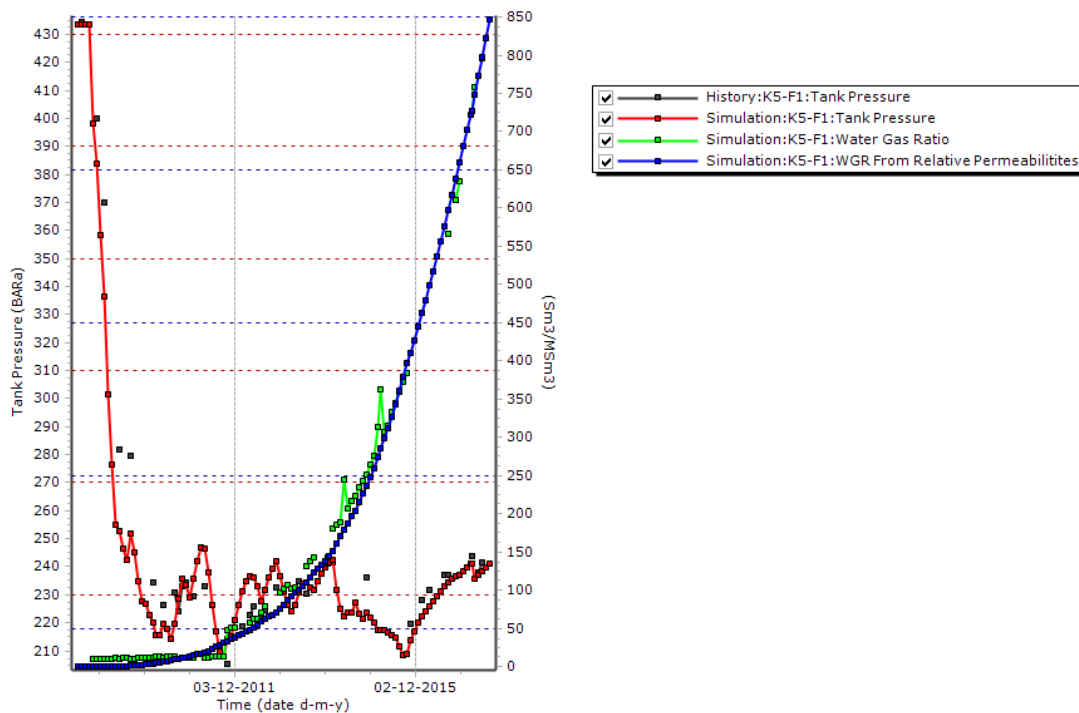
Figure 45: K5-F1 reservoir pressure and WGR measured points vs simulated results with a segmented K5-F1 reservoir.
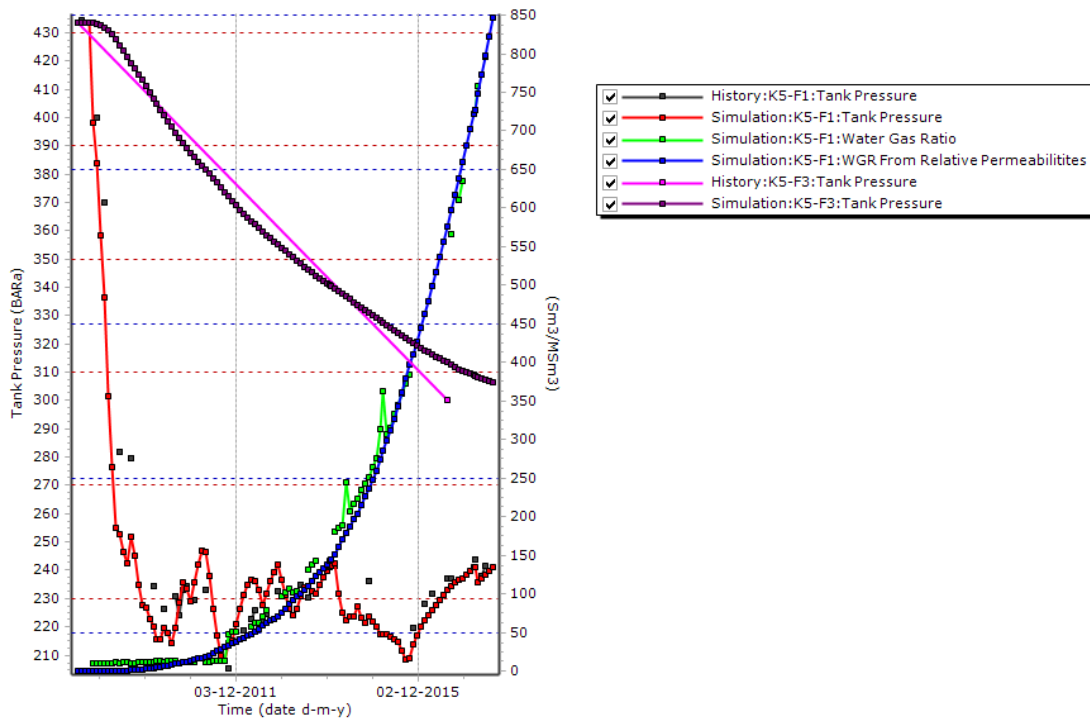
Figure 46: K5-F1 and K5-F3 reservoir pressure measured points vs simulated results and WGR measured and simulated results with a segmented K5-F1 reservoir.

The MBAL model of scenario 2 uses a segmented K5-F1 reservoir. By segmenting the reservoir, it has enables the system to better estimate the pressure change over time in comparison to the previously modelled scenario. Here it was chosen to design a reservoir with three compartments in radial communication with one another. The compartmentalization of the K5-F1 field is shown in Figure 44 where the gas filled tanks are indicated in red and the subsequent transmissibilities per tank modelled in the light blue squares. Aquifers are indicated by the dark blue squares.

7.5.2 K5-F2
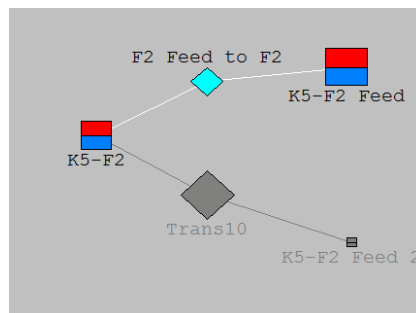
Figure 47: K5-F2 tank model

Scenario 1: Basic MBAL model without K5-F2 reservoir segmentation
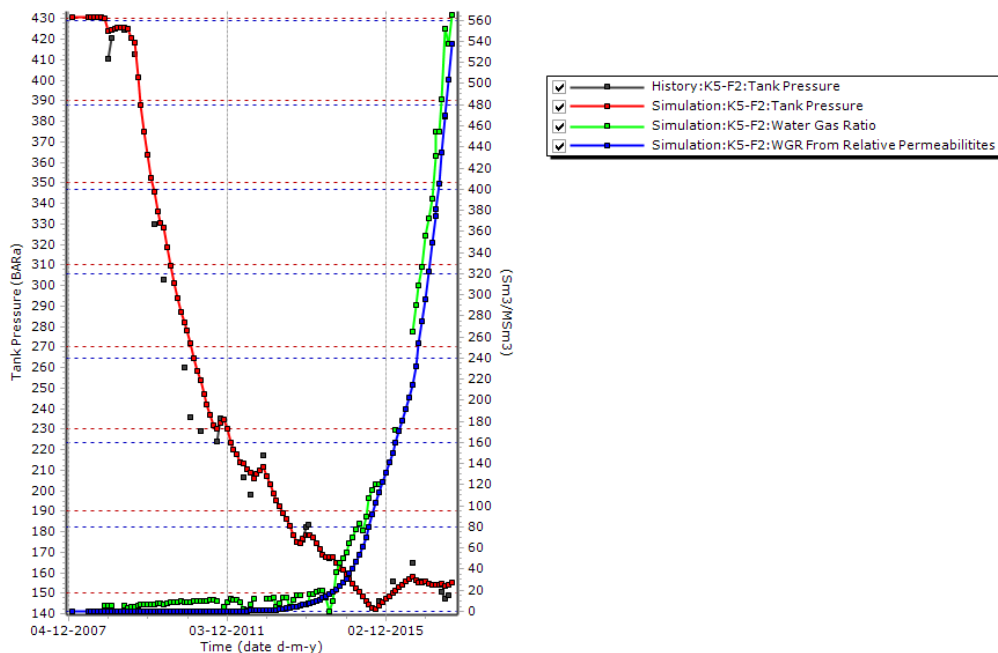
Figure 48: K5-F2 measured vs simulated reservoir pressure and WGR

Figure 47 shows the reservoir geometry of the K5-F2 reservoir and Figure 48 depicts de MBAL simulation results based on scenario 1 mentioned in paragraph 7.5.1 from K5-F1. The results of this simulation show a good match with the observed reservoir pressure and water gas ratio.

Scenario 2: K5-F2 best estimate MBAL model
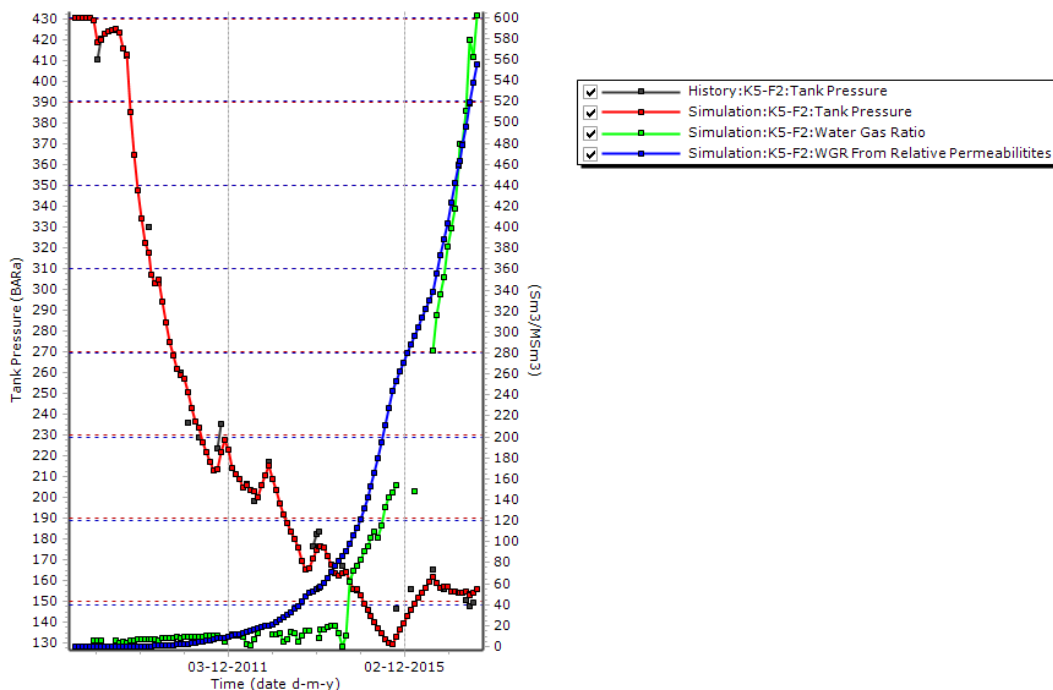
Figure 49: K5-F2 measured points vs simulated match with K5-F1 reservoir segmentation

Figure 49 shows the simulation results from scenario 2 mentioned in paragraph 7.5.1. The reservoir pressure match in this scenario is better than that of scenario 1 which corresponds with the better matched K5-F1 MBAL model.. The water gas ratio is also better matched in the early and late phase.

TANK	T[C]	PI [BARA]	POROSITY	SCW	OGIP [MSM3]
K5-F1 FEED	127	433.8	0.11	0.2	500
WATER TANK F3	127	430.7	0.11	correlation	1e7m3
K5-F3	127	433.8	0.126	0.2	400
K5-F2	127	430.7	0.12	0.15	1000
K5-F3 FEED	127	430.7	0.12	0.15	400

Table 3: MBAL input parameter values from scenario 2

TANK	TRANSMISSIBILITY [M3/DAY*CP/BAR]
K5-F1 FEED TO F1	0.18
WATER TANK F3	4.3
K5-F3	1.5
F2 FEED TO F2	3.5

Table 4: Tansmissibilities of scenario 2 MBAL model

	RESERVOIR THICKNESS [M]	RESERVOIR WIDTH [M]	AQUIFER VOLUME [MM3]	AQUIFER PERMEABILITY [MD]
K5-F2	20	5000	18	10
K5-F2 FEED	20	5000	125	10

Table 5: Reservoir parameters scenario 2 K5-F2

Comparing the two scenarios it was decided that scenario 2 showed a better match and the input values used in this scenario are incorporated in further modelling processes. The values of these parameters are shown in Table 3, 4 and 5.

7.6 Sensitivity & Uncertainty

This paragraphs describes the uncertainty and sensitivity on the developed reservoir model. The shut in bottomhole pressure (SIBHP) needs careful quality checking as this can have a big impact on the linear interpolation used to derive the reservoir pressure. SIBHP carry some uncertainty as the pressure readings can be influenced by the following (Experts, 2007):
- Data usually gathered while surrounding fields are operating;
- If the well was producing at high rates, resulting in a large drawdown, the pressure build up will take longer;
- If the well has been producing for a longer period of time, reservoir pressure has declined and viscosity decreases, the build up will take longer.

If the SIBHP is taken early in the build up phase, the error increases logarithmically. For these reasons, SIBHP points were taken at the moments in time when the well had been unproductive for at least 6 days at which point it is assumed to resemble the reservoir pressure. Additionally, an error of 3 bars is approximated on the reservoir pressure measurement readings (Blandamour H., 2013).

Another uncertainty lies in the definition of the initial gas reserves, aquifer shape and dimensions, petrophysical parameters and boundary conditions as they are unknown making there estimation an uncertainty. (Mesarovic, 1960). There are multiple different internal structures or sets as parameters which can describe the observed reservoir behavior. This means that the initial definition of the reserves cannot be determined uniquely based on past pressure and production reservoir performance. This counts for initial gas as well as water volume estimations (Chierici G.I., 1967).

Additional uncertainty is the presence of communication between K5-F1 and K5-F3. Figure 50 shows the MBAL simulation results of the K5-F1 well in which the aquifer support of the shared aquifer between K5-F1 and K5-F3 is removed. This shows that the measured water gas ratio used as a reference cannot be matched without the extra pressure support provided by the aquifer and communication with K5-F3. The same counts for the reservoir pressure where the simulated reservoir pressure is 30 bars below the measured reservoir pressure. This is further evidence of the communication between the K5-F1 and K5-F3 panel.
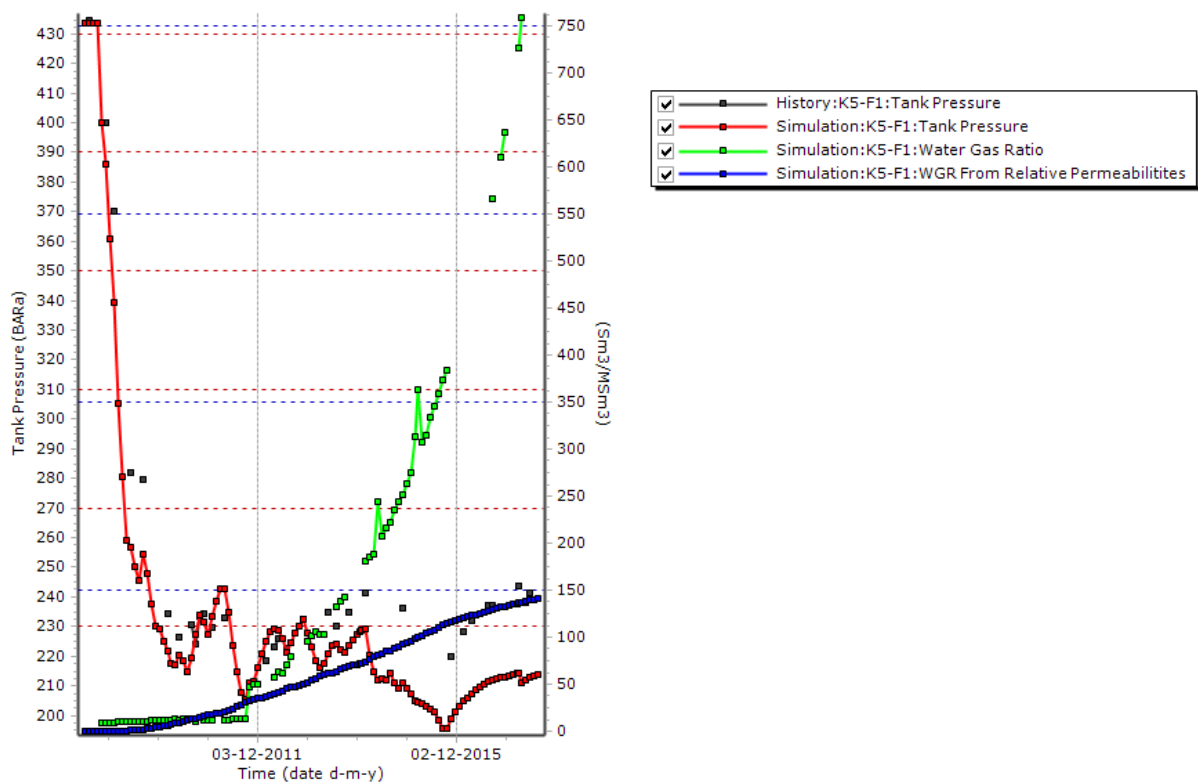
Figure 50: MBAL simulation of the K5-F1 well without aquifer support

8 Well Model Development – PROSPER

As previously mentioned, PROSPER is a design, optimization and well performance program. It is a multiphase well and pipeline nodal analysis tool in which a large variety of field specific information can be utilized. PROSPER has the ability to predict pipeline and tubing temperature and hydraulic changes with high accuracy and speed. It incorporates each aspect required to model a wellbore; PVT data for fluid characterization, vertical lift performance (VLP) for flowline and tubing pressure losses and inflow performance relationships for a reservoir (Coats Engineering, 2009).

The reservoir produces in agreement with a specific platform rate. This platform rate is determined by the specified platform constraints of water handling capacity, gas rate, bottomhole pressure and tubing head pressure. During the simulations, PROSPER will compare the manifold pressure from the surface calculations to each production well, redefining the new tubing head pressure. Here the minimum tubing head pressure is equal to the manifold pressure. The surface model is a steady-state thermodynamic model in which the input streams change over time since the input is determined by the reservoir models (Rahmawati, 2012). The user of the system can verify each model by tuning and matching the system model with the real field data.

8.1 Workflow
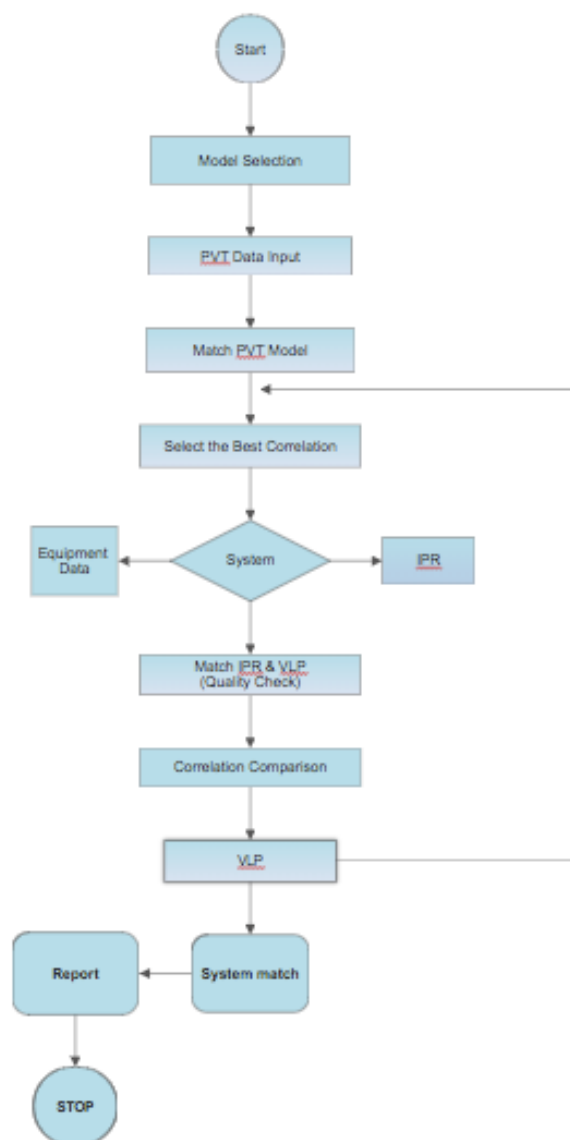
Figure 51: PROSPER Workflow (Okotie Sylvester, 2015)

Figure 51 shows the workflow used in PROSPER modelling. The PVT data needs to be the same as used to develop the tank model, whereas the pressure data is obtained through a link with MBAL.

8.2 Assumptions and Considerations

8.2.1 Well stability
A well is considered stable when it is producing at a steady rate and pressure for a long period of time. In the K5-F field, out of the three wells, K5-F2 is considered the most stable producer and K5-F3 the least. In PROSPER one needs to enter the well specific production rates as an input value. This is easier when your well is stable. However, when it is not some other methods can be chosen:
-    An average rate over the entire day can be chosen;
-    Average rate over a cycle can be chosen;
-    Or one could take the highest rate found within a cycle.

For this model an average rate over a cycle of one month was taken as the input value. This average rate was determined based on the cumulative production for that month and allocating the average rate per day, taking into account the downtime during that month. Since non-producing time is not accounted for in this, a downtime will need to be inserted into the model. This downtime will be applied in GAP.

8.2.2 IPR & VLP Curve Correlation
K5-F1 and K5-F2 produce both gas and water after 2013 making it a multiphase producing system. The presence of multiphase flow makes the pressure drop calculations a lot more complicated since the properties and interaction of each component needs to be taken into account. The productivity of a well strongly depends on how the reservoir and its fluids utilize the compressional energy of the system. The system must be designed to incorporate this energy efficiently. The most common places for energy loss and therefore pressure loss in the entire system are (Amao, 2013):
-    Reservoir;
-    The wellbore;
-    Choke valves;
-    Flowline and tubing string;
-    Separator.

 To be able to predict these pressure losses that accompany multiphase flow, multiphase flow correlations are applied.
$$\Delta P_{Total} = \Delta P_{Hydro} + \Delta P_{Fric}$$
These correlations predict the liquid holdup, the flowing mixture density and the frictional pressure gradient. These correlations consider the gas/liquid interaction. Each well and pipeline system is different which means that there is no universal rule on which correlation is best to apply to a certain situation. Therefore a careful correlation comparison was performed in which the predicted flow regimes and pressure results are inspected after which the researcher can select the correlation that best fits the physical attributes of the reservoir. From this comparison it was found that the inflow and outflow performance of the well was best simulated through the use of the Gray, PETEX 2 or the PETEX 4 correlations. (Experts, 2018) These correlations were able to find matches for stable rates and unstable rates for flowing wells.

The Gray correlation gives good results in gas wells for condensate ratios of up to 50 bbl/MMscf and high produced water ratios. (Maravi, 2003) The Gray correlation contains its own internal PVT model which overrides PROSPER's normal PVT calculations. (Technology, 2017) This correlation was developed specifically for wet gas wells by H.E. Gray. (Associates, 2012) The hydrostatic pressure differences are calculated using the vertical elevation and the frictional pressure losses based on the length of the complete pipeline. This correlation starts by calculating the liquid volume fraction in-site where after this is used to calculate the density of the mixture which then calculates the difference in hydrostatic pressure. The mathematical model describing the Gray correlation can be found in Appendix B.

8.3 Sensitivity & Uncertainty

This paragraph identifies the uncertainties and sensitivities of the developed well model. An uncertainty in the development of the well models lies in the inflow modeling. As previously mentioned, the input data carries measurements and conversion errors which is used for the empirical model. For the analytical model, analysis results from the well tests interpretations is used which in turn carries its own uncertainty. Therefore, it is assumed that for this study the derived data is correct and that the uncertainties are related to the lack of precise knowledge on the geological properties.

The uncertainty quantification on the IPR is more difficult. The IPR relies on the productivity index of a well which in turn depends on well test interpretations. As previously mentioned, well test interpretation can vary depending on the analysis of the user, quality of the data, knowledge of the well geometry, drainage area and quality of the well logs. It is not uncommon that the skin and permeability values can differ by more than 50%. Figure 52 gives an example of the effect a different permeability and reservoir thickness has on the IPR of K5-F1. To test the effect of permeability, the permeability was increased and decreased by 50%. The IPR effect of an increased permeability is indicated by the red line which intersect the VLP at a higher pressure and higher rate whereas the opposite is seen for the decreased permeability indicated by the yellow line. Here a 50% decrease in permeability results in a 5% lower reservoir pressure and a 41% lower gas rate. For a 50% increase in permeability the reservoir pressure is 2.8% higher and the gas rate 25% higher. The same is seen for reservoir thickness where a 50% decrease in reservoir thickness leads to a lower VLP IPR intersection and therefore lower reservoir pressure, gas rate calculation by PROSPER. Here a 50% decrease in thickness results in a 5% lower reservoir pressure and a 42.5% lower gas rate. For a 50% increase in thickness the reservoir pressure is 2.8% higher and the gas rate 27.5% higher. Therefore it can be stated that an overestimation of the permeability leads to an overestimation of the reservoir pressure and gas rate. Examples of the sensitivities of other reservoir parameters such as skin, Darcy coefficient, reservoir pressure and water gas ratio is shown in Appendix C.
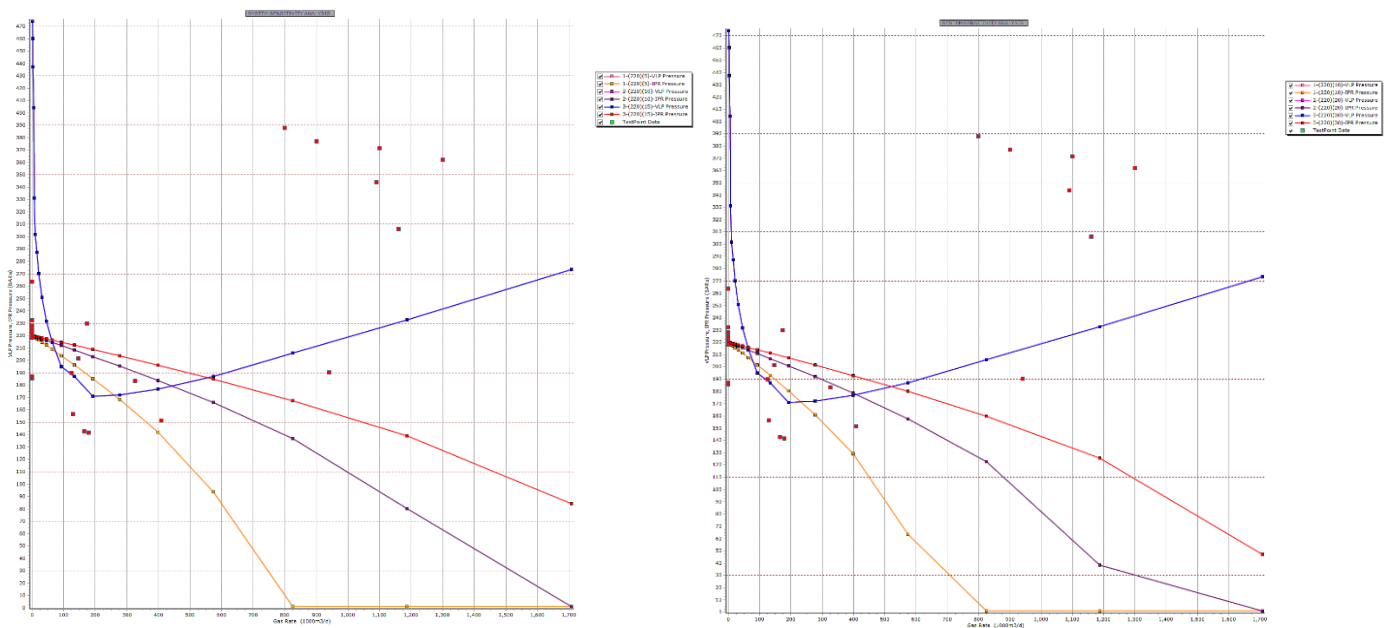
Figure 52: Sensitivity on permeability (left) and reservoir thickness (right) for K5-F1

9 Modeling of Surface Facilities – GAP

9.1 Workflow

In GAP all of the surface facilities are modeled through the process indicated in Figure 53. GAP requires one to input all the details of the well such as the well type, name and location, the pipe- and flow lines, compressor etc. An entire surface network with all the on- and offline wells in the reservoir model is show in Figure 54. The greyed out network areas are offline wells and will not be included in simulating the entire network, whereas the colored areas are active and included in the simulations. In this model a calculated pressure drop is used in order for GAP to assess the node pressure. Included in the system are a compressor and separators for an accurate depiction of the real system for analysis of the steady state production network.

Here GAP was used to back calculate and allocate wellhead and reservoir pressure. For this calculation the system needs a monthly maximum rate and monthly downtime allocated to the nodes of the wells and reservoirs. With these input parameters the model predicts the BHP required for the production of the specified gas rate and calculates the other phases being produced based on the reservoir conditions that surround the well. In Figure 54 the red triangles resemble the wells and the red oval shapes the reservoirs. Also, a separator can be seen in the middle of Figure 54. This compressor was added to the system in June 2013 to increase production.
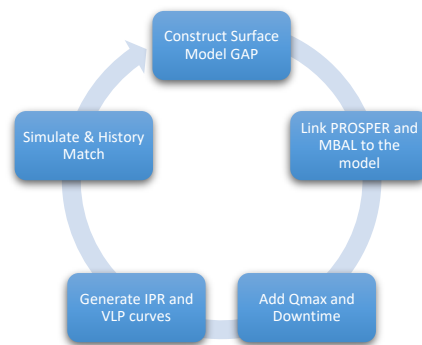
Figure 53: GAP workflow (Experts, 2007)
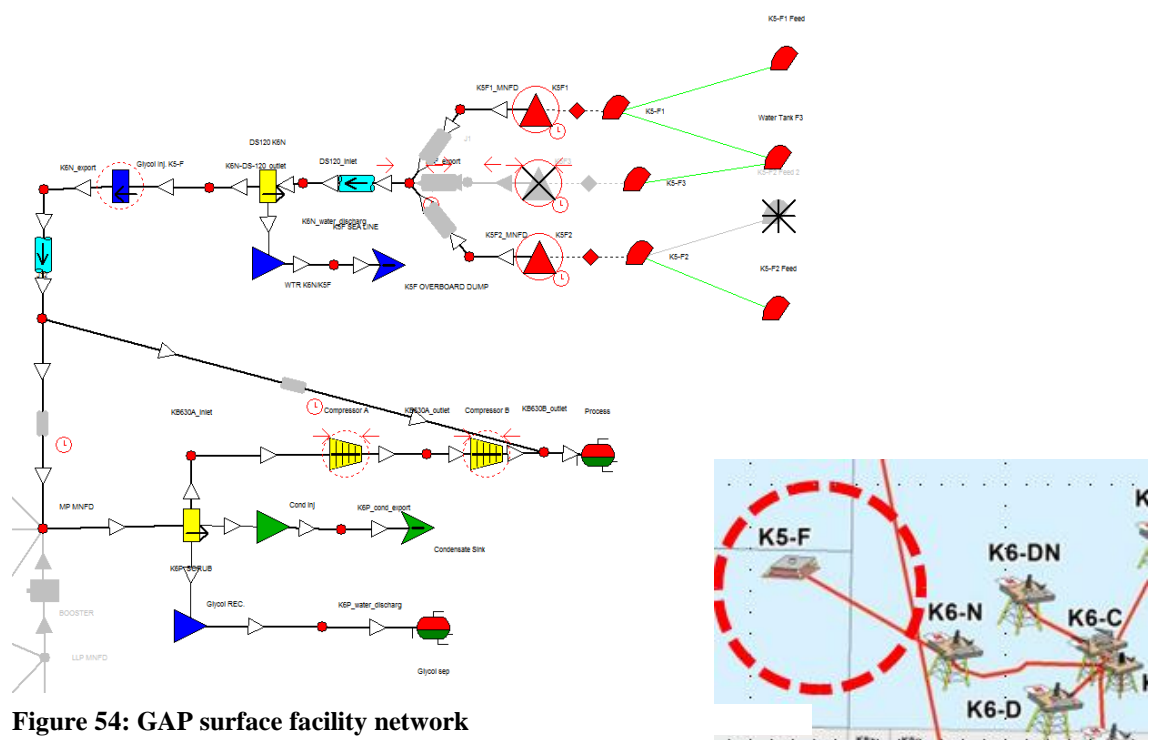
Figure 54: GAP surface facility network

9.2 Assumptions and Considerations

Production Downtime

The downtime of each well is an important parameter in the developed model. This downtime was calculated based on the number of hours a well is not producing, in percentages per month which shows a wells efficiency. This downtime is based on the time at which the well is offline due to production issues or workovers etc. Wells that are not stable producers and have more of a cyclic behavior of bottomhole pressure build up and periods of gas production, need a downtime which incorporates this cyclicity. Not having this would cause an overestimation of the time the wells are online causing an incorrect calculation of the pressures. Therefore, the downtime is estimated based only on the time the wells are actually online.

Surface Facilities

This incorporates all the facilities connected to the wells including all the maximum velocity and pressure constraints for the pipelines.

Compressor

The compressor was modelled with a fixed outlet node and performance curves. The compressor input data consists of minimum and maximum rates, suction pressure and operating range. Inline nodes can be used to constrain the pressure for suction to imitate the operating range of the asset. When a flow rate is outside of the compressor performance curve, GAP extrapolates a value for the performance input data. In reality it was seen that when the value lies outside of the performance curve, it goes either to full capacity or stop.

10 Model Results

10.1 Workflow

Having internal data matches in the Excel, MBAL, PROSPER and GAP should help create full simulation models which are close to the data gathered from the field. During the simulation inconsistencies or errors in the production model will become apparent. Throughout this research, field data has always been used to check the quality of the simulation results and are therefore plotted as a reference in each graph. As previously mentioned, the simulated outcome should be within the 5% range in comparison with the reference data. If the simulation results from GAP were not within this 5% range, the model had to be recalibrated until a match within this range is found. This calibration required careful analysis of the input data, selected models or correlations in Excel, MBAL, PROSPER and GAP.

10.2 Assumptions and Considerations

Timescale

During this programming of this simulation, care was taken when entering the data. All the entered data points are in a time step of 1 month starting at the beginning of each month. The smaller the time scale, the higher the precision but also the longer the computation time. Since there are quite some days in which the meters did not function, daily data has a high chance of being inaccurate in comparison to the monthly approximation.

Well deliverability

The well deliverability resembles a percentage of the amount of time the well is producing in a month. It is the stable rate at which a well can produce determined from the combined plot of the well's inflow performance (IPR) and the vertical lift performance (VLP). (Brown, 1982).

IPR and VLP curve selection

Reservoir characteristics will change over time as it depletes and water encroaches. Some factors affecting the Inflow Performance Relationship are (Amao, 2013):
- Fluid properties
- Rock properties
- Reservoir pressure
- Well geometry
- Well flowing pressure

Whereas the Vertical Lift Relationship is mostly affected by (Amao, 2013):
- Production rate
- Well depth
- Tubing diameters
- WGR

The depletion of reservoirs has the highest effect in the deterioration of the IPR curve over time. During the optimization and calibration of the K5-F1 PROSPER model, three sets of IPR curves needed to be made and programmed in order for GAP to create a model that matches the field data. A first set to describe the reservoir before production, a second in September 2011 and a third in August 2016.

The K5-F2 field required a total of two sets of IPR curves. One to describe the reservoir at the beginning of production and one from August 2013. Figure 30 shows the various well test over time in which a clean change in parameters such as skin and permeability can be seen. This can be a possible explanation for the requirement of a second set of IPR and VLP curves.

The GAP models didn't require the programming of multiple sets of VLP curves since the factors influencing the VLP were compensated through the IPR enough to find a good simulation match.

10.3 Optimization

The goal is to make the model as accurate as possible so that it benefits of utilizing it are high for Total. Hence, any optimization, development (new well drills) and production forecasting scenarios are all allocated resources

which enables pressure response analysis to take place.

The MBAL and PROSPER models were developed for the already producing K5-F field. Evaluating the models in this way allowed for accurate assessment of reserve addition/loss, incremental rates and surface network pressure behaviour. This type of research is beneficial and in the best interest of the company since a working reservoir model directly aids in business and capital investment decisions.

10.4 Model Results

Figure 55 and 56 show the final result of the optimized and calibrated GAP simulation output. The full colour lines resemble the GAP output data which is plotted against the field data depicted in the circles. Yellow is the reservoir pressure, dark green the potential gas rate, light green the gas rate, red the average gas rate and orange the well head pressure.
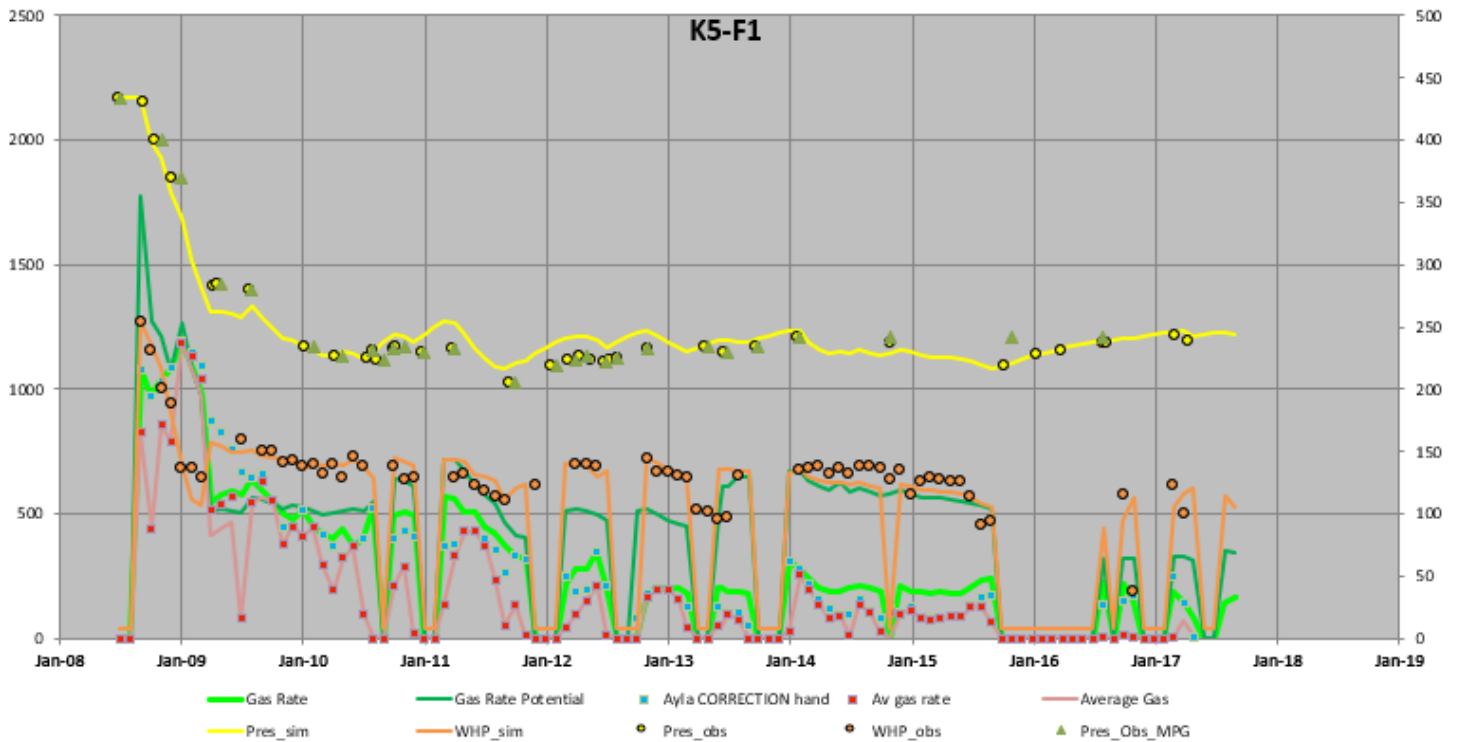
Figure 55: K5-F1 model simulation result vs observed data
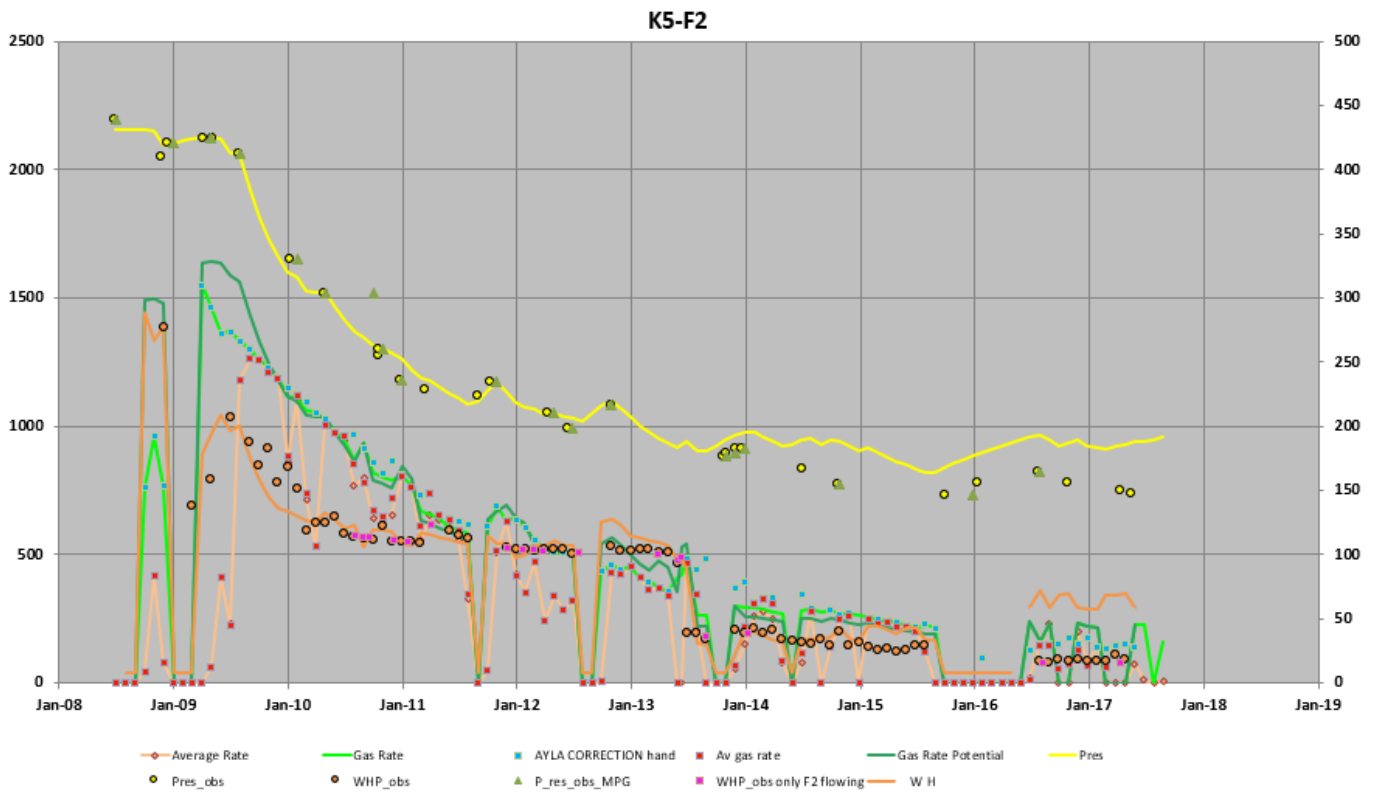
Figure 56: K5-F2 model simulation result vs observed data

10.5 Forecasting Results

A final step in this research is to perform a forecast simulation of each of the wells. Here it is assumed that once the model reacts well under historical constraints just like the real wells, then the same behavior is applicable for future constraints. Care should be taken to always use the normal reservoir engineering principles to prevent making an incorrect model.

In order to run a forecast a BHP or THP is specified for the two wells. These values will let GAP calculate the volumes of the different phases being produced based on these pressures incorporating the programmed reservoir parameters and conditions. The transition between the simulated and predicted data should be smooth and should show a similar decline in production. When this transition is not smooth, it indicates that the well needs more calibration. Since the model is based on the material balance and the movement of fluid in the reservoir, calibration of the productivity of the well could improve the predictability. This is usually an iterative process depending on the connectivity of the wells associated to the field.

Figures 57 and 58 show the forecast results of the K5-F1 and K5-F2 reservoir models. Here the same color coding is applied as before with yellow being the reservoir pressure, dark green the potential gas rate, light green the gas rate, red the average gas rate and orange the well head pressure.
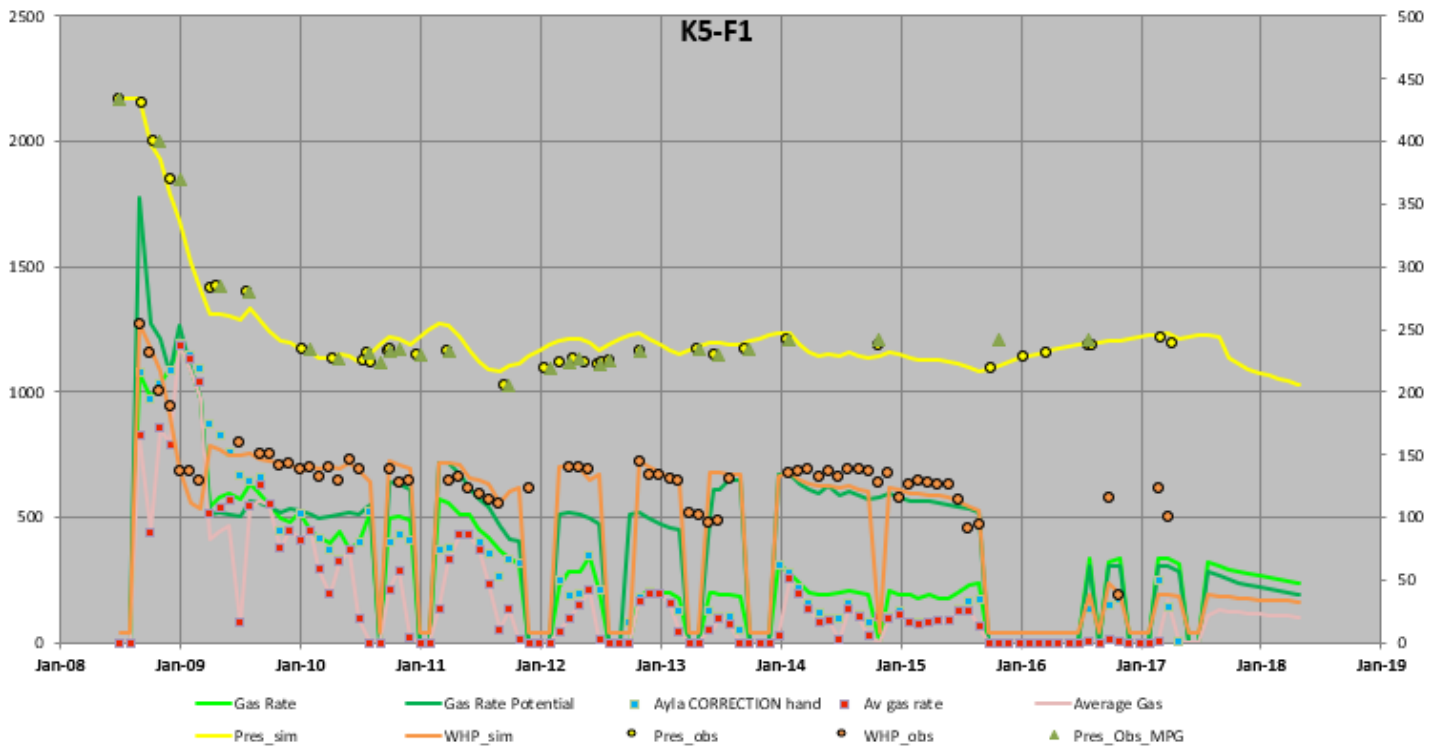
54

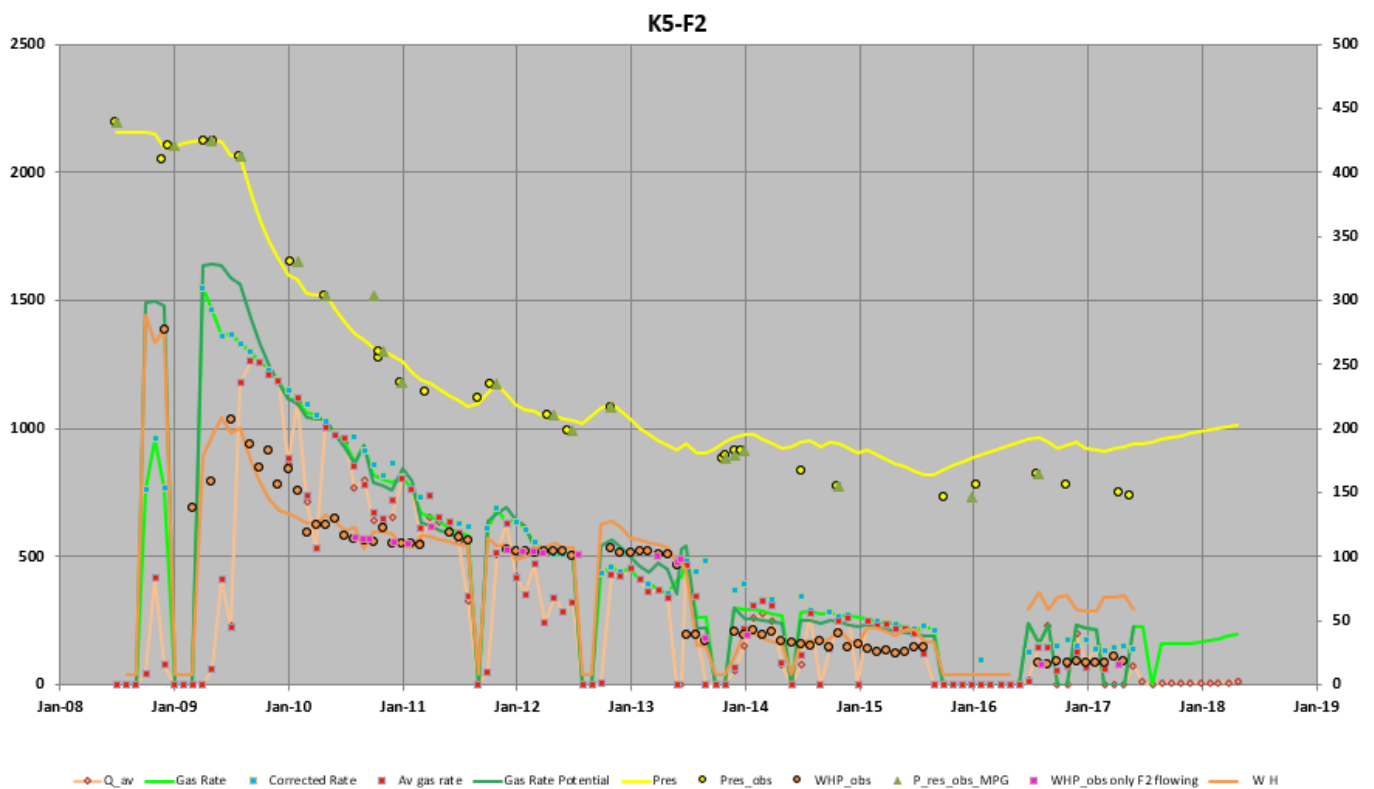**Figure 57: K5-F1 Forecast result vs observed data**

Figure 58: K5-F2 Forecast results vs observed data

11 Discussion

During this thesis, and in depth study of the K5-F field is performed after which this information it utilized to make a reservoir model that is able to simulate and forecast this field. Total has tried modeling the K5-F field in the past but this has been unsuccessful. This could potentially have been caused by production split determination mistakes which give an incorrect production history per well.

The K5-F field is not fitted with individual flow meters and flow is therefore only measured on the K6-N platform where the three wells converge. This requires of a production split to be determined per well. The current production split saved into the database is determined by engineers in Pau. However, after close analysis of this data, the Pau production split is questionable. Some examples of this are:

- The first 2,5 years the total production is simply divided by two to give the production for K5-F1 and K5-F2;
- Some data is stored twice giving unrealistically high production volumes;
- Data is incorrectly stored, or sometimes stored under the wrong well resulting in the system showing a closed in well with pressure build up, but also having production volumes registered during the build-up time.

For these reasons, a new production split is made with a more reliable approach. The new production split resulting from decline curve analysis was accepted by TEPNL Reservoir Engineers and used throughout this research for further analysis and modeling. A comparison between old and new production split is made to study the effect of production history on field analysis, reservoir modeling, history matching and forecasting processes.
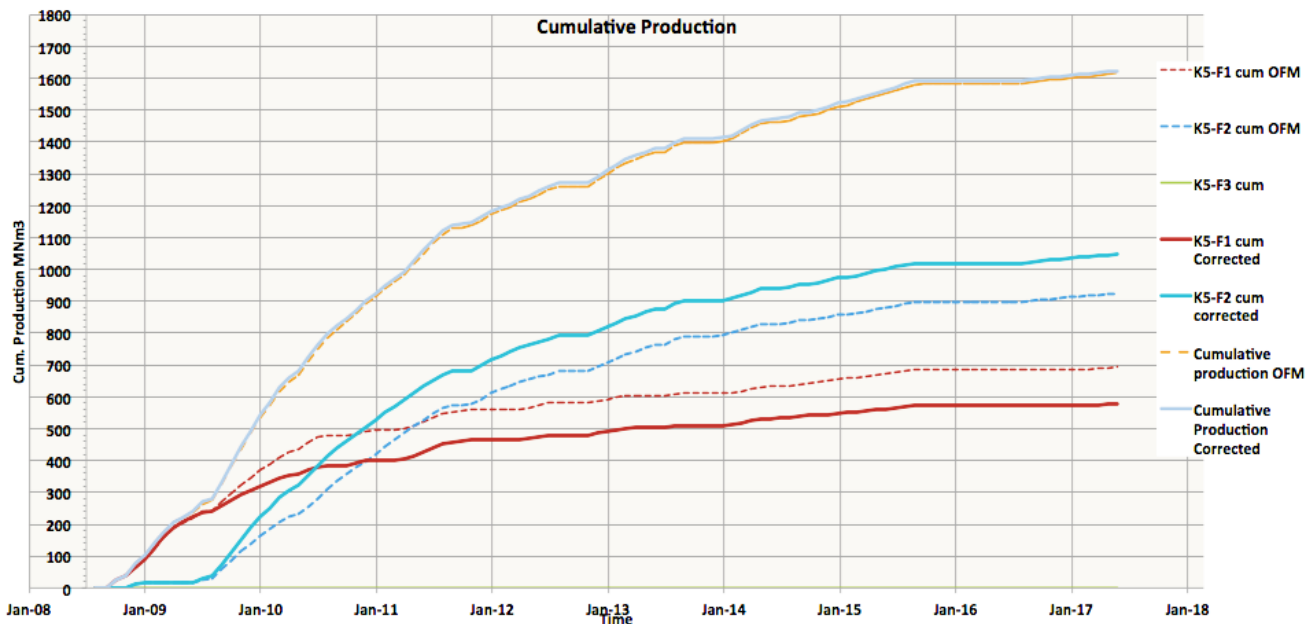
Figure 59: Comparison of the cumulative production profiles for the total production (orange), K5-F1 (red) and K5-F2 (blue) with the Pau allocated data and the new production split.

Comparison of the new and old production split per well results in an overall lower cumulative production for K5-F1 and a higher cumulative production for K5-F2 than previously allocated. This is shown in Figure 59 with the dashed lines resembling the previously allocated cumulative production and the full lines the cumulative production from the new production split. The new production split show an overall 0.4% cumulative production difference with the Pau registered total cumulative production and the cumulative production based on the new production split. For the individual wells this a 16,76% lower cumulative production for K5-F1 and a 13,21% higher cumulative produced volume by K5-F2.

Isolating the production splits per well highlights changes in reservoir behavior over time. Figure 60 shows a comparison between the old and new production history for K5-F1. As previously mentioned, K5-F1 is a field which has production problems causing multiple shut-ins throughout its producing life. Figure 60 also shows an

example of the previously mentioned erroneous production data registration where the production peak seen in June 2012 is not incorporate in the new production split.

Analysis of Figure 60 shows that the new gas production is lower than what has been allocated by engineers in Pau. This is especially true for the first two years where this difference is most apparent.
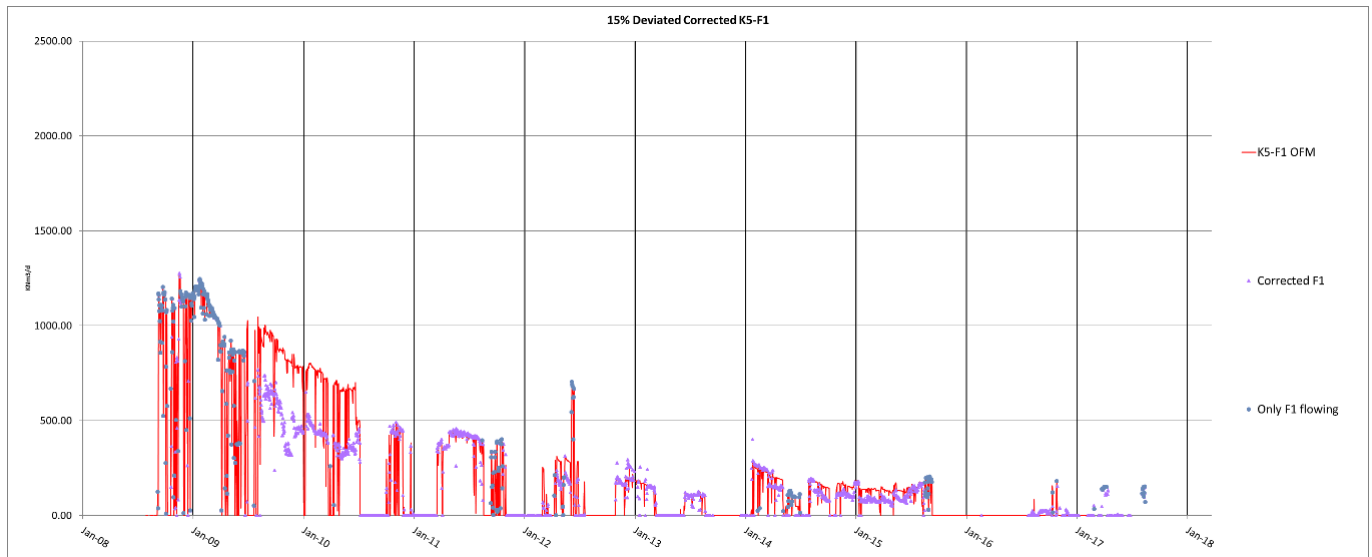
Figure 60: K5-F1 production history with Pau allocated production in red and corrected history in purple

Analysis of Figure 61, which depicts the production split for K5-F2, shows that the corrected production history is higher than what has been allocated by engineers in Pau. The slight rise in production capacity in June 2013 is related to compressor hook up onto the system which has resulted in an 150 m3/d increase in production for the field.
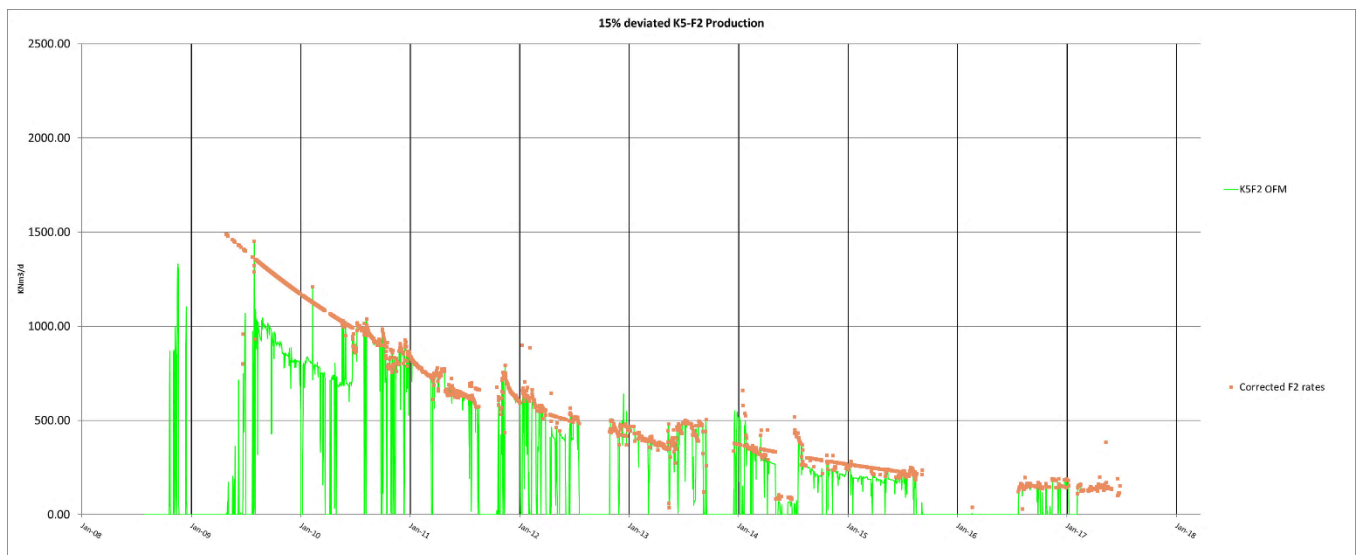
Figure 61: K5-F2 production history with Pau allocated production in green and corrected production in orange

The bottomhole pressures in the reservoirs are measured with downhole gauges which are considered to represent true and correct. As previously mentioned, the corrected production history has resulted in a different cumulative production per well which in turn causes p/Z relationship to change as well. p/Z plots help to determine the initial reservoir pressure, the gas initially in place and help visualize the pressure change trend

57

over time. These values will form the basis of the mass balance model. Figures 62 and 63 show the p/Z plots based on the Pau allocated production data together with the p/Z plots with the corrected production data. Comparing Figures 62 with the old p/Z plot on the left and the new p/Z plot based on the right shows a general decrease in expected initial gas in place (IGIP) for K5-F1 and increased value for K5-F2. The old IGIP for K5-F1 was estimated around 0.89 GNm3 whereas the new production estimates this volume to be closer to 0.71 GNm3. For K5-F2 this IGIP volume estimation has increased from 0.74 GNm3 to 1.4 GNm3. The general trend seen for both wells remain unchanged.

Constant quality checking is a necessity when reservoir modeling to ensure the development of a realistic reservoir model. A quality check when using MBAL is to plot the simulation output in the same p/Z plot. When the MBAL simulated p/Z values follows the same change in pressure trend as the observed pressure changes in the reservoir, the tank model parameter estimations can be considered accurate. Figure 62 and 63 show the p/Z relationship including the simulation output of the K5-F1 and K5-F2 MBAL model compared to the measured reservoir P/z from the field. Since the simulation results closely follow the p/Z trend based on the corrected production history, the parameter value used to describe the tank model are used as input values for the next step in the modeling process.
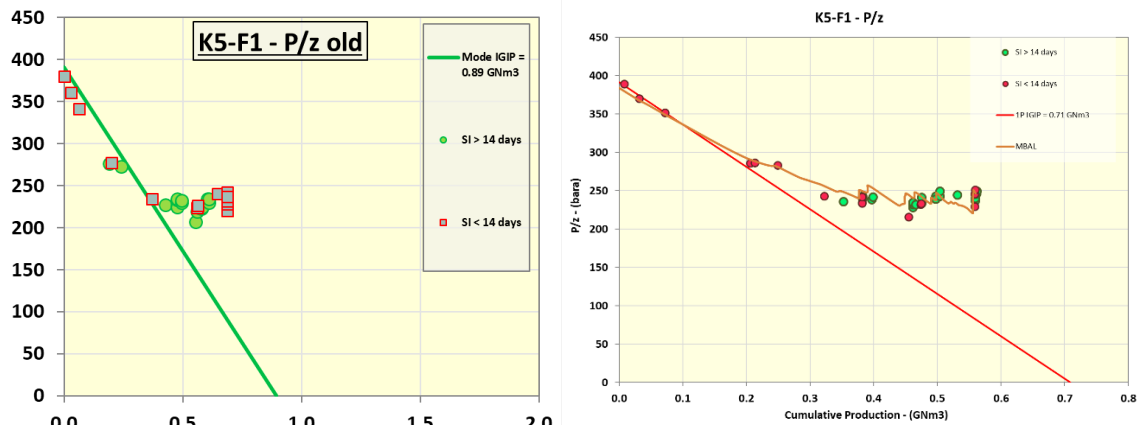
Figure 62: K5-F1 P/z plot with Pau allocated production data (left), P/z plot with corrected production data and MBAL P/z simulation results (right).
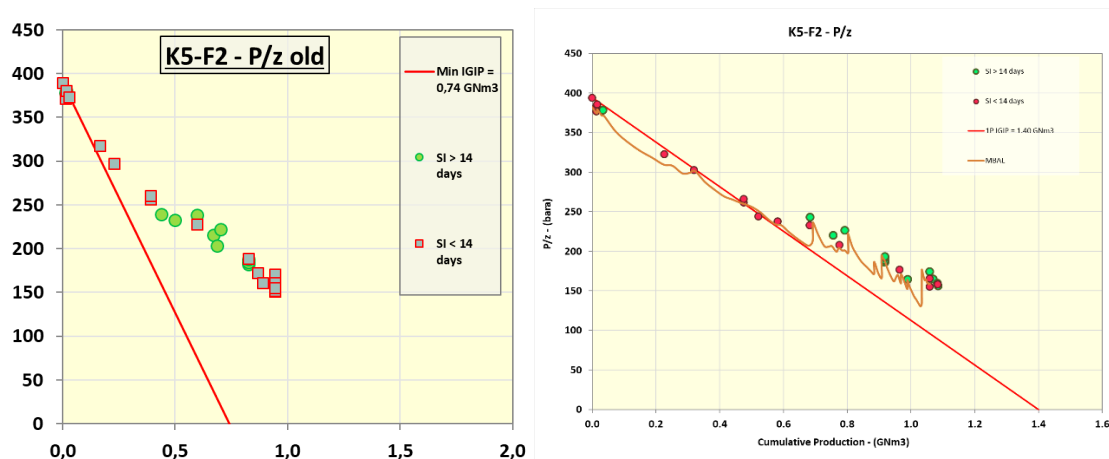
Figure 63: K5-F2 P/z plot with Pau allocated production data (left), P/z plot with corrected production data and MBAL P/z simulation results (right).

The change in gas production history per well requires a recalculation of the corresponding water volumes produced per well. Here the same decline curve principle is applied. Water production split and their following water gas ratios, based on the corrected production history, are shown in Figure 64 and 65. These figures show the old water gas ratio trend at the top and the new water gas ratio trend based on the correct production history.
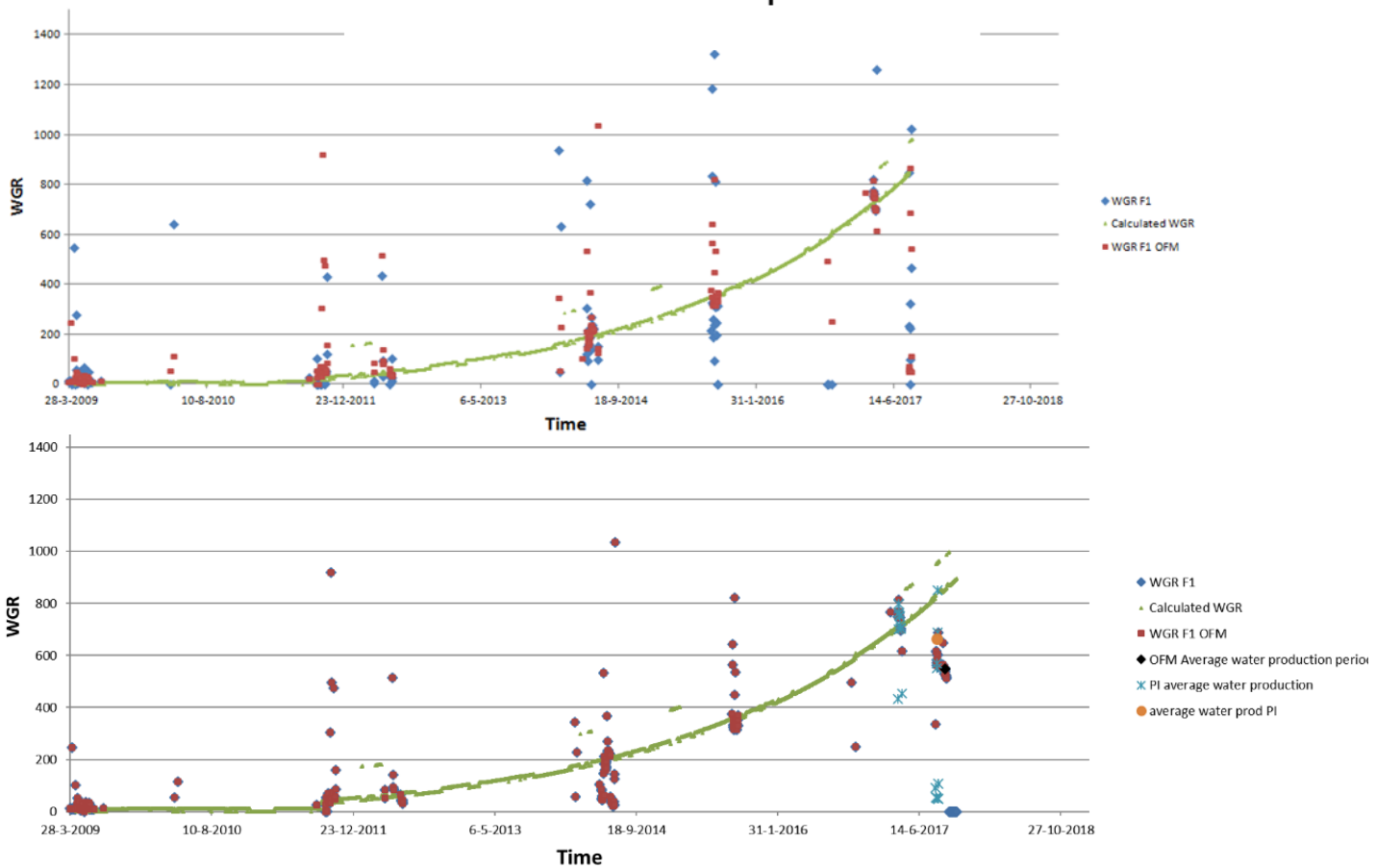
Figure 64: WGR trend of K5-F1 with production history from Pau (top) and corrected production history (bottom).

For K5-F1 both water production histories show an exponential increase in water production over time. However, the water production based on the corrected gas production rates shows a WGR of 880 m3/d in July 2017 whereas this is 810 m3/d for the Pau allocated production history meaning that the new production history, with a lower cumulative gas production also relates to a lower water gas ratio.

Comparing the gas production history of K5-F1 shown Figure 60 and the water production seen in Figure 64, the sudden increase in production in June 2011 coincides with the increase in water production seen in Figure 64. This moment identifies the water breakthrough in the K5-F1 well. The well has been producing for 2 months since the 3 month shut in at the end of 2010, which makes it unlikely that the increase in production seen in 2011 is due any other phenomenon such as the increased gas production caused by the pressure build up from the shut in.
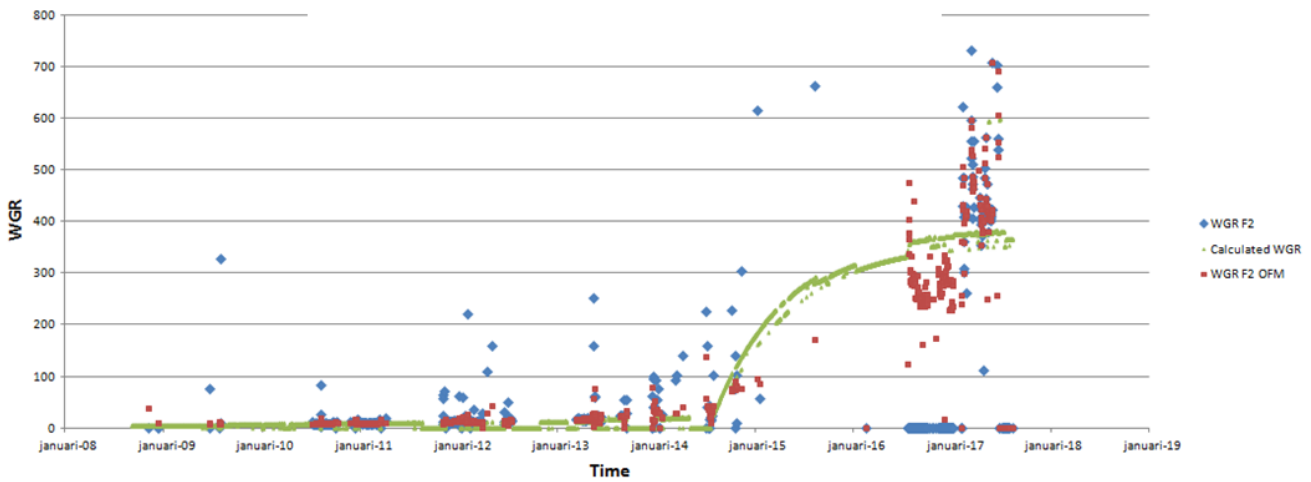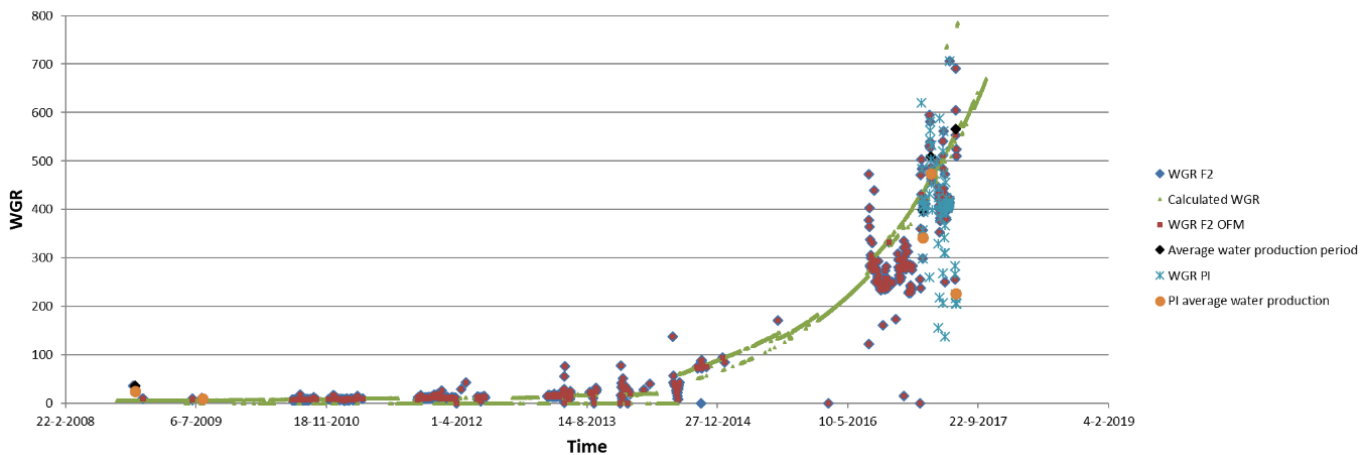
Figure 65: WGR trend for K5-F2 with production history from Pau (top) and corrected production history (bottom).

For K5-F2 the calculated water production based on the production data allocated in Pau and the WGR based on the corrected production history show a completely different trend. The Pau allocated data follows a limited exponential trend whereas the trend based on the corrected production history shows an exponential trend similar to that seen in K5-F1. Calculated average water production volumes during a period when only K5-F2 is producing are shown in Figure 65. These show that the averages based on the new production history are more concentrated which help in determining the best trendline fit. In comparison with Pau production data, the new water production calculations results in 200 m3/d overall increase in WGR. Since the gas and water production volumes are incorporated in the modeling process, changes production quantities have a large influence on how well a model will be able to match.

From the recorded water production from the field and Figure 65 an increase in water production can be seen at the end of 2013. This coincides with the water breakthrough of the K5-F2 well. One of the objectives for this research is to find a reason for the productivity drop in 2016. Normally a long shut-in period is followed by a period of increased production due to the pressure building up when the well is not producing. This, however, is not seen after the shut in of 2016. One hypothesis was based on the old production history and could have been caused by the production allocation. However, since the corrected production history still shows a similar productivity drop other explanations need to be found. A different explanation for the drop in productivity can be that this is caused by an increase in skin due deposition in the well caused by the long shut in period. Secondly, deterioration of the well due to the increasing water production can cause a well to produce less efficiently. To

study the deterioration of the well, pressure build up data is analyzed in which changes in reservoir properties are studied.

The pressure build up data analyzed in Chapter 5 of this thesis shows no indication of K5-F1 reservoir properties changing. However, this observation might not be true as there is only data available from 2 well tests. Since there is only data from 2009 and 2010 available for well test analysis it is impossible to make any definitive conclusions on the evolution of the reservoir parameters over time.

Because there is no pressure build analysis data for K5-F1 available after water breakthrough, assumptions in reservoir parameters changes are made during the modeling process when there is no simulation match with the observed data. In this case parameters such as skin and permeability are changed until a simulated match is found with the reservoir pressure, wellhead pressure, gas rates and the observed field data. It was found that during the modeling of K5-F1 data new inflow performance relationships needed to be modeled after water breakhthrough with lower permeability values. Since the resulting simulation match for the K5-F1 reservoir is good, it can be assumed that the input parameter values that make up the model are good as well. This implies that the reservoir permeability does decrease after water breakthrough.

For K5-F2 more well test data is available which show a significant change in reservoir properties before and after water breakthrough. No well test data is available after 2016 so a decrease in permeability or increase in skin can not be verified. Another possible explanation for the productivity drop is related to the local geology, which for the K5-F2 panel contains faults and is potentially compartmentalized. It is possible that gas has been producing through open faults which have closed due to the declining reservoir pressure. The communication through fault planes could also have decreased due to the increasing water level in the reservoir.

After studying all the separate pressure build up data from the individual wells, the effect of production history on this type of analyses was studied. Figures 66 and 67 show the effect of production history on well test analysis. These figures show that the new production split has a higher effect on well test data taken at an earlier stage in the reservoir production lifetime than on the later well test data. Since the earlier stage saw the biggest change in production rates which explains the derivative has shifted. However when looking at Figure 66, shows that the derivative based on the new production data shows a higher skin that previously thought. This shows that a change in historical production data can cause an underestimation of reservoir parameters, such as skin, which could have a high impact on the fields future potential and economics.
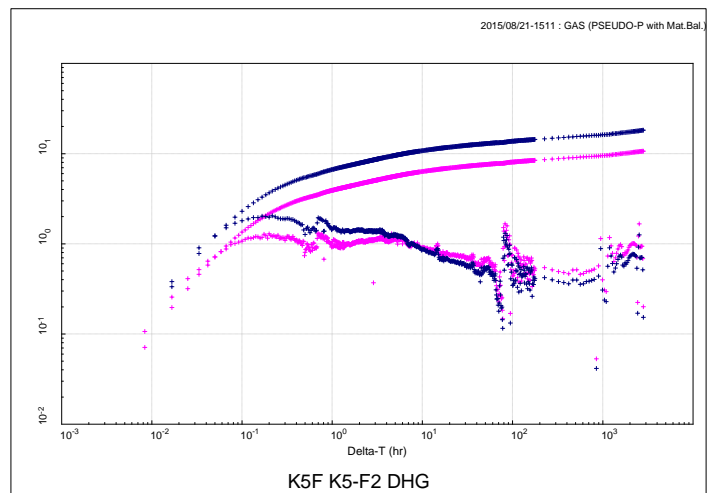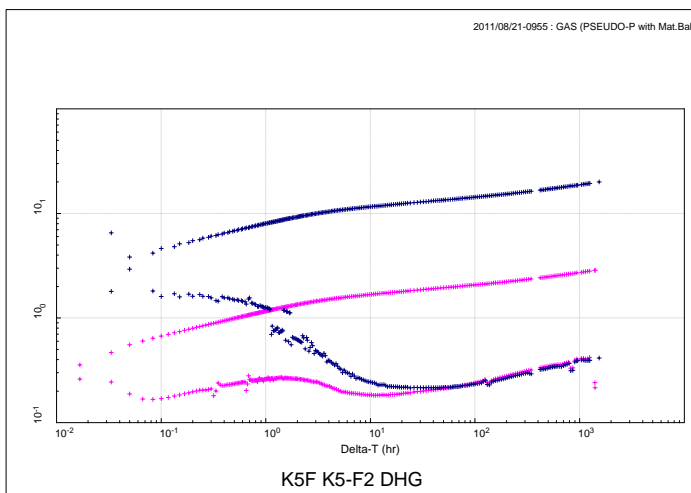
Figure 66: Well test analysis of pressure up data from August 2011 (right) with pink resembling the derivative based on Pau allocated production data, and blue on the new production history.
Figure 67: Well test analysis of pressure build up data from December 2015 (left) with pink resembling the derivative based on Pau allocated production data, and blue on the new production history.

Additionally, the effect of the amount of production history availability is studied. Figures 68, 69 and 70 show the effects of different amounts of production history on the derivative function. These figures show that the amount of production history available influences the pressure build up derivative curve. Having a small amount of production history has a large effect on the late stage of the derivative function causing underestimation on parameters such as skin and permeability. It was concluded that this effect is visible up until 3000 hours of production history, and that it is therefore desirable to have more than 3000 hours of history for pressure build up analysis.
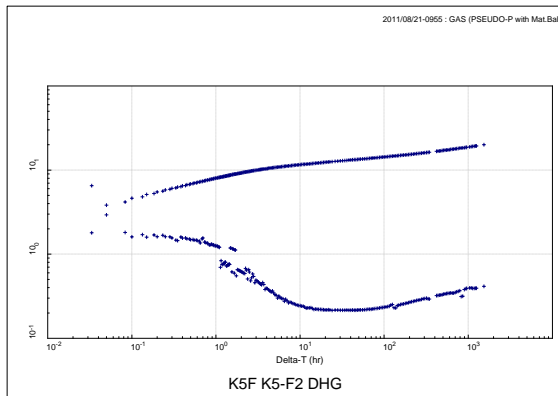
Figure 68: 1000 hours of production history
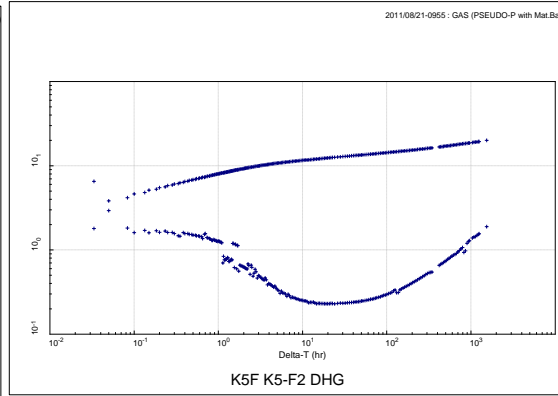
Figure 69: Whole production history

K5F K5-F2 DHG
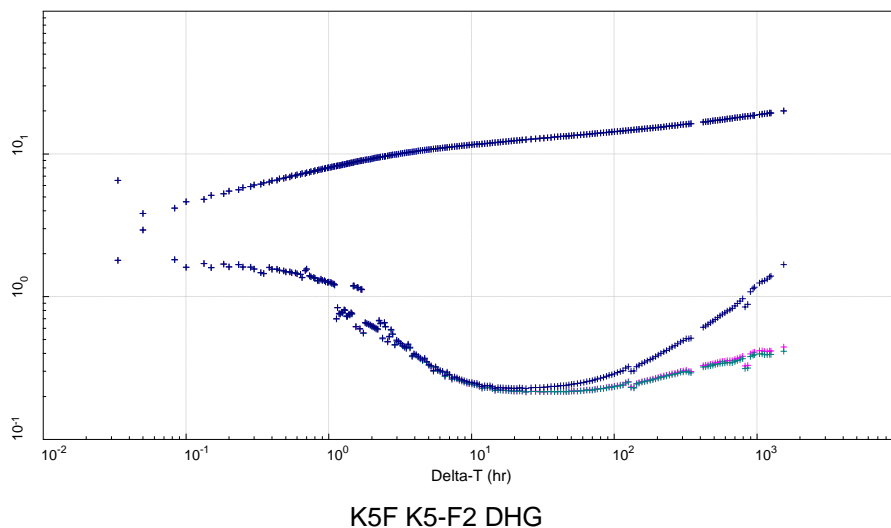
Figure 70: Comparison of the different amounts of production history where the Blue line resembles a 1000 hours of production history available, green half of the production history and red shows all of the production history.

During the programming of PROSPER, the results from the well test analysis as well as the corrected production data are used to match IPR and VLP correlations. Here the VLP takes into account information such as the deviation angle of the well, geothermal gradient, completion diagram and other equipment data. The VLP incorporates the pressure losses over the system from for example the perforations and fluid flow performance. The Inflow Performance Relationship, or IPR, is used to history match the flowing bottomhole pressure and well head rates. The aim is to match the VLP and IPR intersection point within a 2-5% difference from the calculated pressures and rates. An example of a VLP and IPR relationship is shown in Figure 71.
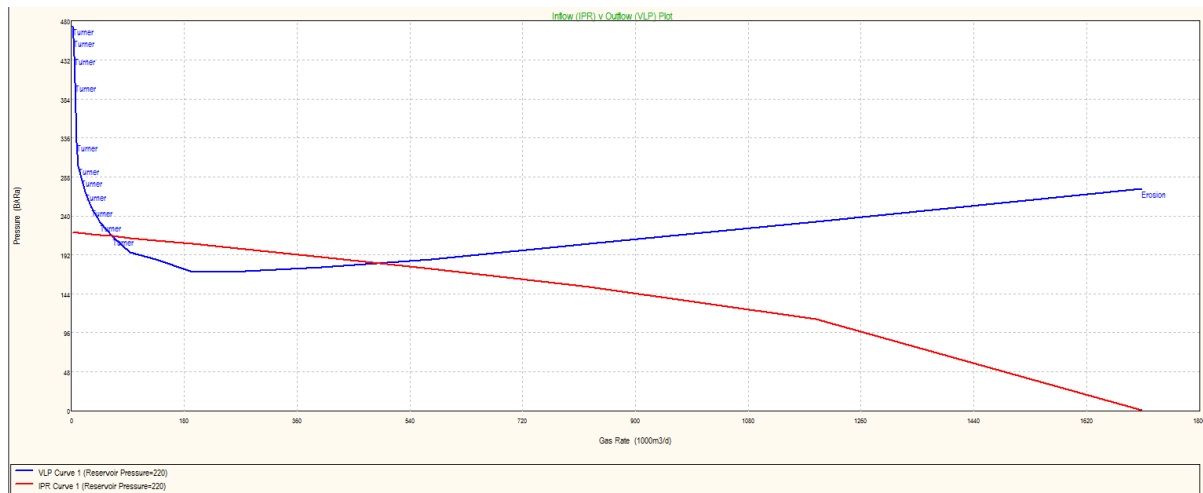
Figure 71: Inflow (IPR) and outflow (VLP) plot showing the pressure and rate correlation intersecting at 480 m3/d and 185 bar.

When PROSPER gives satisfactory pressure and gas rate simulation results, the modeling of the surface facilities in GAP can commence. The reservoir model was developed with the continuous input and review of Total's reservoir and production engineers. Due to the large amount of work, input parameters, assumptions and considerations that the development of each model required, everything was documented. Documented information included the values used as input data from the various data sources as well as the methods, correlations and constraints applied. This approach helps ensure that the fundamental theories and constraints are applied during the development and calibration of the integrated production model as well as safeguard repeatability.

The are no specific rules of thumb in place which determine to correctness of a model history match. However, something can be said about the reliability of a model which mostly relies on the quality and amount of the data. The reliability of a reservoir model history match is higher for a model with 20 years of production history than a model with 1 year of production history. Therefore, when evaluating the quality of a reservoir model is it important to keep in mind that every petroleum reservoir is different and that the simulation model is therefore different too with different amounts of history available. This is why it is important to validate the reservoir model based on more than one aspect.

As seen in Figure 55 in section 10.4, the calibrated model shows an overall good match for the reservoir pressure, well head pressure, average gas rate and the gas rate respectively. Here a quality check can be performed with the gas rate potential which is preferably similar to the simulated gas rate. Although this does not apply to the K5-F1 well which is a choked well. Choke settings are not incorporated in the modelling process and therefore will show an overestimation of the gas rate potential. Therefore, K5-F1 was matched focusing on the other simulation output values. Overall, the difference between the simulated model and the reference field data is within the 5% range.

The simulation model for K5-F2 shows a match within the 5% range until September 2015 as seen in Figure 56 in section 10.4. After a 10 month shut-in period, the simulation output starts to deviate from the field data. Due to time constraints it was not possible to fine tune the model enough to find a match for the last year of production within the acceptable range. The model shows a +/- 40 bar overestimation of the reservoir pressure and wellhead pressure which is the cause for the overestimation of the gas rate and gas rate potential. Reasons for this overestimation could be:
  - Further deterioration of the reservoir which could require a redetermination of the VLP and IPR input parameters;
  - The underestimation of the water gas ratio since this relies on the trend chosen by the user and therefore prone to human error;
  - Underestimation of the downtime of the wells;
  - Overestimation of the monthly cumulative gas production;

Figures 72 and 73 show the simulated model output comparison between the cumulative production data from the Pau allocated production, the corrected production data and the reservoir model output. The goal of integrated production modeling is to recreate the physical reservoir characteristics as closely as possible. Therefore, the difference between the reservoir model output data and the input data should be minimal. For a reservoir model to be consider a good match the cumulative volumes should be within ~5% of the historical values (Blandamour H., 2013). Figure 72 shows that the cumulative production calculated with the corrected data and the reservoir model simulation output differ by 3% and K5-F2 this is slightly higher at 4.8%.
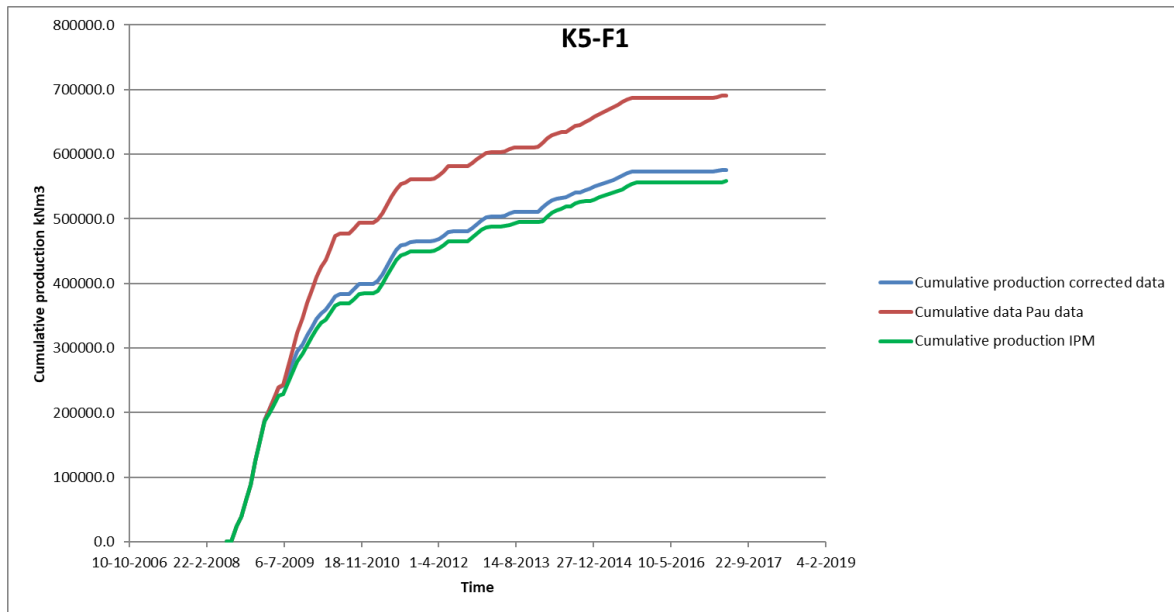
Figure 72: GAP simulated monthly cumulative production compared to calculated monthly cumulative production based on the new production split for K5-F1
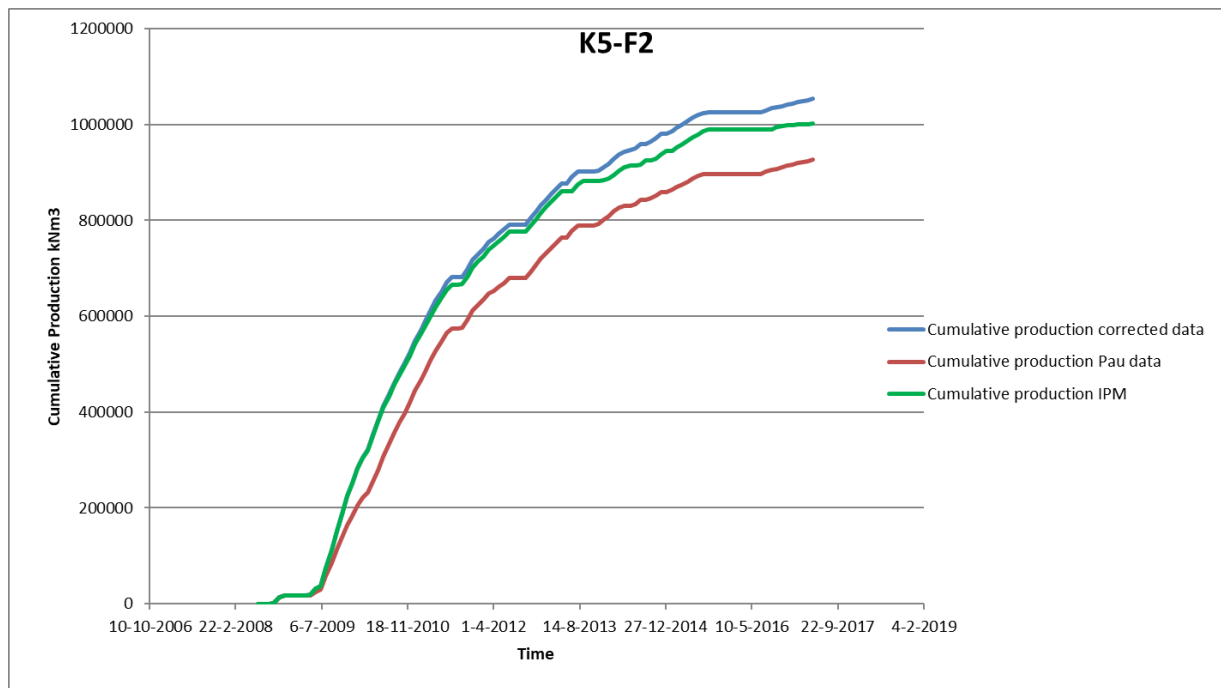
Figure 73: GAP simulated monthly cumulative production compared to calculated monthly cumulative production based on the new production split for K5-F2

In general, it can be stated that a good match for K5-F1 and K5-F2 is found with regards to the pressure and volume tank model made in MBAL, VLP and IPR modeling in PROSPER resulted in representative rate and

pressure calculations and GAP simulations showed a history matched model within the acceptable 5% range for K5-F1 and for 80% of the model for K5-F2. This indicates that the reservoir model designed is a possible representation of the real reservoir and require some more work to get a match for the whole field with both reservoirs.

The last step in this research is to test the reservoir model by its forecasting capabilities. A simulated prediction of a reservoir is considered good if the decline rate of the predicted model is consistent with the historical decline rate. As can be seen in Section 10.5, the forecast for K5-F1 shows a slight drop in reservoir pressure but which trend coincides with the gradual decline in gas rate and gas rate potential. The forecast for K5-F2 is less successful. This is caused by the mismatch between the reservoir model and observed data at the end of the modeled timeframe. The simulated reservoir model shows an overestimation in reservoir pressure and rate before the prediction process, where after this is only enlarged giving an unrealistic reservoir forecast. This exemplifies why it is important to continue to calibrated the reservoir model until it is matched over the whole timeframe.

12 Conclusions

In this thesis a combination of analysis methods are applies to investigate the effect of production history on modeling processes. In comparison to more traditional modeling, where all the different parts of a production system are modeled separately, this integrated model incorporates the interaction between the reservoirs and facilities which gives a better and more accurate results. This allows for engineers to have a better insight in the productiveness and efficiency of the field and its network.

Faults identified through seismic surveys and shown in the contour map were previously thought to be sealing with zero communication between the K5-F1, K5-F2 and K5-F3 panels. Through interference tests, the bottomhole pressure and wellhead pressure gauge data registered in the K5-F3 well during a period where only K5-F1 was producing, found the K5-F3 BHP and WHP pressure to drop approximately 1 bar. This pressure drop is evidence of communication between the K5-F1 and K5-F3 panel.

The wells from the K5-F field have downhole pressure gauges but are not fitted with individual flow meters. The total flow measured at platform level has to therefore be split between the wells contributing to the production of the K5-F field. By analysis of the previously allocated production split it was obvious that this production split was not very reliable which warranted this research to start with the determination of a more dependable production split. This correction in production split has resulted in a change in production history with a 16,67% decreased cumulative production for K5-F1 and a 13,21% increased production for K5-F2.

The production history sees the largest change in the first three years of the production life of K5-F1 and K5-F2. Through application in well test analysis this has led to new skin and permeability value determinations on which the reservoir model is based. However, since there were only two pressure build up test for K5-F1 available to perform analysis on, it is impossible to know whether the quality of the K5-F1 reservoir changes over time. This requires an additional pressure build up test to be performed.

K5-F2 well test analysis does show a clear change in permeability and skin before and 2011 and 2014. Water production and water gas ratio calculation, based on the new production split, show water breakthrough in December 2013 and therefore most likely responsible for the change in reservoir properties. In 2016 the well sees another decrease in productivity after a shut-in period of approximately 1 year. This could be caused by the exponential increase in water, loss of well integrity caused by the shut-in or the closing of a fault by the declining reservoir pressure. However, ideas about the cause of this productivity drop can best be tested through additional pressure build analysis.

Even though the K5-F field is one that has many production difficulties, unknowns and uncertainties, the workflow used and presented in this thesis allowed for the successful development of an integrated production model based on the most recent ideas and findings. The designed and simulated reservoir model resulted in the estimation of unknown reservoir parameters such as volumes, saturation, relative permeabilities, compartmentalization and transmissibilities per well. For both K5-F1 and K5-F2 a tank modelled reservoir pressure and water saturation match with a 2% mismatch with the observed data, cumulative production match is around 3% which is acceptable with overall good reservoir pressure, wellhead pressure and gas rate matches for K5-F1. K5-F2 found a cumulative production match of 4,8% with the K5-F2 reservoir model starting to deviate from the observed reservoir pressures from 2015 till the end of the simulated production time. This overestimation of reservoir results in an overestimation of the wellhead pressure, gas rate potential, gas rate itself and therefore forecast model.

In reservoir modeling it is possible to find good field wide matches while the individual well matches are very poor and vice versa. A poor match can be caused by a number of different factors. Some of these are:
- Reservoir heterogeneities not well modeled;
- Erroneous field data;
- Wrong reservoir geometry or parameters assumptions;
- Wrong saturation distribution.

Adding to this is the effect of production history itself on the development of a reservoir model. This research has shown that the amount and quality of production history available for a field and/or wells can have a huge impact on the analysis on reservoir parameters and model estimations. Besides the quality of the production

data used, the amount of production history plays a large role in well test analysis and reservoir modeling. Small amounts of production history for instance can have a big influence on the late stage of the pressure build up derivative which can lead to an over estimation of the skin. Therefore it can be stated that the quality of a reservoir model and history match of a field has a direct correlation with the quality of the production and field data.

However, it can be concluded that due to the assumptions made throughout the modeling of the K5-F reservoir it was possible to create a simulation model able to forecast the K5-F1 and K5-F2 well simultaneously. Even though the forecasted models are not perfect, the fact that the forecasted model runs without errors suggest that the model used is close to the truth. However, a good history match does not mean that the designed reservoir model resembles the reservoir itself. It is always good to keep in mind that a model is not the reservoir itself. There will always be a level of uncertainty.

13 Recommendations

With companies relying more on technology and reservoir modeling it is important to improve the understanding and quality of data gathering and storage especially since a large part of this research is based on the gas production split allocation per well.

In order to improve reservoir model forecast it is important to remove some of the excess energy seen in the K5-F2 model causing the overestimation of the pressures and rates. This excess of energy can be caused by an overestimation of the tank volumes or aquifer strength in MBAL, underestimation of the relative permeabilities or wrong VLP/IPR correlations. Incorporating vertical permeability variations can help improve the forecast. Vertical permeabilities influence the forecasted production rate of horizontal wells. Once the reservoir and forecast models give satisfactory results, a next step would be to build an eclipse model based on the input parameters from the IPM model.

Besides improving the simulation match of the reservoir model, improvements in the physical field are recommended as well. To improve the production of the K5-F field itself it would be beneficial to increase the water handling capacity of the K6-N platform or to allow some of the production water to be handled at a neighbouring platform. The extra water handling capacity will allow the well to keep producing through the water slugs without it having to be choked or shut in. This will help the well to produce more constantly which improves the field performance and therefore value. Reperforation or sidetracking of the K5-F3 well can improve production rates from this will adding further value.

For the K5-F field it could also be valuable to better estimate aquifer size and strength. Aquifer size and strength is determined by looking at reservoir structure, lateral extension, the fault distribution that compartmentalize the aquifer and the Free Water Level. In areas where the aquifer is not bounded, for example by normal faults with little associated displacement, the area of an aquifer can be very complex. Therefore fault distribution and associated fault properties must be analyzed carefully to determine what area is in hydraulic communication. Moreover, well correlations of the analyzed fields show that the Lower Slochteren reservoir hardly varies in thickness within one field. Therefore the reservoir thickness known from well correlation panels and can be assumed to be constant across the field. Because of the uncertainties, concerning the fault properties and structures controlling the aquifer size as well as the free water level, it might be good to consider P10, P50 and P90 cases to estimate aquifer size and strength. In addition, the pressure data and water fingerprint of the surrounding field must be analyzed to examine whether different fields share the same aquifer and whether several aquifers might be in communication with each other. Moreover, Westphalian reservoirs can be in communication with Lower Slochteren reservoirs increasing the aquifer volume and hereby aquifer strength. According to Lafont (Lafont F., 2000)only Westphalian A and C potentially contain reservoir properties.

Ultimate recovery in water driven reservoir is governed by the heterogeneities in the reservoir, the pressure of the free gas abandoned updip of the highest perforation and the residual gas saturation behind the water front. Normally, the recovery of these reservoirs is between the 30 and 75% (Bassiouni, 1990). For these types of reservoirs, the 'co-production' technique could be applied. Here downdipping wells that begin to water out are turned into high rate water producers where the well in the updip of the reservoir remains a gas producer. Producing enough water will slow down the water influx in the gas well allowing further depletion. This depletion will result in a pressure decrease which in turn will increase the production due to expansion.

14 Nomenclature

ΔV_{wip} = Change in volume caused by water encroachment, bbl, [m^3]

μ_w = viscosity water, cp, [Pa.s]

5.615 = conversion constant in oilfield units, [ft^3/bbl^3]

Bbl = barrel

B_g = Formation volume factor for gas at time t, ft^3/scf,[m^3/m^3]

B_{g1}= Initial gas formation volume factor, ft^3/scf, [m^3/m^3]

B_w= water formation volume factor, ft^3/scf, [m^3/m^3]

D = inside pipe diameter (ft)

E_L = in-situ liquid volume fraction (liquid holdup)

f_{tp} = two-phase friction factor

g = gravitational acceleration (32.2 ft/ s^2)

g_c = conversion factor (32.2 (lb$_m$ ft)/(lb$_f$ s^2))

k = absolute roughness of the pipe (in)

k_e = effective roughness (in)

L = length of pipe (ft)

ΔP_{HH} = pressure change due to hydrostatic head (psi)

ΔP_f = pressure change due to friction (psi)

V_{sl} = superficial liquid velocity (ft/s)

V_{sg} = superficial gas velocity (ft/s)

V_m = mixture velocity (ft/s)

Δz = elevation change (ft)

ρ_G = gas density (lb/ft^3)

ρ_L = liquid density (lb/ft^3)

ρ_{NS} = no-slip density (lb/ft^3)

ρ_m = mixture density (lb/ft^3)

σ = gas / liquid surface tension (lb$_f$/s^2)

DHG = Downhole gauge

DST = Drillstem test

FBHP = flowing bottomhole pressure [bar]

G = original gas in place, Bcf, [m^3]

GAP= General Allocation Package

GIP = Gas in place

G_p = Cumulative gas produced [st.vol]

h = height [m]

IPM = Integrated Production Modeling

IPR = inflow performance relationship

k_a = permeability aquifer

Krg_{max}= maximum gas relative permeability

Krw_{max}=maximum water relative permeability

L_a = length aquifer [m]

L_r = length reservoir [m]

MBAL= material balance software

MMscf = Million metric standard cubic feet

MPG = Massbalance, Prosper and Gaspal

OFM = Oil Field Manager

OGIP = original gas in place

P = pressure, psia, [Pa]

PI = Productivity Index

P_{res} = reservoir pressure [bar]

PROSPER= Production and Systems Performance Analysis Software

R_D = ratio inner and outer radius

S_{cw} = connate water saturation

S_{gr} = residual gas saturation

SIBHP = Shut In Bottom Hole Pressures [bar]

S_{max} = maximum saturation

T = temperature [°C]
t = time, hours, [s]
t_D = dimensionless time
TEPNL = Total Exploration & Production Netherlands
t_{max} = maximum time [years]
U = aquifer constant
VLP = vertical lift performance
V_{pa} = pore volume aquifer [m^3]
V_{pr} = pore volume reservoir [m^3]
W_D = dimensionless cumulative water influx [m^3]
W_e = Water encroachment into the formation, Bbl, [m^3]
WGR = water gas ratio
WHP = wellhead pressure [bar]
W_p = cumulative water produced, Bbl, [m^3]
Z = gas compressibility factor [-]
Z_i = initial gas compressibility factor [-]
ΔP = pressure difference
$ΔP_{fric}$ = frictional pressure difference
$ΔP_{hydro}$ = hydrostatic pressure difference
$ΔP_{total}$ = total pressure difference
$Φ_a$ = porosity aquifer [%]
$Φ_r$ = porosity reservoir [%]

Bibliography

Amao, Matthew. 2013. Performance of Flowing Wells. *Artificial Lift Methods and Surface Operations.* [Online] October 28, 2013. http://fac.ksu.edu.sa/sites/default/files/2-performanceofflowingwells.pdf.

Ambassha A.K., Sageev A. 1987. *Linear Water Influx of an Infinite Aquifer Through a Partially Communicating Fault.* Stanford : Stanford University, 1987.

Ambasyha, A.K. 1990. *Analysis of Material Balance Equation for Gas Reservoirs.* Alberta : Petroleum Society of Canada, 1990.

Associates, Fekete. 2012. Pressure Loss Correlations. *Theory and Equations.* [Online] 2012. http://www.fekete.com/SAN/TheoryAndEquations/PiperTheoryEquations/c-te-pressure.htm.

Bassiouni, Z. 1990. *Enhanced Recovery from Water-Drive Gas Reservoirs.* Baton Rouge : Louisiana State University, 1990.

Blandamour H., P. Benazet. 2013. *Manual for PI Calculations.* Den Haag : Total Exploration and Production Netherlands, 2013.

Brown, Kermit. 1982. *Overview of Artificial Lift Systems.* 1982.

C. Correa Feria, Repsol. 2010. *Integrated Production Modeling: Advanced but, not Always Better.* 2010.

Chierici G.I., G. Pizzi, G.M. Ciucci. 1967. *Water Drive Gas Reservoirs: Uncertainty in Reserves Evaluation From Past History.* Milan, Italy : Journal of Petroleum Technology, 1967.

Coats Engineering, Inc. 2009. *Sensor Reference Manual.* . s.l. : Coats Engineering, Inc. , 2009.

Collinson J.D., C.M. Jones, G.A. Blackbourn, B.M. Besly, G.M. Archard & A.H. McMahon. 1993. *Carboniferous depositional systems of the Southern Noth Sea.* London : The Geological Society, 1993. Vols. 667-687.

Drake, L.P. 1978. *Fundamentals of reservoir engineering.* New York : s.n., 1978.

Engineers, Society of Petroleum. 2015. Water influx models. *Petrowiki.* [Online] 6 12, 2015. http://petrowiki.org/Water_influx_models#Linear_aquifer.
—. 2015. Water Influx Models. *Petrowiki.* [Online] 06 12, 2015. petrowiki.org/Water_influx_models.

Experts, Petroleum. 2007. *An introduction to Prosper, MBAL & GAP.* s.l. : Petroleum Experts, 2007.
—. 2007. *An introduction to PROSPER, MBAL & GAP.* s.l. : Petroleum Experts, 2007.
—. 2018. Integrated Production Modelling and Field Management Tools. *Petroleum Experts.* [Online] 2018. http://www.petex.com/.

F. Lafont, B. Euvard, A. Roumagnac. 2000. *The Netherlands Central offshore update of terminology and facies distribution in the Lower Slochteren.* Structural Geology & Sedimentology Department EP/T/GGC/EUO NL/2000-376. - : -, 2000.

Gray, H.E. 1974. Vertical Flow Correlation in Gas Wells. *Subsurface controlled safety valve sizing computer program.* D.C. Washington : s.n., 1974, Vols. In User manual for API 14B, Appendix B.

IHS Inc. 2014. Material Balance Analysis Theory. *Fekete.* [Online] 2014. www.fekete.com/SAN/WebHelp/FeketeHarmony/Harmony_WebHelp/Content/HTML_Files /Reference_Material/Analysis_Method_Theory/Material_Balance_Theory.htm.

Kabir, C.S. 1983. *Predicting Gas Well Performance Coning Water in Bottom-Water-Drive Reservoirs.* San Francisco, USA : SPE Annual Technical Conference and Exhibition, 1983. SPE 12068-MS.

Kleppe, Professor Jon. 2017. Material Balance Equations. *Reservoir Recovery Techniques.* Norway : Norwegian University of Science and Technology, 2017, pp. 1-6.

Lafont F., B. Euvard, A. Roumagnac. 2000. *The Netherlands Central Offshore Update of Terminology and Facies Definition in the Lower Slochteren.* Nederlands : Structural Geology & Sedimentologt Department, 2000.

Lippolt, J.C. Hess & H.J. 1988. *Subsidenz und Sedimentation im Saar-Nahe-Becken- die Entwicklung eines Molassetrogs im Lichte isotropischer Altersdaten.* s.l. : Nachrichten der Deutschen Geologischen Gesellschaft, 1988. Vols. 26-27.

Maravi, Yanil Del Castillo. 2003. *New Inflow Performance Relationships For Gas Condensate Reservoirs.* Texas : Texas A&M University, 2003.

Mesarovic, M.D. 1960. *The Control of Multivariable Systems.* New York : s.n., 1960.

Moghadam S., O. Jeje, L. Mattar. 2011. *Advanced Gas Material Balance in Simplified Format.* Canada : Journal of Canadian Petroleum Technology, 2011.

Montopoulos, D.A. Marques, S.P. Hunt. 2015. *Best Practice and Lessons Learned for the Development and Calibration of Integrated Production Models for the Cooper Basin, Australia.* s.l. : ResearchGate, 2015.

Okotie Sylvester, Ikporo Bibobra, Ovuema Augustina. 2015. Gas Lift Technique a Tool to Production Optimization. *Science Publishing Group.* [Online] May 2015. [Cited: 12 07, 2017.] http://article.sciencepublishinggroup.com/html/10.11648.j.ogce.20150303.12.html.

Osisoft. PI System . *From data to knowledge to transformation.* [Online] [Cited: December 11, 2017.] https://www.osisoft.com/pi-system/.

Quirk, D.G. 1993. *Interpreting the Upper Carboniferous of the Dutch Cleaver Bank High.* London : Geological Society, 1993. Vols. 697-706.

Rahmawati, Silvya Dewi. 2012. *Integrated Field Modeling and Optimization.* Department of Engineering Cybernetics. s.l. : Norwegian University of Science and Technology, 2012. http://folk.ntnu.no/bjarnean/pubs/others/thesis-Rahmawati.pdf?id=ansatte/Foss_Bjarne/pubs/others/thesis-Rahmawati.pdf .

Ramsbottom, W.H.C. 1978. *Carboniferous.* s.l. : The ecology of fossils: London, Duckworth and Company, 1978. Vols. 146-183.

Rietz D., Palke M. 2001. History matching helps validate reservoir simulation models. *Oil & Gas Journal.* [Online] 12 24, 2001. http://www.ogj.com/articles/print/volume-99/issue-52/drilling-production/history-matching-helps-validate-reservoir-simulation-models.html.

Sanjeev Gupta, Patience A. Cowie, Nancye H. Dawers, John R. Underhill. 1998. *A mechanism to explain rift-basin subsidence and stratigraphic patterns through fault-array evolution.* Edinburgh : Department of Geology and Geophysics, 1998.

Schlumberger. 2017. OFM Well and Reservoir Analysis Software. *Schlumberger Software.* [Online] 2017. [Cited: December 11, 2017.] https://www.software.slb.com/products/ofm.

Technology, Production. 2017. Multiphase flow correlations. *Production Technology.* [Online] November 22, 2017. https://production-technology.org/.

Wilson, Mike. 2003. PIE Frequently Asked Questions. *Well Test Solutions.* [Online] March 12, 2003. http://welltestsolutions.com/faq.htm#FAQ_39.

Ziegler, P.A. 1990. *Geological Atlas of Western and Central Europe (2nd edition).* The Hague : Shell Internationale Petroleum Maatschappij, 1990.

Appendix A

Water Influx Model (Ambassha A.K., 1987)

Aquifers were incorporated into the model due to evidence of external pressure effects as seen in. The modelling of aquifers is quite an uncertain process since there is little known about them. Oil and gas companies hardly drill into aquifers for the sole purpose of gaining knowledge and understanding about the reservoir parameters or fluid properties.

Analytical aquifer models have a large influence on history matching processes through the material balance analysis, since they aid in reproducing the production pressure history. Smaller aquifers can normally be approximated using water influx definitions, whereas large aquifers need to be approximated through a mathematical model taking time dependence into account where it will take a finite time for an aquifer to react to pressure changes in the reservoir (Drake, 1978). This paragraph will introduce the aquifer used in the modelling of the K5-F field aquifers.

In this research we assume the reservoir to have a linear geometry and will be modelled as such. The linear model assumes that the reservoir and aquifer are in juxtaposition to each other which simulates edgewater and bottomwater drives as shown in Figure 74 (Engineers, 2015).
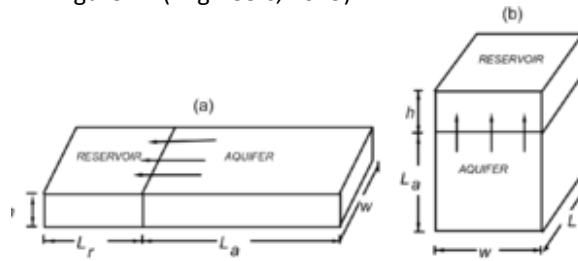

Figure 74: Linear aquifer model for (a) an edgewater drive and (b) a bottomwater drive (Engineers, 2015)

For edgewater drives, the reservoir and aquifer thickness and width is considered identical where only the length is different. In bottomwater drives, the length and width are the same but the depth and height of each is different.

The water influx into the system is described by the following equation:

$$W_{ek}(t) = U x\, \Delta P\, x\, W_D(t_D - R_D)$$

Where U is the aquifer constant, ΔP the difference between initial reservoir pressure and the current reservoir pressure, W_D the dimensionless cumulative water influx, t_D dimensionless time and R_D the ratio between outer and inner radius.

Linear aquifer

The size of the aquifer in the model is given in terms of pore-volume ratio between aquifer and reservoir V_{pa}/V_{pr}.

$$V_{pa} = \left(\frac{V_{pa}}{V_{pr}}\right) V_{pr}$$

The aquifer constant U is:

$$U = V_{pa} c_t$$

For edge water drives the length of the aquifer is given by:

$$L_a = L_r \left(\frac{V_{pa}}{V_{pr}}\right)\left(\frac{\emptyset_r}{\emptyset_a}\right)$$

For bottomwater drives, the depth of the aquifer is given by:

$$L_a = h \left(\frac{V_{pa}}{V_{pr}}\right)\left(\frac{\emptyset_r}{\emptyset_a}\right)$$

Dimensionless time is given by:

$$t_D = \frac{2.309 k_a t}{\emptyset_a \mu_w c_t L_a^2}$$

In linear models t_D is a function of the size of the aquifer. The cumulative influx of water is given by $W_D = 2\sqrt{\frac{t_D}{\pi}}$

for $t_D < 0.47$. The aquifer is considered infinite when it exceeds the critical length given by:

$$L_{ac} = \sqrt{\frac{2.309 k_a t_{max}}{0.5 \emptyset_a \mu_w c_t}}$$

Here t_{max} is the maximum time expressed in years and L_{ac} in feet. The aquifer is infinite when $t_D < 0.50$. The model parameters are estimated through history matching where the most uncertain parameters are treated as adjustable. (Engineers, 2015)

Appendix B

The properties of gas liquid mixtures are used to calculate the roughness of the pipes. This roughness is used with a Reynolds number 10^7 to result in the Fanning friction factor. The Fanning friction pressure loss equation will then calculate the pressure difference caused by friction.

In this research the Gray correlation is used in the model which combines three dimensionless numbers to predict the liquid volume fraction in situ. The three dimensionless numbers are (Gray, 1974):

$$N_1 = \frac{\rho_{NS}^2 V_m^4}{g\sigma(\rho_L - \rho_g)}$$

$$N_2 = \frac{gD^2(\rho_L - \rho_g)}{\sigma}$$

$$N_3 = 0.0814[1 - 0.0554 ln\left\{1 + \frac{730R_v}{R_v + 1}\right\}$$

where:

$$R_v = \frac{V_{sl}}{V_{sg}}$$

They are then combined as follows:

$$E_L = 1 - (1 - C_L) * (1 - \exp(f_1))$$

where:

$$f_1 = -2.314\left[N_1\left\{1 + \frac{205}{N_2}\right\}\right]^{N3}$$

Once the liquid holdup (E_L) is calculated it is used to calculate the mixture density (ρ_m). The mixture density is, in turn, used to calculate the pressure change due to the hydrostatic head of the vertical component of the pipe or well.

$$\Delta P_{HH} = \frac{\rho_m g \Delta z}{144 g_c}$$

Friction Pressure Loss

The Gray Correlation assumes that the effective roughness of the pipe (k_e) depends on the value of R_v. The conditions are as follows:

if $R_v \geq 0.007$ then

$$k_e = k° \text{ if}$$

$R_v < 0.007$ then

$$k_e = k + R_v\left\{\frac{k° - k}{0.007}\right\}$$

where:

$$k^{\circ} = \frac{28.5\sigma}{\rho_{NS}V_m^2}$$

$$R_v = \frac{V_{sl}}{V_{sg}}$$

The effective roughness (k_e) must be larger than or equal to 2.77×10^{-5} in. Where after the relative roughness of the pipe can be calculated by dividing the effective roughness by the diameter of the pipe. This results in the pressure loss by friction to be as follows:
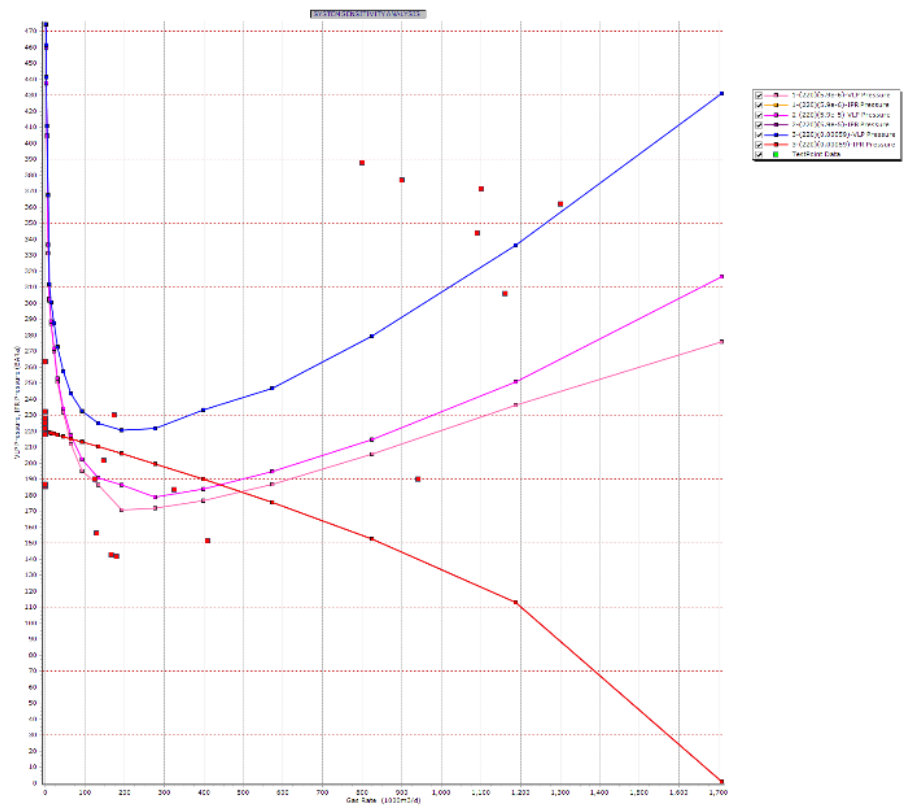
$$\Delta P_f = \frac{2f_{tp}V_m^2\rho_{NS}L}{144g_cD}$$

Figure 75: VLP and IPR sensitivity of the water gas ratio for K5-F1
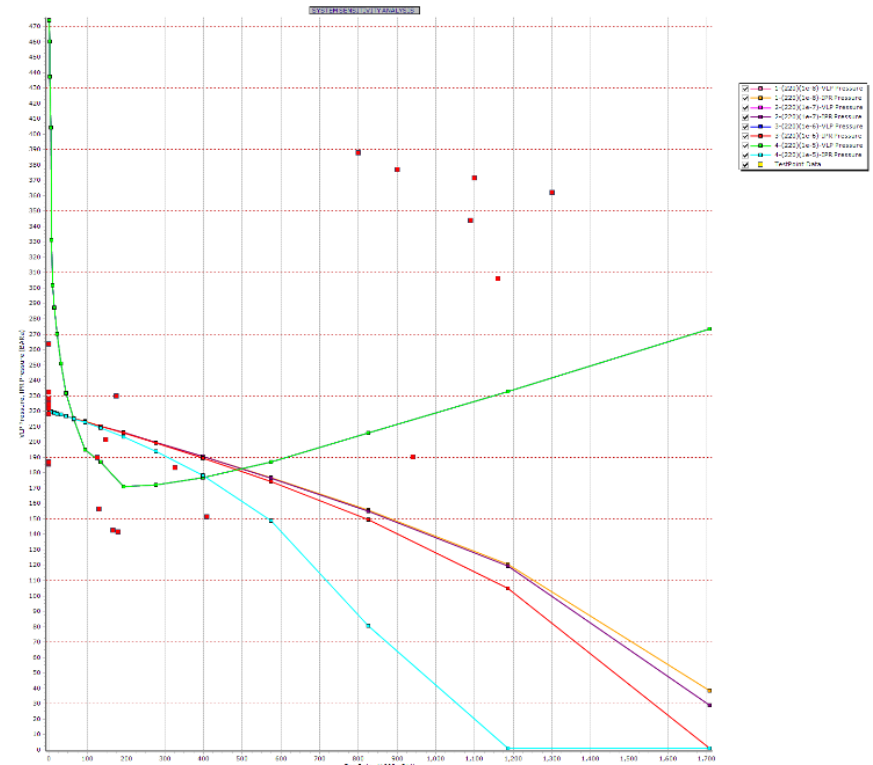

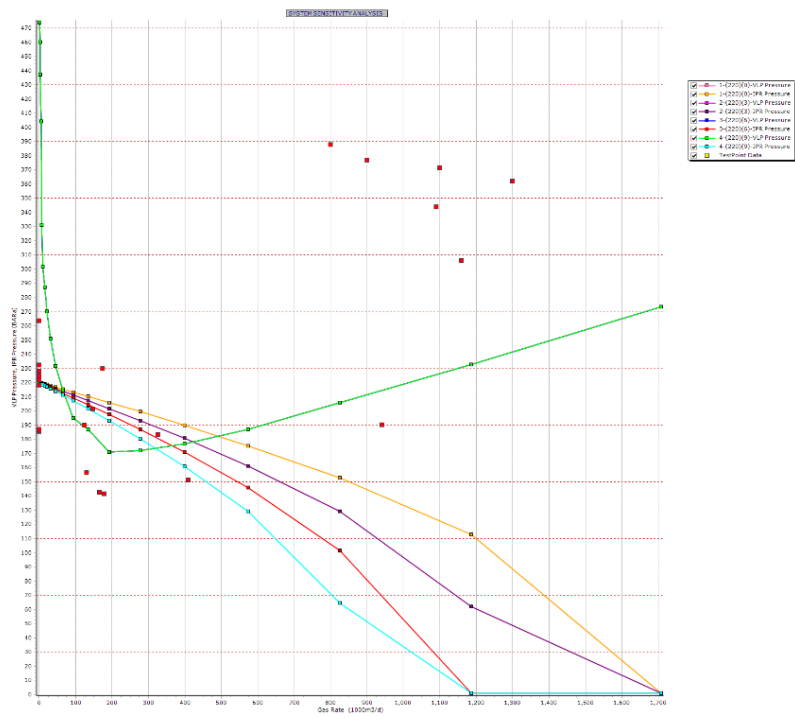**Figure 76: VLP and IPR sensitivity of the non-Darcy factor for K5-F1**

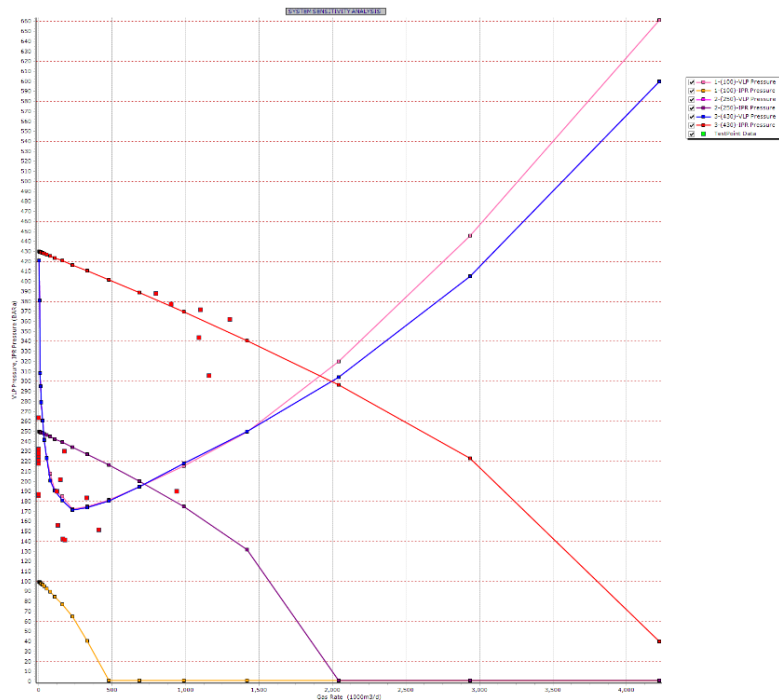**Figure 77: VLP and IPR sensitivity for skin in K5-F1**

Figure 78: VLP and IPR sensitivity on the reservoir pressure for K5-F1